

IMPROVEMENT OF MECHANICAL AND FLAME RETARDANCY  
PROPERTIES OF BIOCOMPOSITES BASED ON LOW DENSITY  
POLYETHYLENE AND POLYLACTIC ACID

A THESIS SUBMITTED TO  
THE GRADUATE SCHOOL OF NATURAL AND APPLIED SCIENCES  
OF  
MIDDLE EAST TECHNICAL UNIVERSITY

BY

YASEMİN ALTUN

IN PARTIAL FULFILLMENT OF THE REQUIREMENTS  
FOR  
THE DEGREE OF DOCTOR OF PHILOSOPHY  
IN  
POLYMER SCIENCE AND TECHNOLOGY

FEBRUARY 2015



Approval of the thesis:

**IMPROVEMENT OF MECHANICAL AND FLAME RETARDANCY  
PROPERTIES OF BIOCOMPOSITES BASED ON LOW DENSITY  
POLYETHYLENE AND POLYLACTIC ACID**

submitted by **YASEMİN ALTUN** in partial fulfillment of the requirements for the degree of **Doctor of Philosophy in Polymer Science and Technology Department, Middle East Technical University** by,

Prof. Dr. Gülbin Dural Ünver  
Dean, Graduate School of **Natural and Applied Sciences**

\_\_\_\_\_

Prof. Dr. Necati Özkan  
Head of Department, **Polymer Science and Technology**

\_\_\_\_\_

Prof. Dr. Erdal Bayramlı  
Supervisor, **Chemistry Dept., METU**

\_\_\_\_\_

Assist. Prof. Dr. Mehmet Doğan  
Co-Supervisor, **Textile Engineering Dept. Erciyes University**

\_\_\_\_\_

**Examining Committee Members:**

Prof. Dr. Teoman Tinçer  
Chemistry Dept., METU

\_\_\_\_\_

Prof. Dr. Erdal Bayramlı  
Chemistry Dept., METU

\_\_\_\_\_

Prof. Dr. Ülkü Yılmaz  
Chemical Engineering Dept., METU

\_\_\_\_\_

Prof. Dr. Necati Özkan  
Polymer Science and Technology Dept., METU

\_\_\_\_\_

Prof. Dr. Mehmet Saçak  
Chemistry Dept., Ankara University

\_\_\_\_\_

**Date:** February 9, 2015

**I hereby declare that all information in this document has been obtained and presented in accordance with academic rules and ethical conduct. I also declare that, as required by these rules and conduct, I have fully cited and referenced all material and results that are not original to this work.**

Name, Last name: Yasemin Altun

Signature:

## **ABSTRACT**

### **IMPROVEMENT OF MECHANICAL AND FLAME RETARDANCY PROPERTIES OF BIOCOMPOSITES BASED ON LOW DENSITY POLYETHYLENE AND POLYLACTIC ACID**

Altun, Yasemin

Ph.D., Department of Polymer Science and Technology

Supervisor: Prof. Dr. Erdal Bayramlı

Co-Supervisor: Assist. Prof. Dr. Mehmet Doğan

February 2015, 145 pages

The main objective of this study was to improve the mechanical and flame retardant properties of low density polyethylene (LDPE) and poly (lactic acid) (PLA) based biocomposites. Wood flour (WF) and jute fabric were used as the fillers.

In the mechanical property improvement studies with LDPE, the effect of two compatibilizing agents MA (random terpolymer of ethylene, acrylic ester and maleic acid) and GMA (random terpolymer of ethylene, acrylic ester and glycidyl metacrylate) functionalized polymers at different concentration on the mechanical, morphological and water uptake properties of LDPE-WF composites were investigated. The effect of solution preimpregnation of WF with dilute

compatibilizer solutions was also studied. . Fourier Transform Infrared Radiation (FTIR), Scanning Electron Microscopy (SEM), Tensile and Impact Tests and water-uptake determinations were conducted to investigate the mechanical, morphological, and water absorption properties of the WF-LDPE. According to the results, it was concluded that MA-composites were more effective than GMA based composites as a compatibilizer in LDPE–WF system. In addition, alkaline treatment and pre-impregnation were effective methods to increase the mechanical properties including tensile modulus, tensile and impact strength of LDPE-WF composites.

In mechanical property improvement studies with PLA, the effect of alkaline treatment, WF ratio and pre-impregnation with dilute solution of polylactic acid (PLA) on the mechanical, morphological and water uptake properties of PLA-WF green-composites were studied. The similar characterization methods were used with LDPE-WF composites. According to results, the tensile strength of the composite increases as the amount of alkaline treated WF reaches 50 wt%. Furthermore, the preimpregnation of WF with dilute PLA solution further increases the tensile strength of the composites.

In the second part of the study, flammability, thermal and combustion properties of LDPE-WF and PLA-jute fabric composites were improved. Limiting Oxygen Index (LOI), UL-94 test, Cone Calorimeter and Thermogravimetric Analysis (TGA) were used to investigate the flammability, thermal and combustion properties of the composites.

Two different approaches were applied for producing flame retardant LDPE-WF composites. In the first approach, the flame retardant LDPE-WF was produced with the reduction of the flammability of both WF and LDPE. Accordingly, WF was treated with bis[tetrakis (hydroxymethyl) phosphonium] sulfate (THPS) or

dicyandiamide-formaldehyde-phosphoric acid (DFP) flame retardants. Treated WF was used with ammonium polyphosphate (APP). As a result, the combined use of THPS or DFP treated WF with APP increased the fire performance of composites as 70% of decrease in peak heat release rate (pHRR) value with respect to the sample without flame retardant. In the second approach, the flammability of the matrix was reduced with the direct mixing of WF, matrix and the flame retardant material. Thus, LDPE, WF, red phosphorous (RP) or APP were directly mixed in the extruder to obtain flame retardant composites. RP was used for its synergistic effect for improving the flame retardant effect of APP. According to the results of the study, the combined use of APP and RP showed adjuvant effect. The maximum adjuvant effect was seen at ratio of 5:1 (APP: RP).

In flame retardancy improvement studies with PLA, one approach was applied to produce flame retardant PLA-jute composites. PLA-jute composites were obtained with the reduction of the flammability of the jute fiber. To this end, jute fabric was treated with ammonium dihydrogenphosphate (ADP) and guanidine dihydrogen phosphate (GDP). The flammability and thermal properties of PLA based biocomposites were investigated. It was found that ADP treated jute fabric containing composite showed better flame retardancy and fire performance than GDP containing one.

**Keywords:** biocomposite, compatibilizer, flame retardancy, low density polyethylene, poly lactic acid, wood flour, jute fabric.

## ÖZ

# ALÇAK YOĞUNLUKLU POLİETİLEN VE POLİLAKTİK ASİT BAZLI BİOKOMPOZİTLERİN MEKANİK VE YANMAZLIK ÖZELLİKLERİNİN İYİLEŞTİRİLMESİ

Altun, Yasemin

Doktora, Polimer Bilimi ve Teknolojisi Bölümü

Tez Yöneticisi: Prof. Dr. Erdal Bayramlı

Ortak Tez Yöneticisi: Yrd. Doç. Dr. Mehmet Doğan

Şubat 2015, 145 sayfa

Bu çalışmanın amacı güç tutuşur veya iyi mekanik özelliklere sahip alçak yoğunluklu polietilen (AYPE) ve polilaktik asit (PLA) bazlı biyokompozitler üretilmesidir. Dolgu malzemesi olarak odun tozu (OT) ve jüt kumaşı kullanılmıştır.

Çalışmanın ilk kısmında, MA (etilen, akrilik ester ve maleik asit terpolimeri) ve GMA (etilen, akrilik ester ve glisidil metakrilat terpolimeri) fonksiyonel grupları içeren polimer uyumlaştırıcıları, farklı konsantrasyonlarda kullanılarak, AYPE-OT kompozitlerinin mekanik, morfolojik ve su tutma özelliklerine olan etkileri araştırılmıştır. Diğer incelenen parametre ise OT'nin seyreltik uyumlaştırıcı çözeltisi ile karıştırma işleminden önce muamele edilmesidir. Ayrıca, OT'ye uygulanan alkali



muamelesinin, kompozitteki OT oranının ve seyreltik PLA çözeltisi ile önemdirme yapılmış OT'nin, PLA-OT yeşil kompozitlerinin mekanik, morfolojik ve su tutma özelliklerine olan etkileri de incelenmiştir. AYPE-OT ve PLA-OT kompozitlerinin bu özelliklerini araştırmak için Fourier Dönüşümlü Kızılötesi Spektroskopisi (FTIR), Taramalı Elektron Mikroskopu (SEM), çekme ve darbe testleri, Dinamik Mekanik Analiz ve su tutma testleri kullanılmıştır.

Çalışmaların sonuçlarına göre, MA uyumlaştırıcısının AYPE-OT kompozitleri için GMA uyumlaştırıcısından daha efektif olduğu ve OT'ye uygulanan alkali muamelesinin ve önemdirme işlemlerinin PLA-OT kompozitlerinin çekme modülüsü, çekme ve darbe mukavemetleri gibi mekanik özelliklerini artırmak için uygun metotlar olduğu bulunmuştur.

Çalışmanın ikinci kısmında ise, AYPE-OT ve PLA-jüt kumaşı kompozitlerinin, güç tutuşurluk, termal ve yanma özellikleri incelenmiştir. Bu özelliklerin incelenmesi için oksijen index testi (LOI), UL-94 testi, Konik Kalorimetre ve Termogravimetrik Analiz yöntemleri kullanılmıştır.

Güç tutuşur AYPE-OT kompoziti elde etmek için 2 yöntem kullanılmıştır. İlk yöntemde hem fiber malzemeyi hem de matriks malzemeyi güç tutuşur yaparak alev dayanıklılık elde edilmeye çalışılmıştır. Bu amaçla OT'ye, bis[tetrakis (hidroksimetil) fosfonyum] sülfat (THPS) veya disiyandiamit-formaldehit-fosforik asit (DFP) alev geciktirici malzemeler ile muamele yapılmış, daha sonra AYPE ve amonyum polifosfat (APP) ile karıştırılmıştır. Çalışma sonucuna göre, THPS veya DFP ile muamele edilmiş OT ile APP karışımı ile hazırlanan kompozitin maksimum ısı salınım değeri (pHRR), güç tutuşurluk sağlayan malzeme eklenmeyen numuneye kıyasla %70 oranında azaldığı ve bu sayede yangın performansının arttığı saptanmıştır. İkinci yöntemde ise kompoziti güç tutuşur yapmak için, yalnızca

matriks malzemenin güç tutuşurluğunu azaltılmıştır. Bu amaçla, matriks malzeme, fiber malzeme ve güç tutuşurluk malzemesi ekstruderde karıştırılmıştır. AYPE, OT, kırmızı fosfor (RP) veya APP karıştırılarak güç tutuşur kompozitler elde edilmiştir. Sonuçta APP ve RP birlikte kullanıldığında adjuvan etki yarattığı ve en yüksek adjuvan etkinin 5:1 oranında APP:RP kullanıldığında elde edildiği saptanmıştır. Ayrıca, amonyum dihidrojenfosfat (ADP) ve guanidin dihidrojen fosfat (GDP) ile jüt kumaşına muamele yapılmış ve bu kumaşlar ile PLA biyokompozitleri oluşturulup, bu kompozitlerin termal ve güç tutuşurluk özellikleri araştırılmıştır. Sonuçta ADP ile muamele edilmiş kumaşlarla oluşturulan kompozitin güç tutuşurluk ve yangın performansının, GDP içeren kompozitlerden daha iyi olduğu olduğu bulunmuştur.

**Anahtar Kelimeler:** biyokompozit, uyumlaştırıcı, güç tutuşurluk, alçak yoğunluklu polietilen, polilaktik asit, odun tozu, jüt kumaşı

*To my deceased father*

## ACKNOWLEDGEMENTS

I would like express my gratitude to my thesis supervisor Prof. Dr. Erdal Bayramlı for his understanding, support and guidance. I am grateful that he always appreciated and encouraged me during my thesis studies.

I would like sincerely thank to my co-supervisor Assist. Prof. Dr. Mehmet Dođan for his invaluable guidance, support and help. He always behaved me like a brother rather than a supervisor and he was the most important reason for starting PhD in this department.

I would like to thank to Prof. Dr. Teoman Tinçer for giving me the opportunity to study in his Rheology Laboratory.

I would also thank Ümit Tayfun and Osman Yaslıtaş very much for their help and friendship whenever I needed.

I gratefully thank to my friends Selbi Keskin, Serdal Kaya, and Selin Kozanođlu for their support, encouragement and friendship.

I would also like to thank my dear friend Dr. Sema Demirci Uzun for her invaluable friendship, support and the great times we spent together during my PhD.

The last, but definitely not the least, I would express my sincere gratitude to my mother, brother and my deceased father for loving and standing by me all through my life.

## TABLE OF CONTENTS

ABSTRACT.....	v
ÖZ.....	viii
ACKNOWLEDGEMENT.....	xii
TABLE OF CONTENTS.....	xiii
LIST OF TABLES.....	xix
LIST OF FIGURES.....	xx
LIST OF SCHEMES.....	xxiii
CHAPTERS	
1. INTRODUCTION.....	1
2. BACKGROUND INFORMATION.....	5
2.1 Composites.....	5
2.2 Biocomposites.....	5
2.2.1 Natural fibers.....	6
2.2.1.1 Wood Fiber.....	9
2.2.1.2 Jute Fibers.....	10
2.2.2 Polymer Matrices.....	11
2.2.2.1 Low Density Polyethylene (LDPE).....	12
2.2.2.2 PLA.....	13
2.3 Methods to enhance biocomposite performance.....	15
2.3.1 Modification of Natural fibers.....	16
2.3.2 Alkaline Treatment.....	16
2.3.3 Use of Compatibilizers.....	18
2.4 Wood Plastic Composites.....	18
2.5 Mechanical Properties of Natural Fiber Composites.....	19

2.6 Definition of Flame Retardant Polymeric Materials.....	19
2.7 General Description of Polymer Combustion.....	20
2.8 Strategies for Obtaining Flame Retardant Polymers.....	21
2.8.1 General Concepts to Obtain Flame Retardancy in Polymers.....	22
2.8.1.1 Additive approach.....	23
2.8.1.2 Surface Approach.....	23
2.9 Flame Retardant Additives.....	24
2.9.1 General Mechanism of Flame Retardant Additives.....	24
2.9.2 Synergism and Antagonism of Flame Retardant Additives.....	27
2.10 Types of Flame Retardant Additives.....	28
2.10.1 Phosphorous containing flame retardants.....	28
2.10.1.1 Red Phosphorus.....	30
2.10.1.2 Ammonium Polyphosphate.....	31
2.10.1.3 Ammonium dihydrogen phosphate.....	35
2.10.1.4 Guanidine dihydrogen phosphate.....	35
2.11 Thermal Behavior of LDPE.....	36
2.12 Thermal Behavior of PLA.....	36
2.13 Characterization Methods.....	36
2.13.1 Characterization of Mechanical and Morphological Properties.....	36
2.13.1.1 Scanning Electron Microscopy.....	37
2.13.1.2 Tensile Test.....	37
2.13.1.3 Impact Test.....	39
2.13.1.4 Dynamic Mechanical Analysis.....	39
2.14.2 Characterization of Flame Retardancy Properties of the Composites.....	41
2.14.2.1 UL-94.....	41
2.14.2.2 Limiting Oxygen Index.....	43
2.14.2.3 Cone Calorimeter.....	44
2.15 Production Methods of Polymer Composites.....	48

2.15.1 Extrusion.....	48
2.15.2 Compression Molding.....	48
2.15.3 Injection Molding.....	49
3. EXPERIMENTAL.....	51
3.1 Alkaline Treatment.....	51
3.2 Production of LDPE-WF Composites.....	52
3.2.1 Materials.....	53
3.2.2 Pre-impregnation with compatibilizer solution.....	54
3.2.3 Preparation of LDPE-WF Composites.....	54
3.2.4 Characterization Methods.....	57
3.2.4.1 FTIR Analysis.....	57
3.2.4.2 Scanning Electron Microscopy.....	57
3.2.4.3 Tensile Test.....	57
3.2.4.4 Impact Test.....	58
3.2.4.5 Water Uptake.....	59
3.3 Production of PLA-WF composites.....	60
3.3.1 Materials.....	60
3.3.2 Preimpregnation with PLA solution.....	60
3.3.3 Mixing of WF-PLA.....	60
3.3.4 Characterization Methods.....	61
3.3.4.1 Tensile Tests.....	61
3.3.4.2 Dynamic Mechanical Analysis.....	61
3.4 Production of Flame Retardant LDPE-WF Composites.....	61
3.4.1 Production of LDPE-flame retardant treated WF.....	62
3.4.1.1 Materials.....	62
3.4.1.2 The Preparation of Dicyandiamide-Formaldehyde-Phosphoric Acid (DFP) Flame Retardant and Treatment of WF.....	63

3.4.1.3 The Preparation of Dicyandiamide-Formaldehyde-Ammonium Dihydrogenphosphate (DFAP) Flame Retardant and Treatment of WF .....	64
3.4.1.4 The Preparation of Urea-Dicyandiamide-Formaldehyde-Phosphoric Acid (UDFP) Flame Retardant and Treatment of WF .....	64
3.4.1.5 The Preparation of Tetrakis(hydroxymethyl)phosphonium sulfate-urea-ammonium dihydrogenphosphate (THPS) Flame Retardant and Treatment of WF .....	65
3.4.1.6 Preparation of LDPE-flame retardant treated WF .....	66
3.4.1.7 Characterization Methods .....	67
3.4.1.7.1 UL-94 Test .....	67
3.4.1.7.2 LOI .....	67
3.4.1.7.3 Cone Calorimeter .....	67
3.4.1.7.4 Thermogravimetric Analysis (TGA).....	67
3.4.2 Direct Mixing of Flame Retardant LDPE-WF Composites .....	68
3.4.2.1 Materials.....	68
3.4.2.2 Preparation of Flame Retardant LDPE-WF Composites. ....	68
3.4.2.3 Characterization Methods .....	69
3.5 Production of Flame Retardant PLA-Jute Fiber Biocomposites.....	69
3.5.1 Materials.....	69
3.5.2 Flame Retardant Treatment of Jute Fabric .....	70
3.5.3 Preparation of PLA-Flame Retardant Treated Jute Fabric Biocomposites	70
3.5.4 Characterization Methods .....	71
4. RESULTS AND DISCUSSION .....	73
4.1 The Effect of Compatibilizers and the Effect of Preimpregnation with a Compatibilizer Solution on Mechanical, Morphological and Water Uptake Properties of LDPE-WF Composites.....	74
4.1.1 FTIR Analysis .....	74
4.1.2 SEM Analysis.....	75



4.1.4 Water Uptake .....	80
4.2 Effect of Alkaline Treatment and Pre-impregnation on Mechanical and Water Uptake Properties of WF-PLA Biocomposites .....	83
4.2.1 FTIR Analysis.....	83
4.2.2 SEM Analysis .....	84
4.2.3 Mechanical Properties .....	86
4.2.4 Dynamic Mechanical Analysis.....	89
4.2.5 Water Uptake of PLA-WF Composites.....	91
4.3 The Effect of Treatment of WF with Flame Retardant Solutions on the Flame Retardancy of LDPE-WF Composites Containing APP .....	92
4.3.1 LOI and UL-94 .....	92
4.3.2 Thermogravimetric Analysis (TGA) .....	93
4.3.3 Cone Calorimeter.....	96
4.4 The Effect of Direct Mixing of Flame Retardants on the Flammability and Thermal Characteristics of WF-LDPE Composites .....	99
4.4.1 LOI and UL-94 .....	99
4.4.2 Thermogravimetric Analysis .....	100
4.4.3 Cone Calorimeter.....	101
4.5 Flammability and Thermal Degradation Behavior of Flame Retardant Treated Jute Fabric Reinforced PLA .....	103
4.5.1 LOI and UL-94 .....	103
4.5.2 Thermogravimetric Analysis .....	104
4.5.3 Cone Calorimeter.....	106
4.5.4 SEM and ATR- FTIR Analysis .....	108
5. CONCLUSIONS .....	111
5.1 Comparative Study of MA and GMA Functionalized Terpolymers as Compatibilizers for LDPE-WF Composites.....	111

5.2 Effect of Alkaline Treatment and Pre-impregnation on Mechanical and Water Uptake Properties of WF-PLA Green Composites .....	112
5.3 The Effect of Treatment of WF with Flame Retardant Solutions on the Flame Retardancy of LDPE-WF Composites Containing APP .....	112
5.4 The Effect of Direct Mixing of Flame Retardants on the Flammability and Thermal Characteristics of WF-LDPE Composites.....	113
5.5 Flammability and Thermal Degradation Behavior of Flame Retardant Treated Jute Fabric Reinforced PLA.....	113
5.6 Overall Evaluation of Compatibilizers and Processing Methods on the Mechanical and Flame Retardancy Properties.....	114
REFERENCES.....	117
APPENDIX.....	133
CIRRICULUM VITAE.....	141

## LIST OF TABLES

### TABLES

Table 2. 1 Mechanical properties of extrusion and injection molding grades of PLA[1].....	15
Table 2. 2 The concentration of P-red required for V0 rating for UL-94 testing for different polymers [50].....	31
Table 2. 3 Criteria for UL-94 classifications.....	43
Table 3. 1 Properties of coupling agents used.....	53
Table 3. 2 The properties of APP.....	63
Table 3. 3 The properties of THPS.....	65
Table 3. 4 The properties of P-red.....	68
Table 3. 5 The properties of ADP and GDP flame retardants.....	70
Table 4. 1 The Mechanical Properties of LDPE-WF Composites.....	78
Table 4. 2 The compositions and the mechanical properties including tensile and impact strength of composites.....	86
Table 4. 3 The composition of formulations, LOI values and UL-94 ratings.....	92
Table 4. 4 TGA data of flame retardant treated WF-LDPE composites.....	95
Table 4. 6 Formulations of composites, LOI values and UL-94 ratings.....	99
Table 4. 7 TGA data of LDPE-WF composites.....	100
Table 4. 8 Mass loss calorimeter data of selected compositions.....	103
Table 4. 9 LOI, UL-94 and TGA data of all composites.....	104
Table 4. 10 Cone calorimeter data of selected compositions of PLA-jute fiber composites.....	108

## LIST OF FIGURES

### FIGURES

Figure 2. 1 Classification of natural fibers [1] .....	7
Figure 2. 2 Cross-section of the three major constituents in the fiber cell wall [16]...	8
Figure 2. 3 Chemical structure of a) cellulose b) hemicelluloses c) lignin [16] .....	9
Figure 2. 4 Schematics of a soft wood and hard wood [29].....	10
Figure 2. 5 The picture of jute plant [37] and jute fabric [38]. .....	11
Figure 2. 6 Repeating unit of polyethylene.....	12
Figure 2. 7 Different chain configurations of polyethylene are caused by branching of main back bone chain [41].....	12
Figure 2. 8 Typical structure of (i) pristine (ii) alkaline treated cellulose fiber [16].	17
Figure 2. 9 Four individual stages of polymer flammability [53].....	21
Figure 2. 10 Schematic representation of general flame retardancy approaches [57]	23
Figure 2. 11 General mechanisms of flame retardant additives [65] .....	26
Figure 2. 12 Chemical structure of Red Phosphorus [68].....	30
Figure 2. 13 The molecular structure of APP [77].....	32
Figure 2. 14 The flame retardant effect of intumescent char [12] .....	33
Figure 2. 15 The order of intumescent reaction processes [58] .....	33
Figure 2. 16 The schematic representation of thermal degradation of APP [50].....	34
Figure 2. 17 The chemical structure of ammonium dihydrogen phosphate.....	35
Figure 2. 18 The chemical structure of guanidine dihydrogen phosphate .....	35
Figure 2. 19 Stress-strain curve for a typical polymeric material [87]. .....	38
Figure 2.20 Response of stress and strain with time for a characteristic polycrystalline polymer above Tg.....	40
Figure 2. 22 The schematic view of LOI test design [95].....	44

Figure 2. 23 Schematic representation of cone calorimeter [95].....	46
Figure 2. 24 Characteristic HRR curves for various typical burning behaviors [98].	47
Figure 3. 1 SEM images of a) pristine WF b) aWF at a magnification of $\times 200$ [5] ..	52
Figure 3. 2 The chemical structures of compatibilizers a) LOTADER $\text{\textcircled{R}}$ 2210 b) LOTADER $\text{\textcircled{R}}$ AX 8900.....	53
Figure 3. 3 The photograph of the twin screw extruder used for the composite production in this study .....	55
Figure 3. 4 The photograph of the laboratory scale injection-molding machine .....	56
Figure 3. 5 The photograph of tensile test machine .....	58
Figure 3. 6 The photograph of impact test machine.....	59
Figure 3. 7 The photograph of hot-press used in this work.....	66
Figure 4. 1 The FTIR spectra of compatibilizers and preimpregnated WFs .....	75
Figure 4. 2 SEM images of freeze-fractured surfaces of selected composites.....	77
Figure 4. 3 The effect of GMA compatibilizer ratio on water uptake values of LDPE- WF composites .....	81
Figure 4. 4 The effect of MA-compatibilizer ratio on water uptake values of LDPE- WF composites .....	82
Figure 4. 5 The effect of preimpregnation on water uptake property of the composites .....	83
Figure 4. 6 FTIR spectra of aWF, PLA and pre-impregnated aWF .....	84
Figure 4. 7 SEM micrographs of fracture surfaces of selected composites .....	85
Figure 4. 8 The stress–strain curves of WF containing PLA composites .....	87
Figure 4. 9 The dynamic storage modulus of PLA composites as a function of temperature .....	89
Figure 4. 10 $\tan \delta$ values of PLA composites as a function of temperature.....	90
Figure 4. 11 The water uptake behavior of the PLA-WF composites.....	91
Figure 4. 12 TGA results of untreated WF and THPS treated WF .....	94
Figure 4. 13 TGA results of untreated WF and DFP treated WF .....	94

Figure 4. 14 The graph of TGA results .....	96
Figure 4. 15 The graph of cone calorimeter results .....	98
Figure 4. 16 TGA graph of LDPE-WF composites .....	101
Figure 4. 17 Cone calorimeter results of selected compositions.....	102
Figure 4. 18 TGA graphs of pristine jute fiber and ADP or GDP treated jute fiber	105
Figure 4. 19 TGA graph of all PLA-jute composites.....	106
Figure 4. 20 Cone calorimeter graph of PLA-jute fiber composites.....	107
Figure 4. 21 SEM results of PLA-jute fiber's char residues .....	109
Figure 4. 22 ATR-FTIR results of PLA-jute fiber char residues .....	109
Figure A. 1 Stress-Strain curve of LDPE-WF composition.....	133
Figure A. 2 Stress-Strain curve of LDPE-WF-3 MA composition.....	134
Figure A. 3 Stress-Strain curve of LDPE-WF-5 MA composition.....	134
Figure A. 4 Stress-Strain curve of LDPE-WF-10 MA composition.....	135
Figure A. 5 Stress-Strain curve of LDPE-WF-15 MA composition.....	135
Figure A. 6 Stress-Strain curve of LDPE-WF-pre 10 MA composition.....	136
Figure A. 7 Stress-Strain curve of LDPE-WF-3 GMA composition.....	136
Figure A. 8 Stress-Strain curve of LDPE-WF-5 GMA composition.....	137
Figure A. 9 Stress-Strain curve of LDPE-WF-10 GMA composition.....	137
Figure A. 10 Stress-Strain curve of LDPE-WF-15 GMA composition.....	138
Figure A. 11 Stress-Strain curve of LDPE-WF-pre 1 GMA composition.....	138
Figure A. 12 Stress-Strain curve of LDPE-WF-pre 3 GMA composition.....	139
Figure A. 13 Stress-Strain curve of LDPE-WF-pre 5 GMA composition.....	139

## LIST OF SCHEMES

### SCHEMES

Scheme 2. 1 Polymerization routes to polylactic acid.....	14
Scheme 2. 2 The chemical reaction of fiber cell with NaOH.....	17
Scheme 2. 3 The proposed radical trap theory of phosphorus compounds [50] .....	29





## **CHAPTER 1**

### **INTRODUCTION**

Slow decay of plastics in the environment, the limiting landfill space, diminishing petroleum resources, concerns over the emission of dangerous gases during annihilation and consumption of packing plastics by fish, fowl and animals have encouraged the development of biodegradable/biobased plastics. Renewable biobased plant and agricultural stock are the contents of this new generation of biobased polymeric products. They are the basis for eco-friendly, sustainable products that can compete with petroleum based products which are dominant in the packing, building products, automotives, furniture applications. There is no necessity for producing 100% biobased products to substitute for the petroleum based products. Petroleum based materials and bioresources are combined to produce useful products for real world applications to fulfill the cost-performance requirements. Synthetic polymers or biopolymers are combined with natural fibers/biofibers are referred to as 'biocomposites'. Biocomposites are the combination of two or more materials; at least one of them is derived from natural resources. Composites produced from natural fibers and petroleum-based nonbiodegradable polymers (e.g. PE, PS) or biodegradable polymers (eg. polylactic acid, PLA) and composites made from biodegradable polymers and reinforced with man-made fibers (e.g. carbon) can be classified as biocomposites [1]. Biocomposites whose matrix and reinforcing material are made from biodegradable polymers are likely to be more ecofriendly and can be referred to as 'green composites' [2]. There are some advantages of using natural fibers over commercial reinforcements: low

price, good specific strength, low density, high toughness, reduced health hazards, good thermal properties, simplicity of separation and biodegradability. However, the main disadvantage of natural fibers is poor compatibility with hydrophobic polymer matrix due to hydrophilic nature of natural fibers. Other drawbacks are low thermal stability, restricted maximum processing temperature, lower impact strength, lower durability, low moisture resistant and poor fire resistance [3],[4]. Accordingly, the studies are focussed on improving the adhesion between polymer matrix and lignocellulosic material, mechanical and flame retardant properties of biocomposites.

Wood plastic composites (WPC) have considerable importance in a wide range of industries especially in automotive and construction industries due to their low cost, low density, and certain specific properties. Despite these advantages, some problems exist for wider application of WPC, such as low thermal stability of lignocellulosics, poor interfacial adhesion between polar lignocellulosics and non-polar matrix material and moisture uptake. The main factors affecting the final mechanical properties of WPC are the degree of filler dispersion and the effective stress transfer at interface between lignocellulosics and matrix material. Better filler dispersion and strong adhesion between matrix and lignocellulosics can be achieved via various physical and chemical methods [1,5-7]. Alkaline treatment, surface treatment with various types of compatibilizers and pre-impregnation with dilute matrix solution are commonly used methods [5,8-11]. In this study, the effect of alkaline treatment, WF ratio and pre-impregnation with dilute solution of PLA on the mechanical, morphological and water uptake properties of PLA-WF green-composites were investigated. In addition, the effect of two different compatibilizing agents, maleic anhydride (MA) and glycidylmethacrylate (GMA) functionalized terpolymers at different concentrations on the mechanical, morphological, and water uptake properties of LDPE–WF composites. The effect of solution pre-impregnation of WF with the compatibilizers were also investigated [5,7].

When a textile or polymeric material is exposed to an igniter and the material does not keep on burning or glowing once the source of ignition has been removed. After the end of burning or glowing even though there are some modifications in the chemical and physical properties, the material can be defined as a flame retardant material. The rise in the utilization of plastic materials in our daily lives in so many areas such as films, fibers, coatings and foams, increases the need for flame retardant materials in recent years. Moreover, the need for flame retardant polymeric materials was increased with the regulations made by European countries [12].

There are three kinds of methods to obtain a flame retardant polymeric material or a textile. During polymerization, a flame retardant co-monomer which provides inherent flame retardancy for the synthesized polymer is used. This is termed as 'reactive approach'. In 'additive approach' the additives which generate flame retardant property, are added into polymer melt during mixing. In 'surface approach', surface modification is applied to get flame retardant polymeric material. Surface approach is widely used for producing flame retardant textiles. In this thesis, both additive and surface approaches were studied [12].

Polyethylene (PE) is widely preferred thermoplastic for household, packaging, and building applications due to good combination of price and properties [13]. There are several reinforcements that have been used to improve the properties of PE, especially composites with natural fibers are becoming more popular. Due to wide range of application, development of its flame retardancy characteristics has attracted a great deal of attention.

PLA has outstanding physical and mechanical properties and this makes it a good candidate to replace with petrochemical thermoplastics in lots of application areas. Some properties (eg. mechanical strength, heat sealability) of commercial PLA is

similar to synthetic thermoplastics, in the mean time some of its properties resembles to bio-based polymers (biodegradability, dyeability). In the past, PLA is mostly used in the production of disposable or semi-durable materials but today market requires more durable materials. PLA is expected to replace polymers such as polypropylene (PP), polyamide or polyethylene terephthalate (PET) in transportation and electric & electronics sectors. In those sectors fire hazards must be prevented by using flame retardant materials [43].

One of the aims of this study is to increase the flame retardancy of LDPE-WF composites with additive and surface approach and to increase the flame retardancy of PLA-jute composites with only surface approach.

Ammonium polyphosphate and red phosphorous were the main flame retardant agents for LDPE-WF composites. Ammonium dihydrogen phosphate and guanidine dihydrogen phosphate were used as main flame retardants for PLA-jute fiber composites.

The characterization methods of the composites for the mechanical, morphological and water absorption studies were performed with tensile tests, impact tests, Scanning Electron Microscope (SEM), Dynamic Mechanical Analysis (DMA), FTIR and daily water absorption measurements. The characterization of flame retardancy properties of the composites were made with UL-94, Limiting Oxygen Index (LOI), Cone Calorimeter, Thermal Gravimetric Analysis (TGA) and Thermal Gravimetric Analysis- Fourier Transform Infrared Spectroscopy (TGA-FTIR).

## **CHAPTER 2**

### **BACKGROUND INFORMATION**

#### **2.1 Composites**

Composites are composed of two or more ingredients having different physical or chemical properties, when combined together, produce a material with different properties from the individual components. A typical synthetic composite is comprised of a reinforcement phase which is stiff, strong material and a continuous matrix phase. The reason for preferring composites is to have stronger, lighter and less expensive materials. The types of engineered composite materials are composite building materials (ex. cements, concrete), reinforced plastics (fiber reinforced polymer), metal composites and ceramic composites (composite ceramic and metal matrices) [14,15].

#### **2.2 Biocomposites**

Biocomposites are the combination of two or more materials; at least one of them is derived from natural resources. Composites produced from natural fiber and petroleum-based nonbiodegradable polymers (e.g. PE, PS) or biodegradable polymers (e.g. PLA) and composites made from biodegradable polymers and reinforced with man-made fibers (e.g. carbon) can be classified as biocomposites [1]. In biocomposites, the reinforcement or filler (discontinuous phase) is mostly the natural fibers. Fibers provide strength and stiffness. The properties of the biocomposites are mostly depending on the inherent properties of these fibers [14]. The other component in biocomposites is a continuous matrix. The matrix acts as a

binder, used to hold the fibers together, transfers external loads to fibers and provides protection from mechanical damage [14,16]. In biocomposites, thermoset matrices such as unsaturated polyesters, epoxies and phenolics, and thermoplastic matrices such as PE, PP and elastomeric materials are widely used [16].

Biocomposites made from natural fibers and biodegradable polymers are likely more eco-friendly and can be referred to as ‘green composites’ [2]. They are completely degraded by anaerobic or aerobic biological processes and water, carbon dioxide, methane, biomass and mineral salts form as a result of degradation [17]. As a result of this, green composites are not detrimental to the environment.

The mechanical properties of biocomposites are close to widely used plastics reinforced with glass fiber. Different kinds of structures such as sandwich plates, tubes, car door panellings have been produced with biocomposites. Besides satisfactory mechanical properties, flame resistance is required to use in some other applications. Since biocomposites are organic based materials, they are combustible. That is why, to be used for aircrafts or in railways, flame resistance is needed in a certain degree. Other applications of biocomposites in furniture industries, irrigation systems, sports and leisure items are recently studied [3].

### **2.2.1 Natural fibers**

In biocomposites, natural fibers reinforce the resulting composite material by increasing its strength and stiffness. There are several kinds of natural fibers having different nature, source, origin, physical and chemical structures [3]. Natural fibers are classified according to their origin; coming from plants, animals or minerals. The classification of natural fibers is illustrated in Figure 2.1.

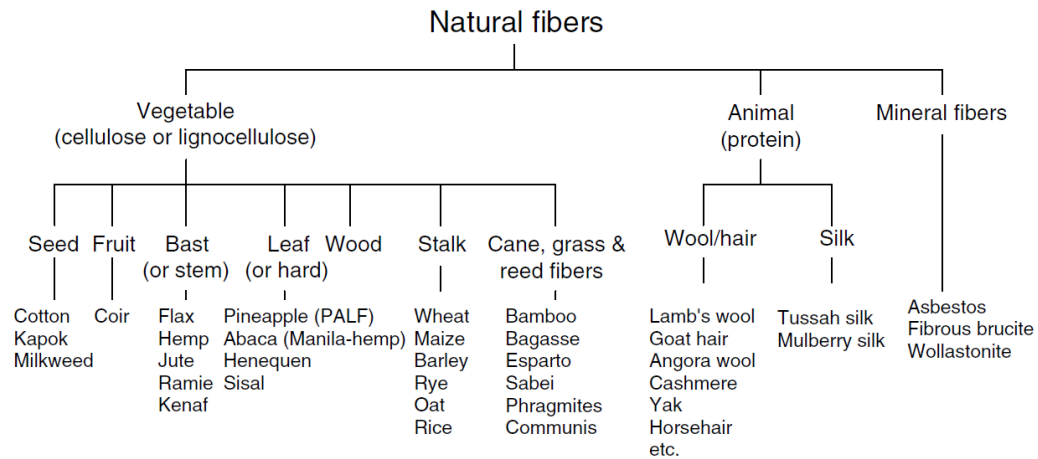


**Figure 2. 1** Classification of natural fibers [1]

Natural fibers have several advantages and drawbacks over glass fibers. They are acceptable mostly in construction industry because of their biodegradability, low cost, wide variety, low energy consumption, high specific properties, safer handling and ecological character. However, they also have some disadvantages such as low thermal stability, forming aggregates while processing, non-uniform dispersion of fibers within the matrix and high moisture absorption decreases the potential usage of natural fibers [18,19].

Plant or vegetable fibers are widely used for the reinforcement of plastics. The plant fibers are classified as seed, fruit, bast, leaf, wood, stalk and grass. Most plant fibers are comprised of cellulose, hemicelluloses, lignin, pectin and some water soluble compounds, where the major constituents are cellulose, hemicelluloses, and lignin. The amount of cellulose can change according to the species and age of the plant in plant fibers [19]. The cross section of the fiber cell wall is shown in Figure 2.2.

Cellulose is hydrophilic polymer having linear chain of 1,4- $\beta$ -bonded anhydroglucose units that includes alcoholic hydroxyl groups in its structure [20]. Intramolecular hydrogen bonds are formed by these hydroxyl groups inside the

polymer itself. This plays a major role having crystalline structure of the cellulose. In addition, hydroxyl groups form hydrogen bonds with the other cellulose molecules and also with the hydroxyl groups in the air resulting in highly hydrophilic nature [3].

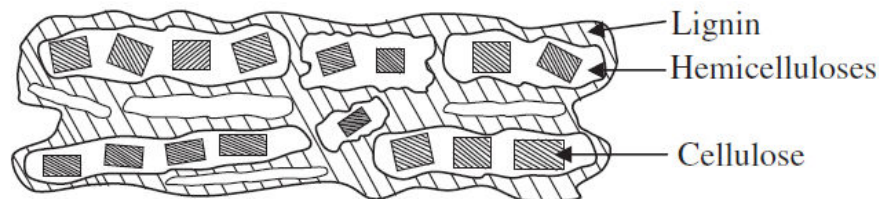


**Figure 2. 2** Cross-section of the three major constituents in the fiber cell wall [16]

Hemicelluloses are polysaccharides comprised of 5- and 6-membered ring sugar molecules. The chains of hemicelluloses are branched and shorter than cellulose, having pendant groups leading to noncrystalline structure. They provide supportive matrix for cellulose microfibrils and also have very hydrophilic nature like cellulose [1].

Lignin, a complex, three-dimensional copolymer of aliphatic and aromatic units, provides rigidity to the plants with very high molecular weight. Although the functional groups of lignin have been identified, its chemistry has not been certainly proved. It has high carbon and low hydrogen content. Lignin has amorphous, thermoplastic and hydrophobic character [1]. The chemical structure of cellulose, hemicellulose and lignin is demonstrated in Figure 2.3.



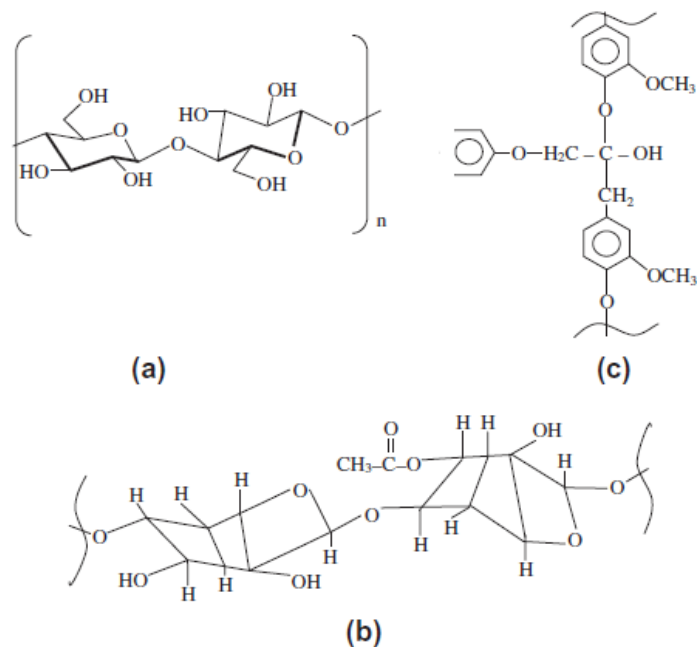


**Figure 2. 3** Chemical structure of a) cellulose b) hemicelluloses c) lignin [16]

### 2.2.1.1 Wood Fiber

Wood, made up of mainly cellulose, hemicelluloses, lignin and other extractives, has a complex chemical structure. It has two different species; hardwood (*deciduous*) and softwood (*coniferous*) and the ratios of their constituents differ according to their origin [1]. Figure 2.4 shows the schematics of softwood and hardwood. Pine, fir, cedar and spruce are the examples of softwoods; oak, maple and ash are those of hardwoods. Wood is comprised of hollow, spindle-shaped, elongated cells that are lined up parallel to each other through the trunk of the tree. The hollow center of the fiber is the lumen and can be entirely or partly filled with resins or gums. These fibers are tightly held together and constituted the structural part of the wood tissue. The length of the wood fibers is 1 mm for hardwoods and 3 to 8 mm for softwoods and the diameters are 15-45 $\mu\text{m}$  [30].

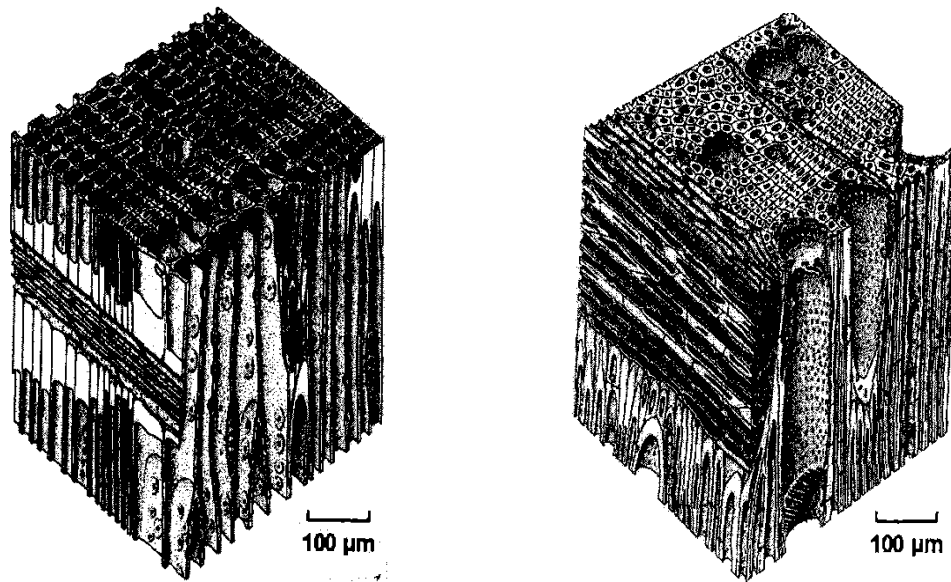


**Figure 2. 4** Schematics of a soft wood and hard wood [29]

#### **2.2.1.2 Jute Fibers**

Jute is one of the most significant fibers within the other types of fibers. It grows 2 to 3.5 m in height in a year, with a 2 to 3 cm diameter stalk. Jute is grown in hot and humid climates such as India and Bangladesh and it is benefited only from its fibers. It is mostly preferable due to its being versatile, ecofriendly, durable, antistatic and natural character. Jute fibers are long, bright, durable and have brown color naturally. They are strong and have a low extension to break. They have high lignin content (up to 20%) which causes brittleness of the fibers [1].

The inherent properties of jute fiber including biodegradability, silky texture and resistance to heat and fire make it convenient for use in different areas such as fashion, luggage, furnishing and carpets. Jute-fiber-reinforced thermoplastic and rubber composites have been produced so far. Jute-epoxy, jute-polyester and jute-

phenolic resin composites have also been studied for the applications of low-price housings and silos for storage [1]. Figure 2.5 shows the picture of both the jute plant and the fabric.



**Figure 2. 5** The picture of jute plant [37] and jute fabric [38].

### **2.2.2 Polymer Matrices**

In a fiber-reinforced composite, the matrix acts as a binder, transfers applied external loads to fibers and provides protection from mechanical damage. The matrix can be a thermoplastic or a thermoset polymer. The widely used examples for thermoplastic matrices are PE, PP, polyvinylchloride (PVC) and PET. Phenolics and epoxies are the most common used examples for thermoset matrices. The production of real biocomposites requests that the matrix is manufactured mostly from biodegradable polymers (green composites), however synthetic thermoplastics and thermosets predominate commercial biocomposite manufacture [14].

### 2.2.2.1 Low Density Polyethylene (LDPE)

LDPE manufactured firstly in 1933 by Imperial Chemical Industries via free radical polymerization of ethylene monomer with the initiation of organic peroxides. The repeating unit of polyethylene is given in Figure 2.6.

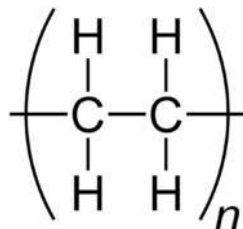


**Figure 2. 6** Repeating unit of polyethylene

Its density is typically 0.915-0.930 g/cm<sup>3</sup> [39]. It is stable at room temperature except by strong oxidizing agents and swelling occurs in certain solvents. LDPE can resist 80°C temperature, quite flexible and tough. In addition, it has more branching than HDPE (Fig. 2.7), so it has weaker intermolecular forces, lower tensile strength and higher resilience. Its density is lower because its molecules are less tightly packed and less crystalline due to side branching [40].

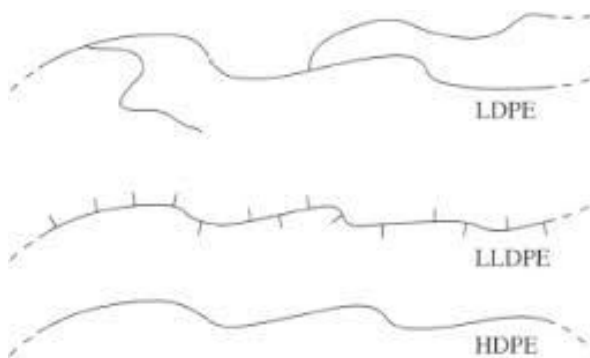


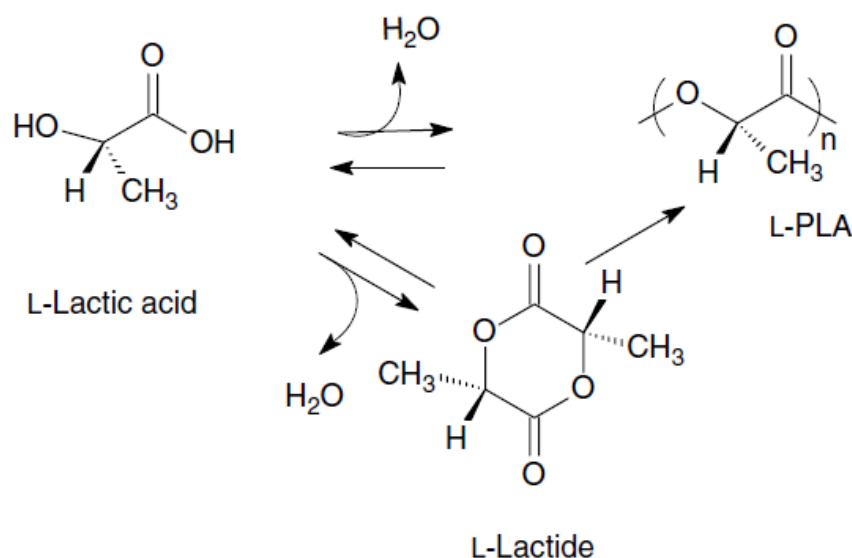
**Figure 2. 7** Different chain configurations of polyethylene are caused by branching of main back bone chain [41].

Since polyethylene has a hydrocarbon structure (contains only hydrogen and carbon) it is easily combusted. Thus, LDPE has a low LOI value of 18 and burns to clamp in UL-94 test.

#### **2.2.2.2 PLA**

PLA is a rigid thermoplastic polymer. It can be semicrystalline or completely amorphous depending upon the stereochemistry of the backbone. The natural and abundant form of PLA is L (-)-lactic acid (2-hydroxy propionic acid) and D form of this acid is formed by microorganisms or through racemization. It is a unique polymer which behaves like PET, acts much like PP. It can be shaped into transparent films, fibers and injection molded for bottles [1].

PLA is not a new polymer. In 1930s Carothers manufactured PLA from cyclic dimer of lactic acid. In 1997, two large companies formed Cargill Dow intended to decrease the cost of production and increase the volume of PLA in the polymer market. In the present green chemistry world, PLA has some advantages that make it unique and popular in the polymer market. Lactic acid which is the starting material of PLA is produced by the fermentation of renewable resources. It is also biodegradable that rapidly degrades in the environment generates by-products having very low toxicity. Cargill Dow has patented a low-cost continuous process for the manufacture of lactic acid-based polymers and this process, for the first time, provides biodegradable commodity polymer produced from renewable sources. There are two routes to prepare PLA. The first one is direct condensation of lactic acid and the second one is ring-opening polymerization of the cyclic lactide dimer [1]. The polymerization routes are given shortly in Scheme 2.1.



**Scheme 2. 1** Polymerization routes to polylactic acid

PLA has reasonable mechanical properties which can be compared with PET and PP that are very popular commodity plastics. It can be melt-processed at a temperature that natural fibers do not degrade [42]. Typical mechanical properties of PLA from Cargill Dow for extrusion and injection molding are given in Table 2.1.

PLA is a flammable polymer with the LOI value of 19. There is only a few literature survey describing the flame retardancy of PLA. This can be attributed to first applications of PLA were planned for disposable materials and semi-durable materials (e.g. textile). Thus, there was no really necessity for flame retardancy. Now the market demands more enduring materials and requires substituting petroleum based thermoplastic polymers like PP, PE and PET by PLA in sectors such as transportation and electrics and electronics. In these sectors protection from fire hazard is important and flame retardancy is required. So development of flame retardancy of PLA or PLA composites became a significant issue [43].

**Table 2. 1** Mechanical properties of extrusion and injection molding grades of PLA[1]

<b>Mechanical Property</b>	<b>PLA Polymer 2000D<sup>a</sup></b>	<b>ASTM Method</b>	<b>PLA Polymer 3010D<sup>b</sup></b>	<b>ASTM Method</b>
Tensile strength at break (MPa)	53	D882	48	D638
Tensile Modulus (GPa)	3.5	D882	-	-
Tensile elongation (%)	6.0	D882	2.5	D638
Notched Izod impact (J/m)	0.33	D256	0.16	D256

a 2000D is a product of Cargill Dow LLC designed as an extrusion/thermoforming grade; properties typical of extruded sheet.

b 3010D is a product of Cargill Dow LLC designed as an injection molding grade; properties typical of injection molded tensile bars.

### **2.3 Methods to enhance biocomposite performance**

The properties of a biocomposite depend on the properties of the components. Therefore, the reinforcing fibers and matrix polymers must be selected carefully to get a biocomposite with the desired properties. In addition, the properties of biocomposites may be enhanced by changing the controlling factors such as fiber architecture and fiber-matrix interface. Fiber architecture includes (i) fiber geometry, (ii) packing arrangement, (iii) fiber orientation, (iv) fiber-volume fraction. Of these, fiber-volume fraction is the most important factor to improve the mechanical properties of the biocomposite and it must be enhanced to some extent, depending on the packing arrangement of the fiber. The fiber-matrix interface is also important in terms of biocomposite performance. The interface transfers the external loads to the reinforcing fiber via shear stresses. Thus, the strength of the interface must be controlled. Moreover, it is essential to have good bonding between matrix and fiber to transfer the stress adequately and to provide good reinforcing function. The general incompatibility between natural fibers and polymer matrix must be overcome with the methods of promoting adhesion. Chemical or physical modifications of the

natural fiber and addition of compatibilizers are the most widely used methods to promote adhesion of polymer matrix and natural fiber [14].

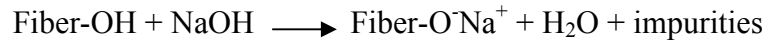
### **2.3.1 Modification of Natural fibers**

There are two main disadvantages of natural fiber reinforcements (i) poor compatibility with the matrix polymer and (ii) their relative high moisture absorption. Thus, modifications are applied to change the fiber surface properties to increase their adhesion with the polymer matrix through surface roughness of the fiber and reducing the moisture absorption of the natural fiber [16,22]. Surface treatment methods are basically divided into two groups; physical methods and chemical methods. The physical methods are Corona treatment and plasma treatment. The chemical methods are alkaline, silane, acetylation, benzoylation, peroxide, sodium chloride, stearic acid and isocyanate treatments and maleated coupling.

### **2.3.2 Alkaline Treatment**

Alkaline treatment or mercerization is one of the widely used methods to change the cellulosic molecular structure of the natural fibers. The orientation of the highly packed crystalline structure of the cellulose is modified with alkaline treatment. This method also provides easy penetration of chemicals through the fiber. In amorphous region, cellulose micromolecules are very far away from each other and water molecules fill those spaces. Alkali sensitive hydroxyl (OH) groups present inside the fiber ionize to alkoxide (fiber-O-Na) with the addition of sodium hydroxide (NaOH). As a result, the amount of hydrophilic hydroxyl groups and the moisture absorption property of the fiber decrease. The chemical reaction of the alkaline treatment is shown in Scheme 2.2.





**Scheme 2. 2** The chemical reaction of fiber cell with NaOH

This treatment takes out a certain amount of hemicelluloses, lignin, pectin, wax and oils covering the surface of the fiber (Fig. 2.8) [23-25]. Consequently, the surface of the fiber becomes clean, more uniform and rough owing to disappearance of the microvoids, therefore; the ultimate cells can transfer stress better and have better mechanical interlocking. Moreover, alkaline treatment decreases fiber diameter and this rises the aspect ratio (length/diameter). As a result, the effective fiber surface area for adhesion with the matrix increases [16].

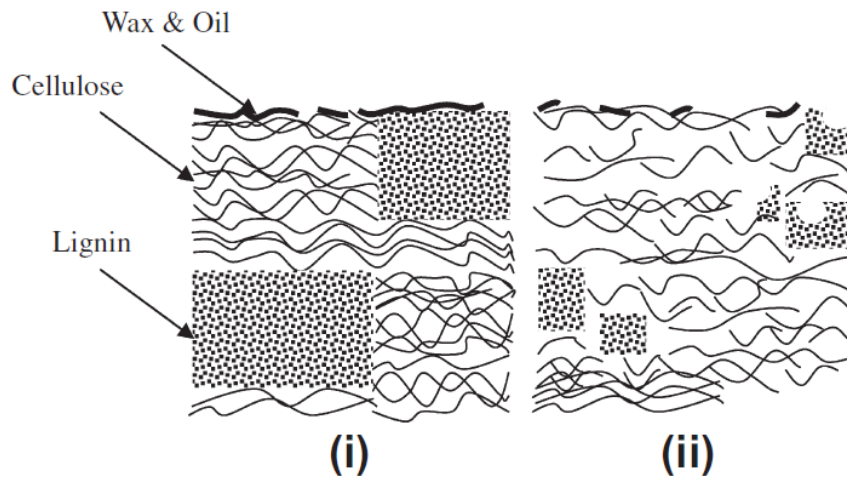


**Figure 2. 8** Typical structure of (i) pristine (ii) alkaline treated cellulose fiber [16]

Figure 2.8 represents the schematic view of pristine and alkaline treated cellulose fiber. NaOH treated fiber has less wax and oil covering materials and the crystalline order of the cellulose is broken down.

### **2.3.3 Use of Compatibilizers**

Most thermoplastics are nonpolar ('hydrophobic') which are not compatible with polar natural fibers. Thus, poor adhesion between the natural fiber and the polymer occurs. To strengthen the adhesion and provide affinity between the fibers and the matrix, coupling or compatibilizing agents have been introduced into the mixture [19]. The coupling agents can be polymers having grafted functional groups onto the polymer chain. The coupling mainly occurs via covalent bonds, secondary bonding (hydrogen bonding and van der Waals forces), polymer entanglement and mechanical interlocking [26]. Silanes and titanates based coupling agents, maleic anhydride functionalized polymers are mostly used compatibilizers to enhance the adhesion [27,28].

### **2.4 Wood Plastic Composites**

Wood plastic composites are the composites that contain wood fibers and a thermoplastic or thermoset matrix. The most widely used thermoplastics for WPC are PP, PE and PVC. They are popular in building, furniture, automotive and construction industry [31]. In addition, epoxy and phenolic resins are the most common used thermosets with wood and bakelite is one of the first examples for wood flour-thermoset composites.

WPC has become popular over the last decade because it has beneficial properties and advantages for the manufacturers such as: relative strength and stiffness, low maintenance, low cost relative to similar materials and the fact that it is a natural source [32]. These composites are manufactured with extrusion process to get structural building products such as profiles, decking and window trims having better thermal and creep performance in comparison with unfilled plastics [33]. However, their physical and mechanical properties must be improved to be popular in the wood composite industry. The ways to improve the properties of WPCs are choosing right

dimensions of the raw material, optimum mixture of the components and adding adequate amount of coupling agents, pigments or antimicrobials during their manufacture [34-36].

### **2.5 Mechanical Properties of Natural Fiber Composites**

The properties of natural fiber composites change according to parameters such as fiber aspect ratio, volume fraction of the fibers, stress transfer at the interface, fiber-matrix adhesion and orientation. Mechanical properties of the natural fiber composites are the most widely studied topic. They are examined as a function of fiber content, effect of different treatments of fibers and the use of coupling agents [44-48].

Both fiber and the matrix properties are significant to have better mechanical properties of the composites. Low stress density, a strong interface and fiber orientation determine the tensile strength. However, fiber wetting in the matrix, high fiber aspect ratio and amount of fiber is necessary to improve tensile modulus. The aspect ratio determines the fracture properties of the composites. In the composites which are reinforced with short fibers, there is a critical fiber length that is needed to develop its full stressed state in the polymer matrix. If the fiber length is shorter than critical value failure occurs owing to debonding at the interface at lower stress. On the other hand, when the fiber length is greater than the critical length, the composite behave stronger under applied load [7]. To have good impact strength, an optimum bonding degree is required. The level of adhesion, fiber pullout and energy absorption mechanism are the factors that can affect the impact strength of the short-fiber-reinforced composite [45].

### **2.6 Definition of Flame Retardant Polymeric Materials**

Flame retardant, flame resistant, fire resistant and fire retardant terms have nearly the same meaning and they can be replaced with each other. When a textile or polymeric

material expose to any igniter and the material does not keep on burning or glowing once the source of ignition has been removed, though there are some modifications in the chemical and physical properties, the material can be defined as a flame retardant material. A perfect fire retardant polymeric material must have special properties;

- i. resistant to ignition and flame propagation
- ii. burns and generates smoke at a low rate
- iii. has low combustibility and toxicity of combustion gases
- iv. has suitable appearance and properties for the specific usage
- v. little or no economic penalty [49-51].

The rise in the utilization of plastic materials in our daily lives in so many areas as films, fibers, coatings and foams, increases the need for flame retardant materials in recent years. Moreover, the need for flame retardant polymeric materials was increased with the regulations enforced by European countries [12].

## **2.7 General Description of Polymer Combustion**

Combustion is a fast and auto-accelerating exothermal redox process that can be spread in the environment with the formation of a flame and luminosity. Natural and synthetic polymers constitute most of our environment in our daily lives. The combustion of polymeric material is comprised of physical and chemical processes which consist of conversion of initial products. This entire transformation process can be divided into stages according to the physical and chemical processes occurring in each stage [52]. Polymer flammability involves four different stages i. heating of flammable sample (pre-heating), ii. degradation and decomposition, iii. ignition of flammable gases evolved, iv. combustion and propagation. The different stages of polymer flammability are demonstrated in Figure 2.9 [53].

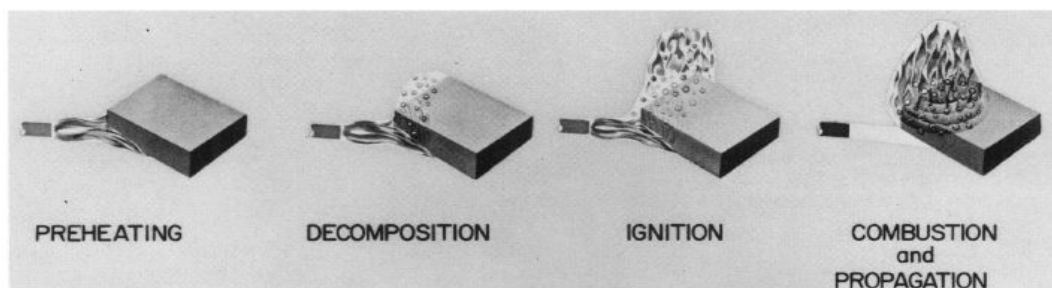


**Figure 2. 9** Four individual stages of polymer flammability [53]

The first stage preheating includes heating of the material with the help of an external source and it increases the temperature of the sample at a rate dependent on the thermal intensity of the ignition source. It also includes thermal conductivity of the material, latent heat of fusion and vaporization of the material and specific heat of the material. When the material is heated enough, the weakest bonds start to break firstly and this causes degradation and lost of its original properties. Combustion products may be formed in a gaseous state and their formation mostly depends on the intensity of external heat source, temperature needed for decomposition and the rate of decomposition. Gaseous products can be ignited and combustion begins with the influence of ignition source. Ignitability depends upon the rate of the temperature rise at the surface that reaches to the ignition temperature. When the heat evolved is greater than the heat spent during combustion, combustion propagates even if the heat source vanishes [53,54].

## **2.8 Strategies for Obtaining Flame Retardant Polymers**

The information about the flame retardation of a polymeric material is based on

- i. chemical and physical properties of the polymer
- ii. stages of the polymer degradation
- iii. combustion of the polymer and its dependence on the nature of the degradation products

- iv. chemical and physical properties of the flame-retardant materials and their interaction with the polymeric substances [51].

In order to choose the right flame retardant strategy to get the flame retardant polymeric substance, degradation mechanism of the polymer should be identified. There are four general mechanisms for the thermal decomposition of polymers which are random chain scission, end chain scission, chain stripping and crosslinking [55].

### **2.8.1 General Concepts to Obtain Flame Retardancy in Polymers**

There are three kinds of methods to obtain a flame retardant polymeric material or a textile. During polymerization, a flame retardant co-monomer which provides inherent flame retardancy for the synthesized polymer is used. This is termed as 'reactive approach'. In 'additive approach' the additives which generate flame retardant property, are added into polymer melt during mixing. In 'surface approach', surface modification is applied to get flame retardant polymeric material. Surface approach is widely used for producing flame retardant textiles [12]. In this study both additive and surface approaches were used. The schematic representation of general flame retardancy approaches is shown in Figure 2.10.

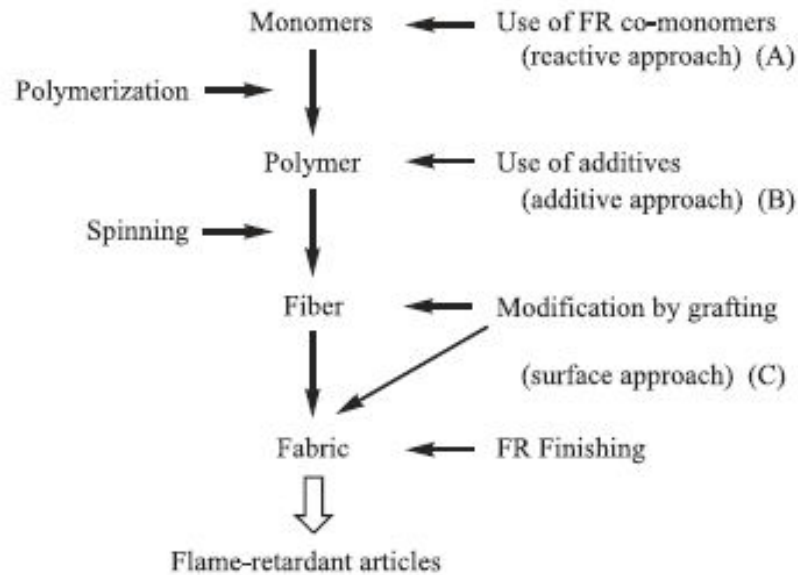


**Figure 2. 10** Schematic representation of general flame retardancy approaches [57]

### 2.8.1.1 Additive approach

Additive flame retardant materials are combined with the polymer either before, during or more frequently after polymerization. They are used especially in thermoplastics. They perform as plasticizers if they are compatible with the polymer, otherwise they can be regarded as fillers. They are occasionally volatile and tend to bleed so their flame retardancy may be slowly lost. The improvement of high molecular weight products creates polymers to be generated permanently fire retardant by the additive method. Additive type flame retardants are mostly incorporated by compounding and are effective in different types of polymer systems [52].

### 2.8.1.2 Surface Approach

Surface modification is another method to obtain flame retardant material. It is widely applied to the fibers or textiles. In this method flame retardant material is coated and covalently linked onto the surface of the textile/fiber [57]. Indeed, it has lots of advantages:

- i. It does not change the inherent properties of the materials such as mechanical properties.
- ii. It is an easy process and can be applied onto lots of materials such as polymers, textiles and wood.
- iii. During inflammation the protective action is occurred at the surface [43].

## **2.9 Flame Retardant Additives**

There are so many flame retardant additives with a range of 150-200 different commercially available compounds that have been improved for polymers. Flame retardants can be classified as additive or reactive materials. Additive flame retardants are combined with the polymer during production, but do not react with the polymer. Reactive compounds are produced with a resin during polymerization to become integrated into the network structure of the polymer [58]. Flame retardant additives can be divided into groups of halogen, phosphorus, nitrogen, silicon, boron containing flame retardants and miscellaneous inorganic additives [52,58]. Phosphorus containing flame retardants were used in this study. Accordingly, information is given only about these flame retardants in the following parts.

### **2.9.1 General Mechanism of Flame Retardant Additives**

Flame retardant additives differ from each other in terms of their chemical structure and general modes of action. All flame retardants perform chemically and/or physically in the condensed phase and/or in the gas phase by retarding at least one of the stages of burning process [59,60]. An effective flame retardant additive affects more than one of these stages physically or chemically. The presence of flame retardant materials provides the result of retardation and elimination of burning process mechanism [54].

Gas phase active flame retardants perform through cleaning free radicals that cause branching of radical chain reactions inside the flame. This can be termed as the



chemical action mechanism in the gas phase. For the physical action mechanism in the gas phase, large amounts of noncombustible gases are produced that dilute combustible gases, decompose endothermically and reduce the temperature by absorbing heat [55,60].

Flame retardant additives act in two different modes of action in the condensed phase mechanism. In the first mode of action, flame retardants speed up the degradation of polymer and this increases the dripping of the polymer. Increasing the dripping behavior of the polymer removes the fuel source from the combustion zone. In the second mode of action, flame retardants form a layer of carbon (charring) on the material surface [60]. The formed intumescent char performs as a physical barrier to decrease the mass (fuel and oxygen) and heat transfer between the gas and the condensed phases so it protects the underlying material from flame. Flame retarding effect of the intumescent system can be determined according to the amount and the properties (stability, integrity and foam structure) of the char. The main advantage of this system is the reduction in the heat produced during the combustion as a result of the formation of carbon layer rather than CO and CO<sub>2</sub> [61-64]. The general mechanisms of flame retardant additives are given in Figure 2.11.

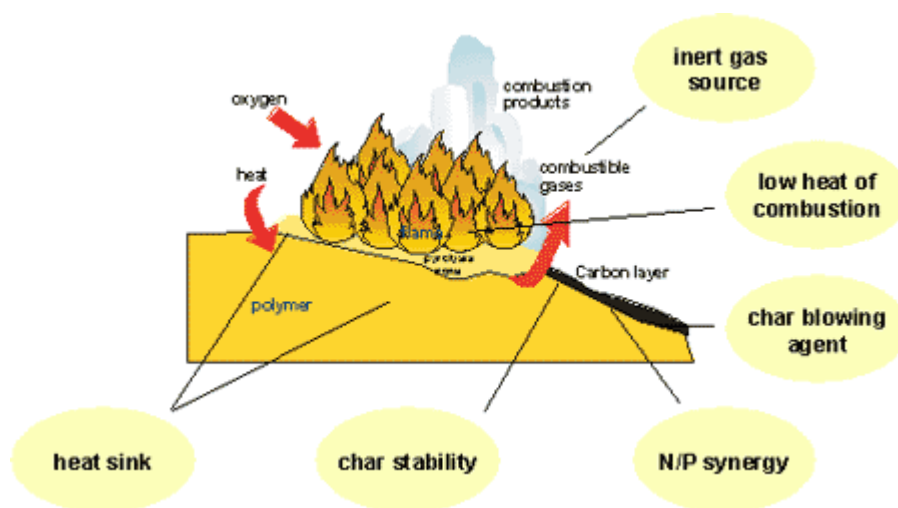


**Figure 2. 11** General mechanisms of flame retardant additives [65]

When the stages of burning process is examined one by one, in the first stage a glassy layer is formed due to the presence of an effective flame retardant. This layer has poor thermal conductivity and/or high reflectivity which permits repelling radiant heat from the heat source before decomposition of the material. Materials that swell on heating to create an intumescent layer are the examples of flame retardant additives forming a surface coating with low thermal conductivity [54,60].

The flame retardant material can chemically change the thermo-oxidative decomposition of the substrate during the degradation and decomposition stages proceed in the burning process. Lower concentration of combustible gases is required in this process. This can be provided by promoting char formation, hydrogenation or dehydration [54].

In the ignition part of the burning process, there are number of ways of retarding the burning process. Essentially, any kind of mechanism that supports decrease in the production of combustible gases or increase in the concentration of noncombustible decomposition gases will provide inhibition of the burning process at the ignition

stage. In addition to these ways the flame retardant additive may also form free radical terminating species by its own degradation or interaction with the substrate. These gaseous inhibitors decelerate the flame as a result of their interaction with the highly energetic chain-propagating species, such as OH radicals. A flame retardant additive may also form a very dense gas that behaves like a blanket on the surface of the flammable substrate and keep out oxygen needed for the ignition [54].

Even after the ignition process has started, combustion and the propagation of burning may be inhibited by reducing the heat transfer at the surface of the burning material. This can be accomplished with the formation of particulate matter in the pre-flame zone. These smoke particles create a surface that has less radiative thermal energy in the flame zone [54].

### **2.9.2 Synergism and Antagonism of Flame Retardant Additives**

Synergism means an effect greater than the summation of individual effects. Antagonism is a phenomenon wherein two or more flame retardants in combination have an overall influence less than the addition of their individual influence. The researches made on flame retardancy usually focused on creating synergy using different flame retarding agents. Nanoparticles (clay, polyhedral oligomeric silsesquioxanes, and carbon nanotubes), metal oxides and boron compounds are mixed with traditional flame retardants for providing synergistic effect. When a synergy is established among different flame retardants, less amount of flame retardant can be consumed to get same flame retardant effect [50,66]. There are several synergisms found among different flame retardants such as nitrogen-halogen, nitrogen-phosphorous, boron-phosphorous, silicon-phosphorous [50].

## **2.10 Types of Flame Retardant Additives**

Flame retardant additives are generally classified according to their content that is most probably named from an element. The types of flame retardant additives are listed below:

- Halogen containing flame retardants
- Phosphorous containing flame retardants
- Nitrogen containing flame retardants
- Boron containing flame retardants
- Silicon containing flame retardants
- Inorganic flame retardants

In this study only phosphorous containing flame retardant additive is used. That is why the information is given only about this kind of additive.

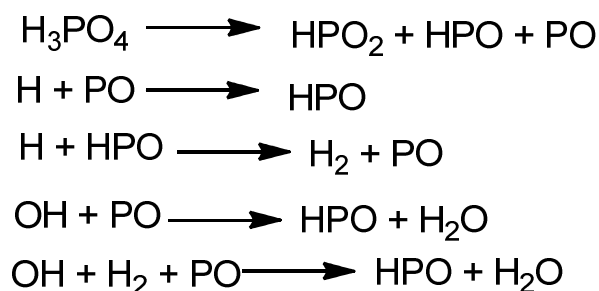
### **2.10.1 Phosphorous containing flame retardants**

Phosphorus containing flame retardants are known as the second popular flame retardant additives for thermoplastics, thermosets, textile, coating and paper [50,55]. Phosphorus is present in both organic and inorganic substances which have flame retardant properties [60]. Phosphorus has several oxidation states and this provides a variety of phosphorus containing flame retardants. Phosphine oxides, phosphonium compounds, phosphines, phosphonates, phosphites, elemental red phosphorus and phosphates are all used as flame retardants [59].

The flame retardant mechanisms of phosphorus containing flame retardants change according to the chemical structure of the polymer and the type of the phosphorus containing compound. They can perform more effectively in oxygen or nitrogen containing polymers [55]. Moreover, they can function both in the condensed and gas phases [50] but mostly in the condensed phase [59,66,67].

The flame retarding effect of the phosphorus compounds in the condensed phase can be described as the following: (1) they may change the direction of the chemical reaction involved in decomposition, produce carbon rather than CO or CO<sub>2</sub>. This results in promotion of char formation. (2) Phosphoric acid and its derivatives perform as a heat sink because they retard the oxidation of CO to CO<sub>2</sub>. This reduces the heating process. (3) The acids form a liquid or thin glassy protective layer on the condensed phase. Thus, this layer inhibits the oxygen diffusion and mass and heat transfer between gas phase and the condensed phase. This protective barrier disrupts the oxidation of carbon at the carbon monoxide stage and this decreases the exothermic heat of combustion. (4) They decrease the melt viscosity of the material to form a melt drip mode of flame quenching [52,66,67].

The flame retarding effect of phosphorus compounds in the gas phase is explained as the following; (1) They form reactive phosphorus containing small molecules such as PO•, P•, PO<sub>2</sub>•, HPO•, HPO<sub>2</sub>• which can react with the free radicals that drive combustion [60]. Volatile phosphorus compounds are the most effective inhibitors of combustion [55]. The proposed radical trap theory is shown in Scheme 2.3. (2) They can dilute the combustible pyrolysates with less combustible vapor [66].



**Scheme 2. 3** The proposed radical trap theory of phosphorus compounds [50]

In this study, red phosphorus, ammonium polyphosphate, ammonium dihydrogenphosphate and guanidine dihydrogen phosphate compounds are used as flame retardants. The detailed information will be given about these additives.

### 2.10.1.1 Red Phosphorus

Red phosphorus (P-red) is one of the allotropes of phosphorus having an amorphous, complex three dimensional inorganic polymeric structure. The chemical structure of P-red is illustrated in Figure 2.12.

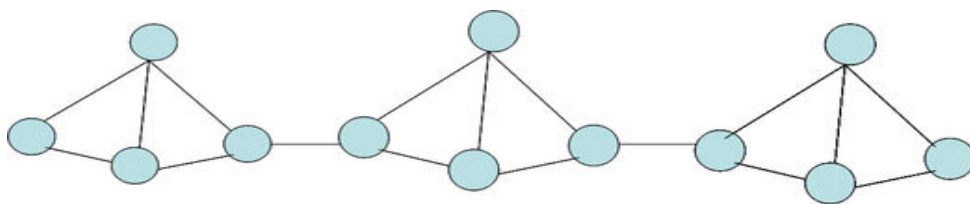


**Figure 2. 12** Chemical structure of Red Phosphorus [68]

P-red is a highly effective flame retardant especially for nitrogen and/or oxygen containing polymer since it has a high content of phosphorus. It has a weak flame retarding effect in polystyrene and polyolefins. P-red shows its flame retardancy effect at a concentration ranging from 2-15 wt% depending on the polymer [50,55]. The Table 2.2 illustrates the amounts of P-red needed for V0 rating for UL-94 testing for different polymers [50].

**Table 2. 2** The concentration of P-red required for V0 rating for UL-94 testing for different polymers [50].

<b>POLYMER</b>	<b>% wt</b>
Polystyrene	15
Polyethylene	10
Polyamide	7
Filled phenolic	3
Polycarbonate	1
Polyethylene terephthalate	3

There are some advantages and disadvantages of P-red. The advantages are high phosphorus content, good flame retardant properties at lower amounts and low cost [69,70]. Nevertheless, P-red has some disadvantages involving thermal instability (produces highly toxic phosphine gas), high water absorption and reddish brown color that restricts the commercial applications [50,55,67,69,71,72]. In order to decrease the disadvantages of P-red, surface treatments involving inorganic or polymeric coating or microencapsulation are needed. Different kinds of resins such as epoxy, urea-formaldehyde, phenol-formaldehyde and melamine formaldehyde are widely used for the encapsulation of P-red [50,67,69,71-73].

The flame retardant mechanism of P-red is not well understood. The mechanism is considered to be through the formation of phosphoric acid, though some proofs also propose free radical scavenging. P-red demonstrates its flame retarding action in gas phase in LDPE. It increases the LOI values of the material, produces char on the surface thus preventing the material from oxygen attack [74].

#### **2.10.1.2 Ammonium Polyphosphate**

APP is an inorganic salt of polyphosphoric acid and ammonia. It is widely used as flame retardant in polymers, especially with polyolefins. It is also used in textile materials to get flame retardant textiles [75,76]. APP has two crystal types; crystal

phases I and II. Phase I is identified by a variable chain length, having lower decomposition temperature and higher water solubility than phase II. Phase II has a crosslinked and branched structure and is more preferable than phase I for flame retardancy. The structure of APP is shown in Figure 2.13. APP has a condensed phase mechanism with the formation of intumescent char. To describe the flame retardant mechanism of APP, intumescent system and the formation of char by APP is explained in detailed.

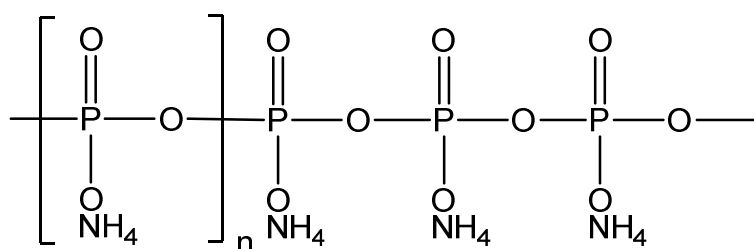


**Figure 2. 13** The molecular structure of APP [77]

In intumescent system there is a protection of underlying material with the generation of thick, thermally stable, highly porous char layer [58]. This layer performs as a physical barrier to decrease the heat and mass (oxygen, fuel) transfer between the gas and the condensed phases. So it provides protection of the polymer material from the influence of flame. The properties (stability, foam structure and integrity) and the amount of the char specify the flame retardant influence of the intumescent system. The main benefit of this system is the reduction of heat produced during combustion due to the generation of carbon rather than CO and CO<sub>2</sub> [61-64]. The flame retardant effect of intumescent char is represented in Figure 2.14.



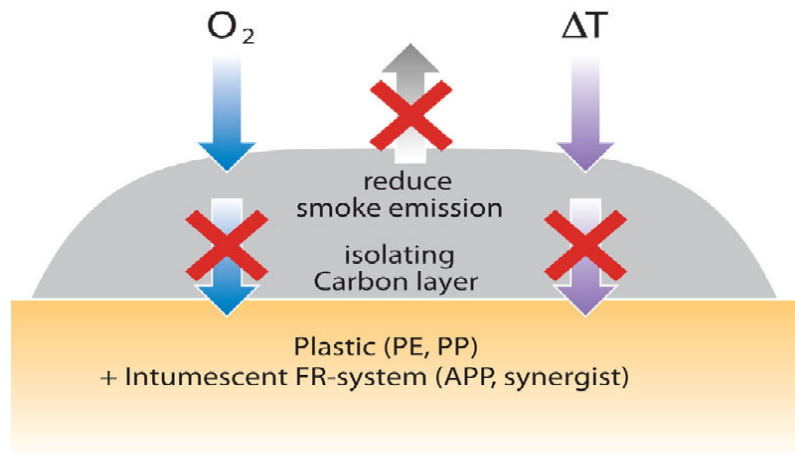


**Figure 2. 14** The flame retardant effect of intumescent char [12]

An intumescent system is mainly constitutes 3 parts which are a char forming agent (carbonific), an acid source and a blowing agent (spumific). Intumescent char is generated by a series of decomposition reactions and physical processes of the component of the system [58,78]. The order of intumescent reaction processes is illustrated in Figure 2.15.

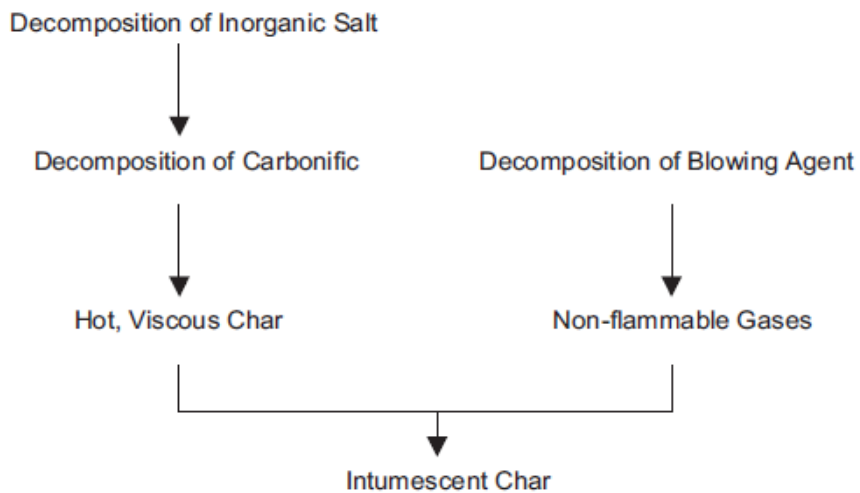


**Figure 2. 15** The order of intumescent reaction processes [58]

When APP is used for the flame retardant additive, it performs as a blowing agent and acid source during combustion. APP produces polyphosphoric acid, phosphoric acid, orthophosphates, ammonia and water as result of thermal degradation [61-63,78-81]. Thermal degradation of APP is shown in Figure 2.16.

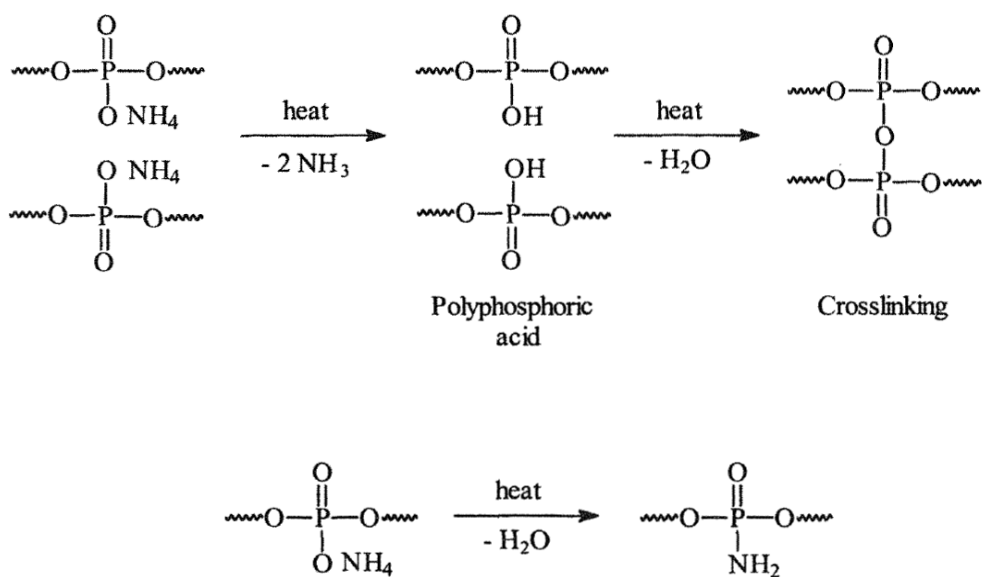


**Figure 2. 16** The schematic representation of thermal degradation of APP [50].

Phosphoric acid, polyphosphoric acid and orthophosphates are the acid source for the esterification reaction with the carbonizing agent. Ammonia and water perform as the blowing agent. Barrier effect of the intumescent char can be increased by using different blowing agents with APP. Urea, melamine, dicyandiamide, and polyamides are the most widely used blowing agents [78-81]. Dextrin, mannitol, starch, pentaerythritol (PER), sorbitol and char forming polymers can be the carbonizing agent in intumescent systems.

### 2.10.1.3 Ammonium dihydrogen phosphate

Ammonium dihydrogen phosphate, or monoammonium phosphate, ( $\text{NH}_4\text{H}_2\text{PO}_4$ ), is prepared with the addition of phosphoric acid in ammonia until the solution becomes distinctly acidic. It is mostly used in blending of agricultural fertilizers [82]. In addition, this material is termed as ABC Dry Chemical, tri-class or multi-purpose dry chemical which is a dry chemical extinguishing agent used on fires [83]. The extinguisher spray disperses finely powdered ADP, which coats the fuel and rapidly smothers the flame. The chemical structure of ADP is illustrated in Figure 2.17.

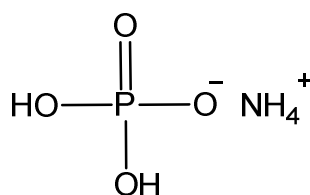


**Figure 2. 17** The chemical structure of ammonium dihydrogen phosphate

### 2.10.1.4 Guanidine dihydrogen phosphate

Guanidine was first isolated in 1861 as a degradation product of guanine. Even though free guanidine or guanidine salts are present in nature in trace amount, many guanidine derivatives are significant constituents of living organisms. Guanidine and its derivatives are mostly used in building blocks in the synthesis of pharmaceutical and agricultural chemicals, in production of textile and plastics and in biochemistry [84]. GDP is a derivative of guanidine compounds and the chemical structure of it is shown in Figure 2.18.

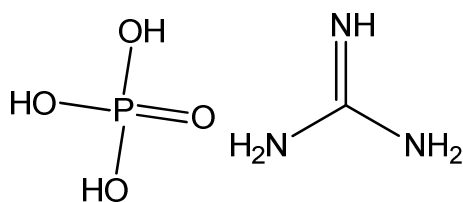


**Figure 2. 18** The chemical structure of guanidine dihydrogen phosphate

GDP is also named as guanidine phosphate monobasic, guanidinium phosphate or guanidine phosphate. It is generally used as flame retarding agent for cellulosic products like wood, textiles, paper and laminates. The decomposition of it occurs above 300 °C forming noncombustible gases and polymetaphosphates [84].

### **2.11 Thermal Behavior of LDPE**

LDPE is easily flammable and burns readily in air with a hot and clean flame. It melts and the molten polymer drips or flows without any char residue. The flammable nature of LDPE arises from long-chain saturated hydrocarbon structure that results in excellent physical, chemical and electrical properties. It yields low-molecular weight volatile saturated and unsaturated fragments that are very flammable [54].

### **2.12 Thermal Behavior of PLA**

PLA is flammable, burns readily and produces less visible smoke than other non-flame retardant materials so visibility hazards in a fire are decreased. Moreover, the peak energy release rate of burning PLA is 60% less than that of PET. So, especially when it is combined with other flame retardant materials, PLA fires can spread less to neighboring articles.

### **2.13 Characterization Methods**

#### **2.13.1 Characterization of Mechanical and Morphological Properties**

Different kinds of test methods are used for the determination of mechanical and morphological properties of the composites. In this study, Scanning Electron Microscopy, Tensile Tests, Impact Tests and Dynamic Mechanical Analysis are used for the composite material characterization. Fourier Transform Infrared Analysis is also used to prove the applied treatments on wood are successful.

### 2.13.1.1 Scanning Electron Microscopy

SEM is a kind of electron microscope that scans the sample with a focused beam of electrons and produces images of it. The interaction of the electrons from the instrument with the atoms in the sample produces signals that provide information about the surface topography and the composition of the sample. The electron beam is usually scanned in a raster scan pattern, and the image is produced with the combination of detected signal and beam [85].

The surface of the material to be scanned may or may not be polished or etched, but it has to be electrically conductive. Thus, it must be made conductive by applying a very thin metallic surface coating before the measurement. 10 to in excess of 50000 diameters of magnification range are possible [85].

### 2.13.1.2 Tensile Test

ASTM D 638 test method is used for the characterization of tensile properties of the polymeric material with a specified dog-bone shaped sample. The sample is clamped from the two ends and pulled apart at a constant rate of elongation until the specimen fails. The initial length of central section included the narrow part of the dog-bone is named as gauge length,  $L_0$ . Force is determined as a function of elongation during deformation. The tensile response graph is generally drawn as engineering stress  $\sigma$ , vs. engineering strain  $\epsilon$ ,

$$\sigma = F/A_0 \quad (2.1)$$

$$\epsilon = \Delta L/L_0 \quad (2.2)$$

where  $A_0$  is the initial (undeformed) cross-sectional area of the gauge region and  $\Delta L$  is the change in sample gauge length ( $L-L_0$ ) due to the deformation [86]. Figure 2.19 shows the stress-strain curve over the entire strain range for a typical polymeric material [89].

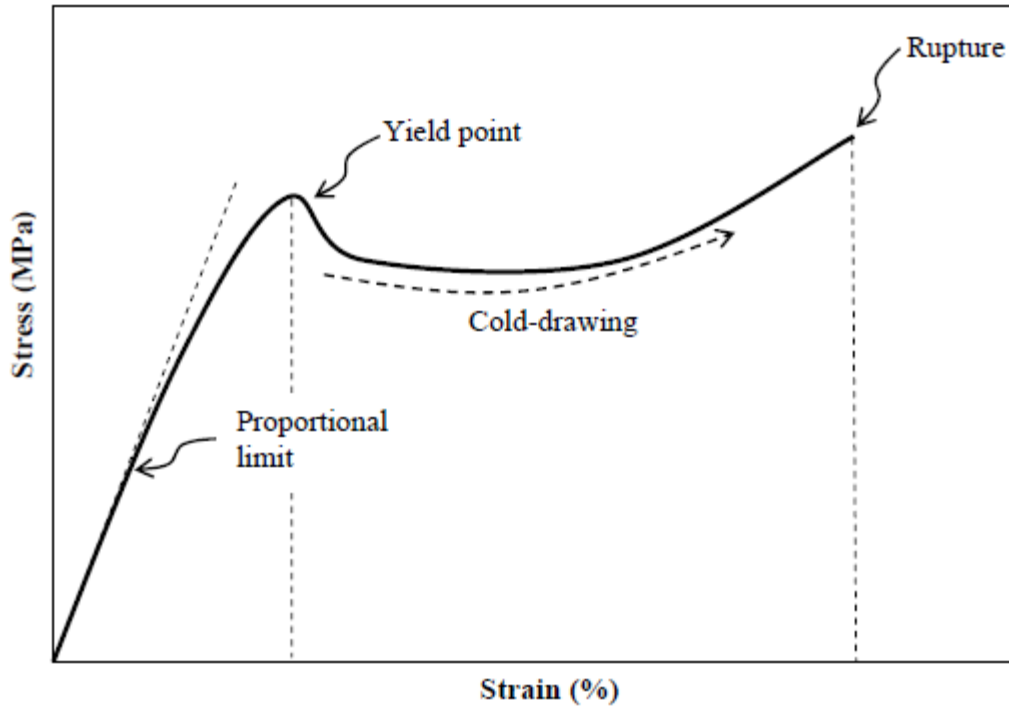


**Figure 2. 19** Stress-strain curve for a typical polymeric material [87].

Tensile strength,  $\sigma_m$  (Eq. 2.1) is the maximum tensile stress that the specimen sustains during the tensile test. Tensile strength at yield is observed when the maximum stress takes place at the yield point. If the maximum stress happens at break, it is defined as tensile strength at break [89].

Tensile strain,  $\epsilon$  is the proportion of the elongation to the gauge length of the specimen, in other words the change in length of the specimen per unit of initial length (Eq. 2.2).

Modulus of elasticity,  $E$  is the ratio of stress to strain below proportional limit and it is the measure of the stiffness of the elastic material. It is also named as elastic modulus or Young's modulus or tensile modulus and expressed in force per unit area (Eq. 2.3) [88].

$$E = \sigma/\varepsilon \quad (2.3)$$

### **2.13.1.3 Impact Test**

Impact test measures the energy absorbed for the fracture when the specimen exposed a rapid stress. This energy is the measure of the material's toughness. Izod and Charpy tests (ASTM D256-92) are the most common impact tests for the determination of the impact strength of a polymeric material [90]. In both Izod and Charpy tests, a pendulum known weight strikes the specimen and the energy-to-break is measured from the loss in the kinetic energy of the pendulum [91]. Falling ball or dart test are the other types of impact tests used for the determination of impact strength [89].

### **2.13.1.4 Dynamic Mechanical Analysis**

Polymeric materials may be sustained to variable stress at a slightly high frequency. To study the response of these materials to such variable stress dynamic mechanical analysis is used. In DMA, low load is applied to the sample in a sinusoidal style. The stress and strain must be completely in phase for a perfectly elastic material since stress is directly proportional to strain. For the perfectly viscous fluid, the strain lags behind the stress with a phase angle of  $90^\circ$ . For a polymeric material, the response is the combination of elastic and viscous responses. That is to say, they both have elasticity and viscous flow properties and the strain lags behind the stress by a phase angle. Therefore, polymeric materials are termed as viscoelastic. The characteristic response of stress and strain with time for a polymeric substance is demonstrated in Figure 2.20.

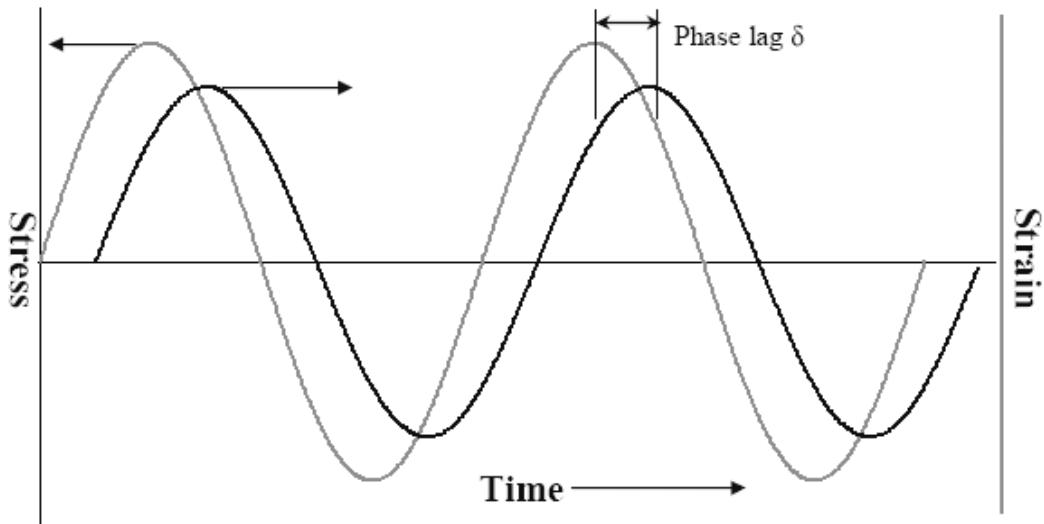


**Figure 2.20** Response of stress and strain with time for a characteristic polycrystalline polymer above  $T_g$

As it is seen in Figure 2.20 the strain lags behind the stress by an angle,  $\delta$ , ranging from  $0^\circ$  and  $90^\circ$ . Lagging of the strain behind the stress is defined as damping process [92]. The strain and stress formulas are expressed as follows:

$$\varepsilon = \varepsilon_0 \sin(\omega t) \quad (2.4)$$

$$\sigma = \sigma_0 \sin(\omega t + \delta) = \sigma_0 \sin \omega t \cdot \cos \delta + \sigma_0 \cos \omega t \cdot \sin \delta \quad (2.5)$$

In these equations  $\omega$  is frequency and  $t$  is time. Equation 2.5 shows that stress has two components:

- $\sigma_0 \cos \delta$  component is in-phase with the strain and it is called as storage component of stress (elastic component). The corresponding modulus is the storage modulus,  $E'$ .
- $\sigma_0 \sin \delta$  component is  $90^\circ$  out of phase with the strain is the loss component of the stress. The corresponding modulus is the loss modulus,  $E''$ .



In terms of the moduli, the stress can be written as

$$\sigma = \varepsilon_0 E' \sin \omega t + \varepsilon_0 E'' \cos \omega t \quad (2.6)$$

As a result of these the phase angle is  $\delta$ .  $\tan \delta = E''/E'$  which is the dissipated energy during the loading/unloading cycle and this provides a direct result of the damping effect in the material. This discussion reveals that a perfect elastic material's  $\tan \delta$  is zero whereas a perfect viscous material's  $\tan \delta$  is infinite. Therefore, in DMA elastic modulus ( $E'$ ) and loss modulus ( $E''$ ) of a material are determined by studying in sine wave. These moduli provides to find the ability of the material to store ( $E'$ ) or lose ( $E''$ ) energy and the damping property from the proportion of loss and storage moduli ( $\tan \delta$ ). Furthermore,  $T_g$  of the material is found from the peak point of  $\tan \delta$  vs. temperature plot [93].

#### **2.14.2 Characterization of Flame Retardancy Properties of the Composites**

Different kinds of test methods are used for the flame retardancy properties of the composites. Underwriters Laboratory UL-94 Test, Limiting Oxygen Index (LOI), TGA-FTIR and Cone Calorimeter are used for the flame retardancy properties of the composite materials.

##### **2.14.2.1 UL-94**

UL-94 test is the most widely used, easy and practical method for the determination of the ignitability and the flame spread property of polymeric materials exposed to a small flame at vertical position. The schematic view of the UL-94 test design is illustrated in Figure 2.21 [94].

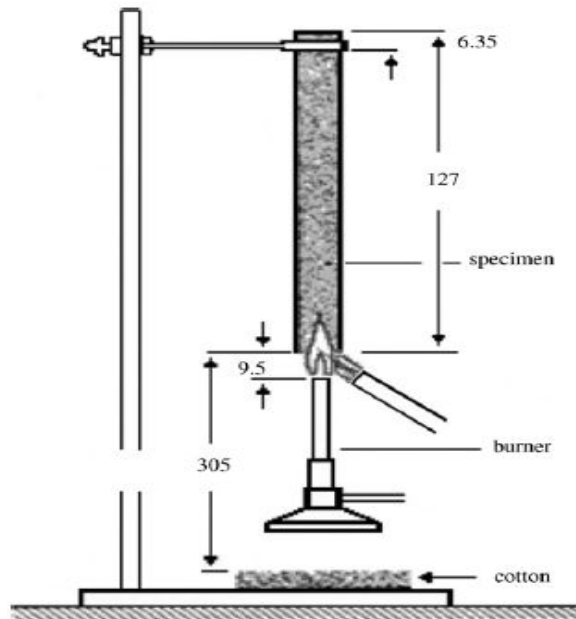


**Figure 2. 21** The Schematic view of UL-94 test design [94]

The specimen is exposed to the flame from the bottom part and the top of the burner is placed at 10 mm from the bottom edge of the specimen. The flame is applied for 10 seconds and taken off. The flame time  $t_1$  (the time passed for the flame to extinct) is recorded. After extinguishing, the flame is applied again for 10 seconds. The flame time  $t_2$  is recorded in addition with the afterglow time  $t_3$  (time passed for the fire glow to vanish). A piece of cotton is placed under the sample and if a burning piece of sample falls down, it causes ignition of the cotton during the test. This information must also be noted. In the view of these data, the flammability of the material is categorized in to three parts (V0, V1, V2) according to its performance regarding the individual time of burning for every specimen, total burning time for all samples and the presence or absence of burning drips [94-96]. Criteria for UL-94 classification are demonstrated in Table 2.4 [94,96].

**Table 2. 3** Criteria for UL-94 classifications

	<b>V0</b>	<b>V1</b>	<b>V2</b>
t <sub>1</sub>	<10	<30	<30
t <sub>2</sub>	<10	<30	<30
t <sub>1</sub> + t <sub>2</sub> (for five samples)	<50	<250	<250
t <sub>2</sub> +t <sub>3</sub>	<30	<60	<60
Cotton ignited by burning drips	No	No	Yes
Afterglow or afterflame up to the holding clamp	No	No	No

#### **2.14.2.2 Limiting Oxygen Index**

LOI is used for the quantification of the flammability of polymers. LOI test was standardized as NF T 51-071, ASTM D 2863, ISO 4589 [94-96]. The schematic view of LOI test is demonstrated in Figure 2.22 [95]. Oxygen/nitrogen gas mixture is provided from the bottom of the tube. The proportion of oxygen and nitrogen is altered during the test to find the oxygen concentration that will sustain the combustion of the material for at least 3 minutes or the combustion of 50 mm of the specimen. The calculation of the LOI value is done with this formula:  $[O_2 / (O_2 + N_2)] * 100$ . Since the air contains 21% oxygen, materials having LOI value lower than 21 are classified as combustible and materials having LOI value higher than 21 are classified as self-extinguishing. Higher LOI value means better flame retardancy [94-96]. LOI is a widely used method, however it has some insufficiencies; i. The test condition does not reflect to real full size fires, ii. For the definition of oxygen index of a material, downward flame spread for a distance of 50 mm is used which has a trivial importance in real fires, iii. LOI test is performed at oxygen percentage generally above the normal oxygen content of air that occurs rarely in most fires [58].

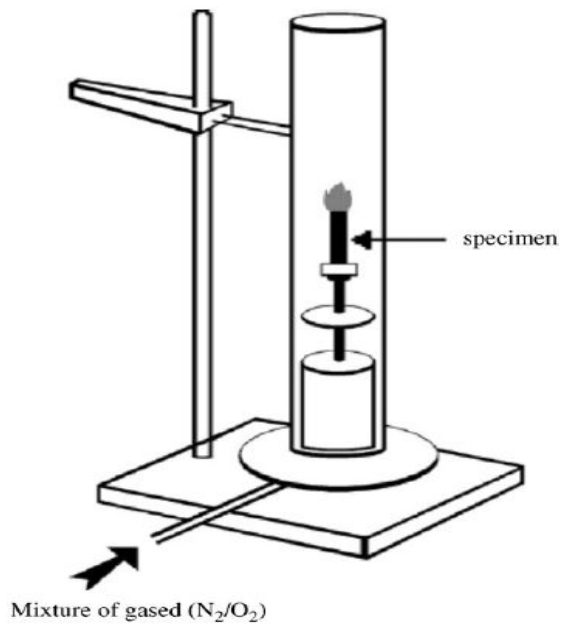


**Figure 2. 22** The schematic view of LOI test design [95]

### 2.14.2.3 Cone Calorimeter

Cone calorimeter has conical shape heater for the heating of specimen during the test and its name comes from this conical shape heater. Cone calorimeter can provide information about large number of fire reaction properties in a single test with a small sample and the burning medium during the test reflect the real fire conditions well. Because of these reasons cone calorimeter test become popular among the scientists. It is standardized as ASTM E 1354 ( in the United State ) and ISO 5660 ( International Standard ) [58].

Cone calorimeter works with a principle of exposing the sample to an incident heat flux by a heater. The schematic representation of cone calorimeter is illustrated in Figure 2.23 [95]. The material begins to decompose and flammable gases evolve from the specimen with the effect of heat. An electric spark ignites these evolved

gases and these gases pass through the heating cone. They are captured by an exhaust duct system with centrifugal fan and hood. Gas flow and oxygen concentration measurements are used to determine the fire properties of samples. Cone calorimeter gives information about Heat Release Rate (HRR), Time to Ignition (TTI), the peak Heat Release Rate (PHRR), Total Heat Release (THR), Mass Loss Rate (MLR), Time of Combustion (TOF), mass loss quantities of CO and CO<sub>2</sub> and total smoke released values of the materials [58,95-98].

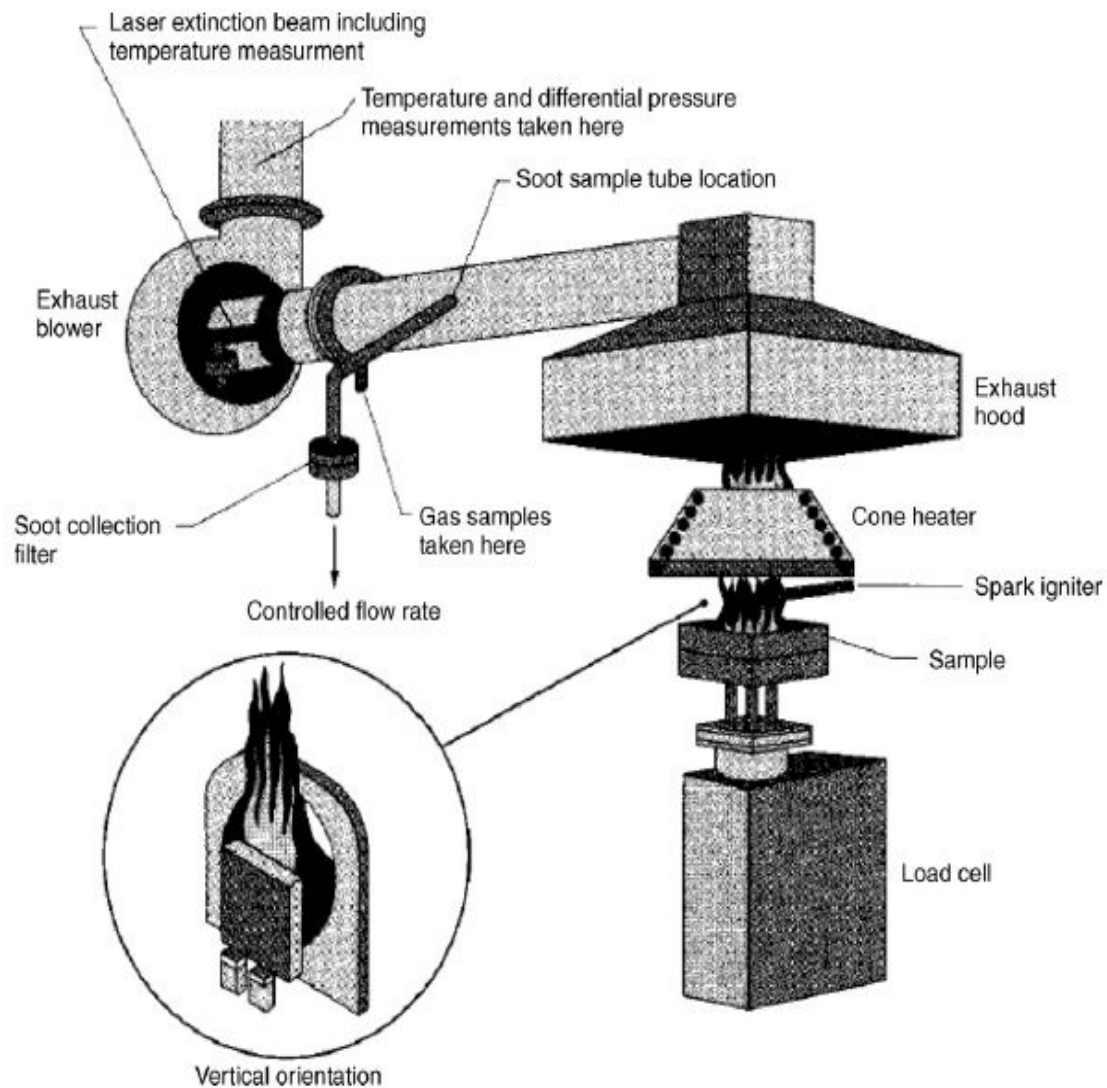


**Figure 2. 23** Schematic representation of cone calorimeter [95]

In cone calorimeter test heat flux range is  $10-100 \text{ kWm}^{-2}$ . The values of  $35$  and  $50 \text{ kWm}^{-2}$  heat fluxes which correspond to heat flux values found in developing fires are the most widely used values in the tests. The sample can be positioned either horizontally or vertically. Tests are generally carried out in the horizontal direction because convective component of heat transfer is almost trivial. The position of the

sample is 2.5 cm below the heater in horizontal direction. Sample dimensions should be 10 x 10 cm<sup>2</sup> with varying thickness up to 50 mm. The thickness of the sample is very important since the results are strongly dependent on it. Thin sample exhibits lower TTI and higher PHRR values than the same sample having higher thickness [58,95-98].

Different polymers and polymer composites showing different kinds of burning behavior give different kinds of HRR vs. time curve. The shape of this curve also reveals information about the burning characteristics of polymer and polymer composites. Some examples of HRR vs. time curves are illustrated in Figure 2.24 [98].

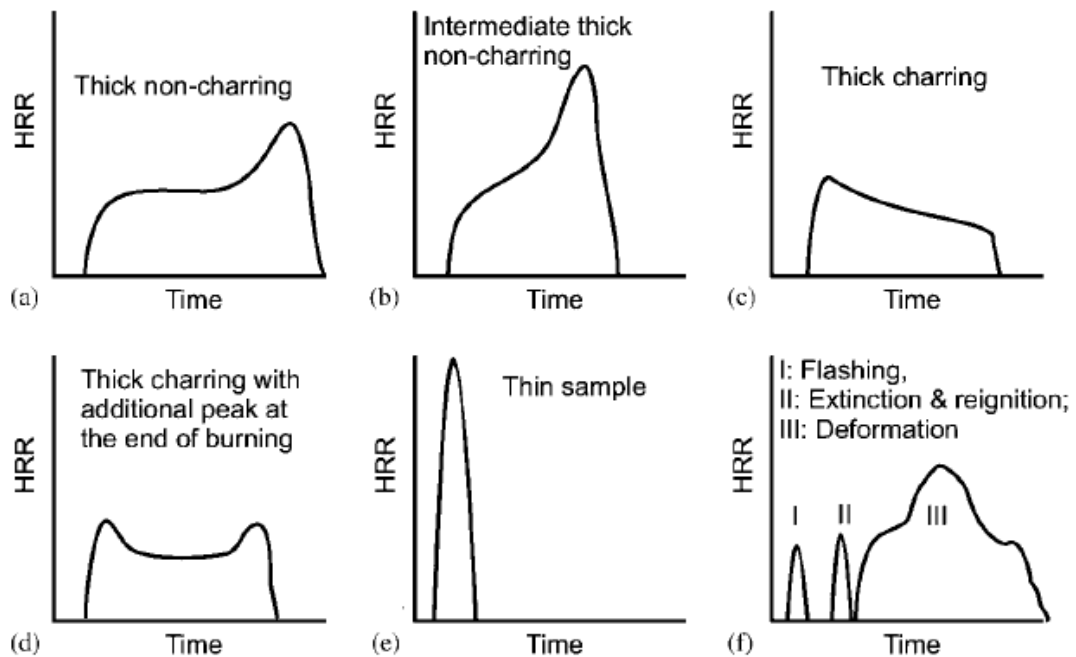


**Figure 2. 24** Characteristic HRR curves for various typical burning behaviors [98]

## **2.15 Production Methods of Polymer Composites**

In this thesis, the additives are mixed with the polymer by twin screw extruder for the manufacture of polymer composites. Composite pellets obtained after extrusion is injection molded and compression molded in order to get desired shape for tensile tests or flammability tests.

### **2.15.1 Extrusion**

Extrusion is the most widely used method in plastic industry for melting the polymer and mixing it with the other ingredients of a composite such as colorants, fillers and other types of additives. In spite of thermoplastics are the mostly extruded plastics, there are also some thermosets (especially rubbers) that can be extruded. As a result of extrusion process, plastics are produced in different shapes such as fibers coating on wire, pipes, cables, sheets and long thin rods that are cut into pellets [100,101].

Polymer pellets or granules and other ingredients of the composite are fed in the hopper part of the extrusion machine during the process. The materials coming from the hopper go through a hole at the top of the screw. The screw pulls the plastic forward until it leaves from a hole at the end of the extruder barrel named as die. Screw also melts the plastic both with external heat and heat evolved from the friction of polymers. The molten plastic is shaped by the die, instantaneously cooled to become solid; therefore it retains its shape [100,101].

### **2.15.2 Compression Molding**

Compression molding is the most common technique for molding the polymeric materials. In compression molding, firstly the material to be molded is usually preheated in a heated, open mold cavity. Then, the mold is closed and pressure is applied to be contacted with all mold areas. Heat and pressure are kept up until the



molding process is over. Finally, after applying pressure is completed, the molding material is waited to be cooled and the cooled material is removed from the mold. In this study, the samples used for flame retardancy studies are prepared with compression molding.

### **2.15.3 Injection Molding**

Injection molding is a process for manufacturing parts by injecting molten material into a mold. There are several kinds of materials used for injection molding, generally thermoplastics and thermoset polymers. The material to be injected is fed into a preheated barrel, mixed, pushed into a mold cavity with a high pressure and then the material is cooled, hardened and taken the shape of the mold. In this study the samples (dog- bone shaped) of tensile tests were produced with laboratory scale injection molding [102].



## CHAPTER 3

### EXPERIMENTAL

Experimental part of the thesis is comprised of four parts. In the first and second parts, the materials and the preparation procedure of the LDPE-WF and PLA-WF composites for the mechanical studies are explained. Preparation procedure and the materials of the LDPE-WF and PLA-jute fabric composites for the flame retardancy studies are mentioned in the third and fourth part. Alkaline treatment is applied to all WF used in this thesis. In few parts alkaline treatment is not applied and it is explained where it is necessary.

#### 3.1 Alkaline Treatment

The purpose of alkaline treatment is to dissolve partially alkali soluble components from the WF structure like resins, hemicelluloses, lignin and pectin [23-25]. It is thought that surface cleaning and activation is achieved via NaOH (aq) treatment. SEM images of pristine WF and alkaline treated WF are shown in Figure 3.1. As it is seen in SEM images, alkaline treated surface becomes more rough and this provides more interaction between WF and the compatibilizer. WF was treated with 18 wt % solution of NaOH for 45 minutes under continuous mixing. The volume of the solution was equivalent to 5 times the volume of WF. WF was then washed with water until all NaOH was eliminated. A few drops of acetic acid were added to neutralize the last rinsing solution. The WF was air-dried at 60 °C for 52 hours. After the drying process, WF was stored in a desiccator until the extrusion process.

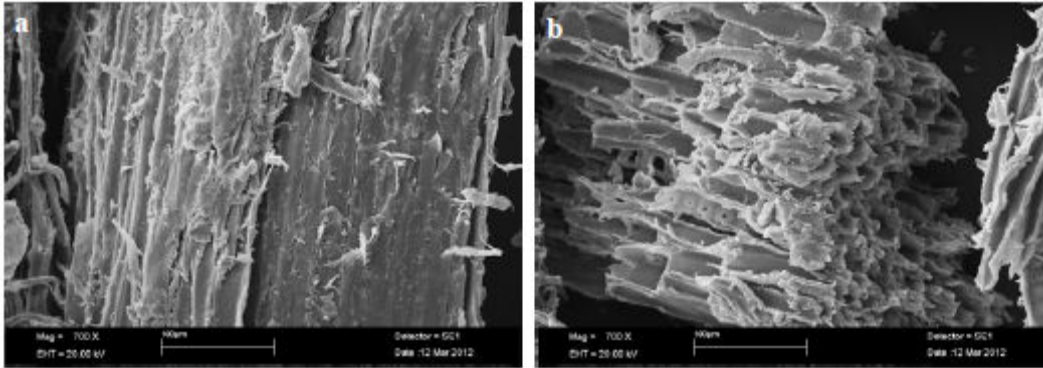


**Figure 3. 1** SEM images of a) pristine WF b) aWF at a magnification of  $\times 200$  [5]

### 3.2 Production of LDPE-WF Composites

For the production of WF-LDPE composites two different compatibilizers were used. 12 different compositions were prepared with compatibilizers; LOTADER® 2210, a random terpolymer of ethylene, acrylic ester and MA and LOTADER® AX 8900, a random terpolymer of ethylene, acrylic ester and GMA. The chemical structures and the properties of compatibilizers are given in Table 3.1 and Figure 3.2. 8 of them were prepared with direct mixing the ingredients by the use of extruder and 4 of them were firstly preimpregnated with the compatibilizer and then mixed with LDPE in the extruder. ATR-FTIR was used to assign peaks to the compatibilizers involved at the surfaces of the fillers before and after surface treatment. The composites were immersed into liquid nitrogen and broken. The morphology of freeze-fractured surfaces of composites was examined by SEM. Tensile tests and impact tests were applied to obtain mechanical properties of the samples. Water absorption values of the samples were also obtained.

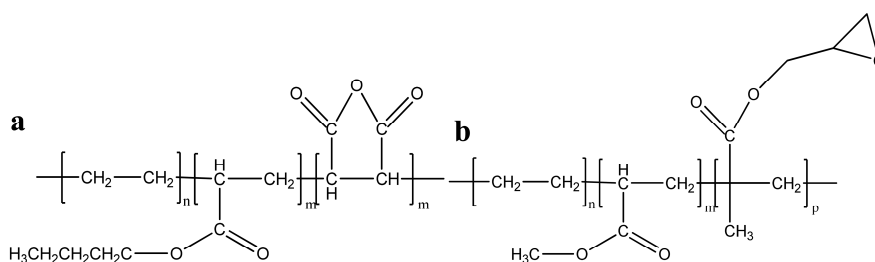


**Figure 3. 2** The chemical structures of compatibilizers a) LOTADER ® 2210 b) LOTADER ® AX 8900

**Table 3. 1** Properties of coupling agents used

Coupling Agent	Density (g/cm <sup>3</sup> )	Melt Index <sup>a</sup> (g/10 min)	Tm <sup>b</sup> (°C)	Composition wt%
LOTADER® 2210	0.94	3	107	Butyl Acrylate (6) Maleic Anhydride (2.8) Ethylene (91.2)
LOTADER®AX 8900	0.94	6	65	Methyl Acrylate ( 24) Glycidyl Methacrylate (8) Ethylene (68)

**a:** Measured at 190 °C under 2.16 kg load **b:** Melting Temperature

### 3.2.1 Materials

The main materials used in this study were LDPE, WF and two kinds of functionalized terpolymers. LDPE was obtained from PETKIM A.S. (Turkey) under the trade name LDPE F2-12. The density was 0.92 g/cm<sup>3</sup> and the melt flow index was 2-3.5 g/10 min (2.16 kg, 190 °C) as provided by the supplier. WF from pine (20-mesh size) was obtained from local sources. LOTADER® 2210, and LOTADER® AX 8900, were purchased from ARKEMA (France). Sodium hydroxide (NaOH), chloroform and toluene, all reagent grades were supplied by Sigma Aldrich.

### **3.2.2 Pre-impregnation with compatibilizer solution**

The WF was pre-impregnated with both compatibilizer solutions. The pre-determined amount of GMA-comp was dissolved in chloroform at 50 °C. After the complete dissolution of compatibilizer, the pre-determined amount of WF was added and mixed vigorously for 30 minutes. After mixing, chloroform was evaporated at 50 °C for 48 hours. The amount of GMA-comp in solution was adjusted to the 1, 3 and 5 wt % of WF. Wt % of WF was 30% in each composition. In addition to those compositions 40% and 50% WF was also prepared and the amount of GMA-comp was 3% of WF. The pre-determined amount of MA-comp which corresponded to 10 wt % of WF was dissolved in toluene at 110 °C. After the complete dissolution, WF was added and mixed vigorously for 30 minutes. After mixing, toluene was evaporated at 80 °C for 48 hours.

### **3.2.3 Preparation of LDPE-WF Composites**

The mixing of LDPE, WF and compatibilizers at various composition ratios was carried out with a counter rotating twin screw microextruder (15 ml microcompounder®, DSM Xplore, Netherlands) at 100 rpm at 190 °C for 3 minutes (see Figure 3.3). The extrudate was pelletized and then oven-dried for 48 h at 60 °C and was stored in desiccator for injection molding. The specimens for mechanical tests were molded by a laboratory scale injection-molding machine (Microinjector, Daca Instruments) at a barrel temperature of 190°C and mold temperature of 30°C and were stored in a desiccator (see Figure 3.4). The following procedure was applied for the preparation of composites; all compositions contain the same amount of WF (30 wt %) and the added amount of compatibilizer was removed from the LDPE content. WF and LDPE were also mixed without using compatibilizer as for reference sample. The WF, LDPE and compatibilizers were directly extruded with

different compatibilizer ratio which corresponds to 3, 5, 10, 15 wt % of WF content to determine the optimum compatibilizer to WF ratio. After the mechanical tests of these 9 trials, pre-impregnation ratios were decided.

For MA-comp, pre-impregnation was made at 10 wt % loading of WF. For GMA-comp, pre-impregnation was carried out at loading levels of 1, 3 and 5 wt % of WF.



**Figure 3. 3** The photograph of the twin screw extruder used for the composite production in this study



**Figure 3. 4** The photograph of the laboratory scale injection-molding machine



### **3.2.4 Characterization Methods**

#### **3.2.4.1 FTIR Analysis**

FTIR was used to assign peaks to the compatibilizers involved at the surfaces of the fillers before and after surface treatment. IR absorption spectra of compatibilizers, NaOH treated WF and pre-impregnated WFs were obtained with FTIR (Bruker Optics IFS 66/S series FT-IR spectrometer) at an optical resolution of  $4\text{ cm}^{-1}$  with 32 scans.

#### **3.2.4.2 Scanning Electron Microscopy**

The morphology of freeze- fractured surfaces of composites in liquid nitrogen was examined with SEM (LEO 440 computer controlled digital, 20 kV). All specimens were sputter-coated with gold before examination.

#### **3.2.4.3 Tensile Test**

The specimens were stored in a desiccator for some days before testing. Tensile measurements were performed using Lloyd LR 5K tensile testing machine equipped with 5 kN load cell at room temperature according to ASTM D 638 standard. The photograph of tensile test machine used in this study is shown in Figure 3.5. Tensile measurements were conducted on a sample ( $7.4 \times 2.1 \times 80\text{ mm}^3$ ) at a crosshead speed of 5 mm/min. Tensile strength, percentage elongation at break and modulus values were recorded.



**Figure 3. 5** The photograph of tensile test machine

#### **3.2.4.4 Impact Test**

Notched Izot impact energy was measured with Coesfeld-Material impact tester according to ASTM D256 with notched samples at room temperature. The photograph of impact test machine used in this study is shown in Figure 3.6. All the results represent an average value of five samples with standard deviations.



**Figure 3. 6** The photograph of impact test machine

### 3.2.4.5 Water Uptake

The samples of dimensions (7.4×2.1×80 mm<sup>3</sup>) were used for the measurement of water absorption. The specimens were periodically taken out of the water, wiped with tissue paper to remove surface water, reweighed and immediately put back into water. The pre-dried ( $W_0$ ) was determined and used to calculate the degree of water absorption as the following formula:

$$\text{Water Absorption (\%)} = (W_f - W_0) / W_0 \times 100,$$

where  $W_f$  is the mass of the sample after immersion.

### **3.3 Production of PLA-WF composites**

5 different PLA-WF compositions were prepared. One of them was prepared with WF which had no alkaline treatment. The compositions had different WF ratios and prepared with direct mixing by the use extruder. In one composition WF was preimpregnated with PLA at a ratio of 10 wt % of WF, then mixed with the rest amount of PLA by using extrusion. ATR-FTIR, SEM, Tensile and Impact tests, Dynamic Mechanical analysis and water-uptake measurements were performed for the characterization of the samples.

#### **3.3.1 Materials**

PLA under the trade name 6202D was purchased from Cargill-Dow. The density was 1.24 g/cm<sup>3</sup> (ASTM D792) and the melt flow index was 15-30 g/10 min (2.16 kg, 210 °C) as provided by the supplier. WF from pine (20-mesh size) was obtained from local sources. NaOH and chloroform, all reagent grade were supplied by Sigma Aldrich.

#### **3.3.2 Preimpregnation with PLA solution**

The WF was pre-impregnated with dilute PLA solution. The pre-determined amount of PLA (2.5 g) was dissolved in 200ml chloroform at 50 °C. After the complete dissolution of PLA, the pre-determined amount of WF (25 g) was added and mixed vigorously for 30 minutes. After mixing, chloroform was evaporated at 50 °C for 48 hours.

#### **3.3.3 Mixing of WF-PLA**

The mixing of PLA and WF at various composition ratios was carried out with a counter rotating twin screw microextruder (15 ml microcompounder®, DSM Xplore, Netherlands) at 100 rpm at 190 °C for 3 minutes (see figure 3.3). The extrudate was pelletized and then oven-dried for 48 h at 60 °C and was stored in desiccator for injection molding. The specimens for mechanical tests were molded by a laboratory

scale injection-molding machine (Microinjector, Daga Instruments) at a barrel temperature of 200 °C and mold temperature of 30 °C (see figure 3.4).

### **3.3.4 Characterization Methods**

The characterization methods used were mentioned previously in Sections 3.2.4.1, 3.2.4.2, 3.2.4.4 and 3.2.4.5.

#### **3.3.4.1 Tensile Tests**

The specimens were stored in a desiccator for some days before testing. Tension test measurements were performed using Shimadzu AG-X tensile testing machine equipped with 50 kN load cell at room temperature according to ASTM D 638 standard. Tension tests were conducted on 7.4×2.1×80 mm<sup>3</sup> samples at a crosshead speed of 5 mm/min. Tensile strength, percentage elongation at break and modulus values were recorded.

#### **3.3.4.2 Dynamic Mechanical Analysis**

DMA experiments was carried out using Perkin Elmer DMA 8000 in dual cantilever bending mode at a frequency of 1 Hz to determine elastic moduli and tan  $\delta$  of the composites. The test was carried out in the temperature sweep mode from 18 to 100 °C at a heating rate of 5 °C/min. The sample with dimensions of 50×7.5×2.5 mm<sup>3</sup> was obtained from injection molded tensile bar.

### **3.4 Production of Flame Retardant LDPE-WF Composites**

Flame retardant LDPE-WF composites were produced by two approaches. In the first approach, the flammability of both WF and LDPE were decreased. WF was treated with amino resins together with phosphoric acid solutions. Treated WF was then mixed with LDPE and other ingredients. In the second approach, the flammability of the matrix (LDPE) was reduced with direct mixing of LDPE, WF and the flame retardants in the extruder.

In the first part, four different kinds of reactions were made to obtain flame retardant solutions for WF treatment. The reactants and abbreviations of each reaction are listed below:

- Dicyandiamide-formaldehyde-phosphoric acid (DFP)
- Dicyandiamide-formaldehyde-ammonium dihydrogenphosphate (DFAP)
- Urea- dicyandiamide-formaldehyde-phosphoric acid (UDFP)
- Tetrakis(hydroxymethyl)phosphonium sulfate-urea-ammonium dihydrogenphosphate (THPS)

Certain amounts of WF was treated in each solution and then mixed in an extruder with LDPE and APP. The composites that their WF was treated with DFP, DFAP, UDFP, and THPS solutions, characterized with UL-94, LOI, thermogravimetric analysis (TGA) and cone calorimeter test.

In the second part, two different commercial flame retardants were used. These flame retardant materials were APP and red phosphorous. These materials were used in different combinations and compositions to determine the synergistic effect. To determine the synergistic effect UL-94, LOI and thermogravimetric analysis (TGA) and cone calorimeter tests were performed.

### **3.4.1 Production of LDPE-flame retardant treated WF**

#### **3.4.1.1 Materials**

LDPE was obtained from PETKIM A.S. (Turkey) under the trade name LDPE F2-12. WF from pine (20-mesh size) was obtained from local sources. LDPE and WF properties are present in section 3.2.1. APP was also used as a flame retardant and the properties of it are given in Table 3.2.

**Table 3. 2** The properties of APP

<b>Material</b>	<b>Commercial Name and Supplier</b>	<b>Specifications</b>
Ammonium polyphosphate (APP)	Exolit AP-750, Clariant	Appearance: White free-flowing powder Density: 1.8 g/cm <sup>3</sup> Bulk density: 0.6 g/cm <sup>3</sup> P content: 20-22 %(w/w) N content: 11.5-13.5 %(w/w) Decomp Temp>250°C

#### **3.4.1.2 The Preparation of Dicyandiamide-Formaldehyde-Phosphoric Acid (DFP) Flame Retardant and Treatment of WF**

4.05 g (0.05 mol) of 37 % formaldehyde solution (F) was taken to round bottom flask and adjusted its pH to 8-8.5 with NaOH solution and heated in an oil bath. 4.2 g (0.05 mol) dicyandiamide (D) was added to the mixture and stirred with a magnetic stirrer until dissolved. The mixture was refluxed for 10 minutes and then the heating was stopped and the reaction was allowed to cool to room temperature. Finally, 5.75 g (0.05 mol) 85% phosphoric acid (P) solution was added slowly to the cooled mixture [103].

The product was diluted with 15 ml of water and 10 g of WF was added to the solution. The suspension was stirred with a magnetic stirrer for 30 minutes at room temperature. The mixture was filtered and WF was heat treated at 160°C for 10 minutes. After heat treatment, WF was washed with water, filtrated and dried. At the end 11.64 g of WF was obtained. WF was impregnated with 1.64 g (16.4%) flame retardant product.

#### **3.4.1.3 The Preparation of Dicyandiamide-Formaldehyde-Ammonium Dihydrogenphosphate (DFAP) Flame Retardant and Treatment of WF**

4.05 g (0.05 mol) of 37 % formaldehyde solution (F) was taken to round bottom flask and adjusted its pH to 8-8.5 with NaOH solution and heated in an oil bath. 4.2 g (0.05 mol) dicyandiamide (D) was added to the mixture and stirred with a magnetic stirrer until dissolved. The mixture was refluxed for 10 minutes and then the heating was stopped and the reaction was allowed to cool to room temperature. Finally, 5.75 g (0.05 mol) ammonium dihydrogenphosphate was added to the cooled mixture [103].

The product was diluted with 15 ml of water and 10 g of WF was added to the solution. The suspension was stirred with a magnetic stirrer for 30 minutes at room temperature. The mixture was filtered and WF was heat treated at 160°C for 10 minutes. After heat treatment, WF was washed with water, filtrated and dried. At the end 13.26 g of WF was obtained. WF was impregnated with 3.26 g (32.6%) flame retardant product.

#### **3.4.1.4 The Preparation of Urea-Dicyandiamide-Formaldehyde-Phosphoric Acid (UDFP) Flame Retardant and Treatment of WF**

8.1 g (0.1 mol) of 37 % formaldehyde solution (F) was taken to round bottom flask and adjusted its pH to 8-8.5 with NaOH solution and heated in an oil bath. 2.1 g (0.0125 mol) dicyandiamide (D) and 1.5 g (0.025 mol) urea (U) were added to the mixture and stirred with a magnetic stirrer until dissolved. The mixture was refluxed for 10 minutes and then the heating was stopped and the reaction was allowed to cool to room temperature. Finally, 5.75 g (0.05 mol) 85% phosphoric acid (P) solution was added slowly to the cooled mixture [103].

The product was diluted with 15 ml of water and 10 g of WF was added to the solution. The suspension was stirred with a magnetic stirrer for 30 minutes at room

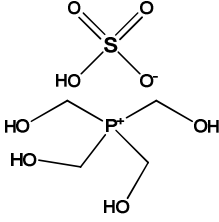


temperature. The mixture was filtered and WF was heat treated at 160°C for 10 minutes. After heat treatment, WF was washed with water, filtrated and dried. At the end 11.40 g of WF was obtained. WF was impregnated with 1.4 g (14.0 %) flame retardant product.

### 3.4.1.5 The Preparation of Tetrakis(hydroxymethyl)phosphonium sulfate-urea-ammonium dihydrogenphosphate (THPS) Flame Retardant and Treatment of WF

The properties of commercial available chemical THPS are given in Table 3.3.

**Table 3. 3** The properties of THPS

Material	Chemical Structure	Commercial Name and Supplier	Specifications
Bis[Tetrakis(hydroxymethyl)phosphonium] sulfate		Bis[tetrakis (hydroxymethyl) phosphonium] sulfate- Sigma Aldrich	Appearance: Clear colorless viscous liquid Density: 1.4 g/ml MW: 406.28 g/mol

7.5 g of THPS solution (75 %) was neutralized with NaOH solution to get a pH value of 6.5. To obtain 22.5% urea solution 5,625 g of urea was dissolved in 25 ml of water. Urea solution was mixed with THPC solution and then the pH was again adjusted to 6.5. After mixing the two solutions 0.375 g of ADP was added to the mixture. The resulting mixture was used for the treatment of WF [104].

10 g of WF was added to the resulting solution. The suspension was stirred with a magnetic stirrer for 30 minutes at room temperature. The mixture was filtered and

WF was heat treated at 160°C for 10 minutes. After heat treatment, WF was washed with water, filtrated and dried. At the end 11.20 g of WF was obtained. WF was impregnated with 1.2 g (12.0 %) flame retardant product.

#### **3.4.1.6 Preparation of LDPE-flame retardant treated WF**

LDPE, WF and the flame retardant materials were mixed in a counter rotating twin screw microextruder (15 ml microcompounder®, DSM Xplore, Netherlands) at 100 rpm at 190 °C for 2.5 minutes (see figure 3.3). The extrudate was chopped into small pellets and then oven-dried for 48 h at 60 °C and was stored in desiccator for compression molding. The samples for thermal or flammability tests were produced by compression molding at 190 °C. A laboratory scale hot-press (Pneumo Hydraulic Press, Ats Faar, Italy) was used (see Figure 3.7).



**Figure 3. 7** The photograph of hot-press used in this work

The following procedure was applied for the preparation of composites; all compositions contained the same amount of LDPE (40 wt %), WF (30 wt %) and flame retardant (30 wt %) and also APP was used in all compositions. After all treatments of WF, the amount of flame retardant material that had been impregnated, was determined. The amount of impregnated flame retardant was subtracted from the total amount of flame retardant (30 wt %) and the rest amount of APP was added to all compositions.

### **3.4.1.7 Characterization Methods**

#### **3.4.1.7.1 UL-94 Test**

UL-94 rating was obtained according to ASTM D3801 where V0 indicates the best flame retardancy and V2 is the worst. The dimensions of bar specimens are  $130 \times 13 \times 3.25 \text{ mm}^3$ .

#### **3.4.1.7.2 LOI**

LOI value was determined by using LOI instrument (Oxygen Index, Fire Testing Technology Limited, England) instrument with test bars of size  $130 \times 6.5 \times 3.25 \text{ mm}^3$ , according to the standard oxygen index test ASTM D2863.

#### **3.4.1.7.3 Cone Calorimeter**

The cone calorimeter test was carried out without replication following the procedures in ISO 13927 using Mass Loss Cone with thermopile attachment (Fire testing Technology, U.K). Square specimens ( $100 \times 100 \times 4 \text{ mm}^3$ ) were irradiated at a heat flux of  $35 \text{ kW/m}^2$ , corresponding to a mild fire scenario.

#### **3.4.1.7.4 Thermogravimetric Analysis (TGA)**

TGA was carried out on Perkin Elmer Pyris 1 TGA & Spectrum 1 FTIR Spectrometer at a heating rate of  $10 \text{ }^\circ\text{C/min}$  up to  $800 \text{ }^\circ\text{C}$  under nitrogen flow of  $50 \text{ ml/min}$ .

### 3.4.2 Direct Mixing of Flame Retardant LDPE-WF Composites

#### 3.4.2.1 Materials

LDPE was obtained from PETKIM A.S. (Turkey) under the trade name LDPE F2-12. WF from pine (20-mesh size) was obtained from local sources. LDPE and WF properties are present in section 3.2.1. APP and P-red were used as flame retardants and the properties of APP are given in Table 3.2 and the properties of P-red are given in Table 3.4

**Table 3. 4** The properties of P-red

<b>Material</b>	<b>Commercial Name and Supplier</b>	<b>Specifications</b>
P-red	Phosphorus (red), Merck	Appearance: Brownish Powder Molecular weight: 30.97 g/mol P content $\geq$ 97% (w/w)

#### 3.4.2.2 Preparation of Flame Retardant LDPE-WF Composites.

LDPE, WF and the flame retardant materials were mixed in a counter rotating twin screw microextruder (15 ml microcompounder®, DSM Xplore, Netherlands) at 100 rpm at 190 °C for 2.5 minutes (see figure 3.3) The extrudate was chopped into small pellets and then oven-dried for 48 h at 60 °C and was stored in desiccator for compression molding. The samples for thermal or flammability tests were produced by compression molding at 190 °C. A laboratory scale hot-press machine (Pneumo Hydraulic Press, Ats Faar, Italy) was used (see Figure 3.5). The following procedure was applied for the preparation of composites; all compositions contain the same amount of WF (30 wt %). WF, LDPE and P-red composition and WF, LDPE and APP combinations were also mixed as for reference sample. The WF, LPPE, P-red

and APP were directly extruded with different P-red ratio which corresponds to 3, 5, 10 wt % of WF.

#### **3.4.2.3 Characterization Methods**

The characterization methods used were mentioned previously in Section 3.4.1.7.

### **3.5 Production of Flame Retardant PLA-Jute Fiber Biocomposites**

One approach was applied to produce flame retardant PLA-jute composites. The properties of ADP and GDP flame retardants are given in Table 3.5. Thermal gravimetric analysis, LOI, vertical UL-94 and cone calorimeter tests were used for the characterization of samples. Char residues remained after cone calorimeter test were investigated by scanning electron microscopy and ATR-FTIR.

#### **3.5.1 Materials**

PLA under the trade name 6202D were purchased from Cargill-Dow (Nebraska, USA). The density was  $1.24 \text{ g/cm}^3$  (ASTM D792) and the melt flow index was 15-30 g/10 min (2.16 kg, 210 °C) as provided by the supplier. Plain woven jute fabric was purchased from Kumascı bilisim ve tekstil hizmetleri (İstanbul, Turkey) and it was originated from Pakistan. Ammonium dihydrogenphosphate (ADP) and guanidine dihydrogen phosphate (GDP) were purchased from Sigma Aldrich.

**Table 3. 5** The properties of ADP and GDP flame retardants

<b>Material</b>	<b>Commercial Name and Supplier</b>	<b>Specifications</b>
Ammonium dihydrogenphosphate (ADP)	Merck	Appearance: White solid crystal Density: 1.8 g/cm <sup>3</sup> Melting point:190°C
Guanidine dihydrogen phosphate (GDP)	Sigma Aldrich	Appearance: White powder Solubility in H <sub>2</sub> O: 0.1 g/ml- clear,colorless Decomp. Temp<300°C

### **3.5.2 Flame Retardant Treatment of Jute Fabric**

10 wt% aqueous solutions of ADP and GDP were prepared for flame retardant applications. Before the flame retardant treatment, jute fabrics were dried at 60 °C for 24 hour. Jute fabrics were treated with the aqueous solution of flame retardants at room temperature for 120 minutes. The treated fabrics were dried at 60 °C for 12 hours. The resulting fabrics contained 25 ± 1 wt% flame retardant.

### **3.5.3 Preparation of PLA-Flame Retardant Treated Jute Fabric Biocomposites**

PLA films used as matrix material were produced by compression molding using laboratory hot press (ATSFAAR, Milano, Italy) at 190 °C. In the production of PLA-jute biocomposites, 5 films and 4 reinforcing material with the dimensions of 40x40 mm were stacked into the stainless steel mould (40x40mm). The composites with a thickness of 3 ± 0.1 mm were produced using same laboratory hot press with the production of films at 190 °C. The resulting composites had a jute fabric content of 50 wt % with respect to PLA. The resulting composites had a flame retardant content of 12±0.5 wt%.

### **3.5.4 Characterization Methods**

The characterization methods used were mentioned previously in Section 3.2.4.1, 3.2.4.2 and 3.4.1.7.





## CHAPTER 4

### RESULTS AND DISCUSSION

In the first part, the studies made on improving the mechanical properties of LDPE-WF and PLA-WF composites are mentioned. In the second part, the studies made on improving the flame retardant properties of LDPE-WF and PLA-jute fabric are mentioned. Initially, the effects of MA and GMA functionalized compatibilizers, on the tensile, impact, morphological and water uptake properties of LDPE-WF composites are discussed. The effect of preimpregnation with compatibilizer solutions is also investigated. Later, the effect of surface treatment and WF ratio on the mechanical, morphological and water uptake properties of PLA-WF composites are investigated.

In the second part, thermal and flammability analysis results of flame retardant LDPE-WF and PLA-jute fabric composites studies are given. Two different approaches are applied for the production of flame retardant LDPE-WF composites. In the first approach, the flame retardant properties of the composites are improved with the reduction of the flammability of both WF and LDPE. In the second approach, only the flammability of matrix is reduced with using flame retardant mixture. Single approach is mentioned for the production of PLA-jute composites. Jute fabric is treated with two different flame retardants, and then combined with PLA to obtain flame retardant PLA-jute biocomposites. The thermal and flammability analysis results of PLA-jute composites are also discussed.

#### **4.1 The Effect of Compatibilizers and the Effect of Preimpregnation with a Compatibilizer Solution on Mechanical, Morphological and Water Uptake Properties of LDPE-WF Composites**

All compositions contained the same amount of WF (30 wt %), and the added amount of compatibilizer was removed from the LDPE content. WF and LDPE were also mixed without using compatibilizer as for reference sample. The WF, LDPE, and compatibilizers were directly extruded with compatibilizer ratios, which corresponded to 3, 5, 10, and 15 wt % of WF content to determine the optimum compatibilizer to WF ratio. After the mechanical tests of these nine trials, preimpregnation ratios were determined. For MA-comp, preimpregnation was performed at 10 wt % loading of WF. For GMA-comp, preimpregnation was carried out at loading levels of 1, 3, and 5 wt % of WF [13].

##### **4.1.1 FTIR Analysis**

The FTIR spectra of compatibilizers and preimpregnated WFs are shown in Figure 4.1. The spectra of both compatibilizers show a pair of very strong absorption bands at 2850 and 2920  $\text{cm}^{-1}$  due to symmetrical and asymmetrical  $\text{CH}_2$  stretching vibrations of ethylene part of compatibilizers [105,106]. The absorption bands at 1460 and 718  $\text{cm}^{-1}$  arise from deformation and skeletal vibrations of  $\text{CH}_2$  group in ethylene part of compatibilizers [105]. MA-comp (LOTADER 2210) shows two distinct peaks at 1730 and 1780  $\text{cm}^{-1}$  that can be attributed to carbonyl groups in the anhydride structure [105,107]. GMA-comp (LOTADER AX 8900) shows a single absorption band at 1730  $\text{cm}^{-1}$  arising from carbonyl group in the ester bond and a broad peak at 1160  $\text{cm}^{-1}$  arising from C-O group in the ester bond and epoxy group that masks each other [108]. The FTIR spectra of WF treated with compatibilizers show two characteristic broad peaks at 3300 and 1025  $\text{cm}^{-1}$  associated with hydroxyl group vibrations and C-O vibrations of cellulose in WF structure, respectively [108]. The presence of compatibilizers adsorbed on WF is confirmed by the peaks at 2850

and  $2920\text{ cm}^{-1}$  arising from the ethylene unit of them in FTIR spectra of WF treated with compatibilizers.

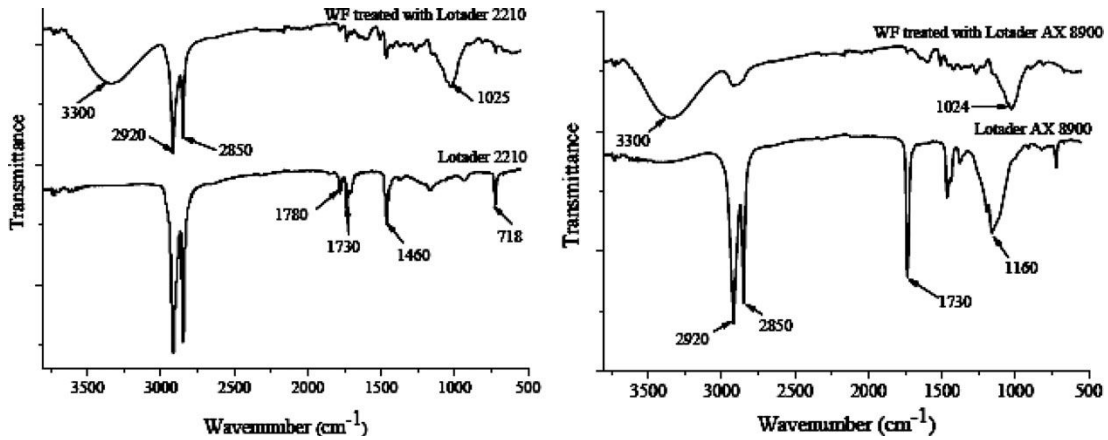


**Figure 4. 1** The FTIR spectra of compatibilizers and preimpregnated WFs

#### 4.1.2 SEM Analysis

The effect of compatibilizer inclusion and preimpregnation on the morphology of the composites is studied by SEM. Representative SEM micrographs of freeze-fractured surfaces of selected composites are shown in Figure 4.2. From SEM image of LDPE–WF (image 1), a wide gap is observed between WF and LDPE at the interface after fracture indicating poor adhesion. However, the addition of MA-comp greatly improves the interfacial adhesion between WF and LDPE (image-2), because the LDPE still covers the WF surface after fracture. This provides qualitative evidence for the existence of adhesive bonds between surfaces in the presence of MA-comp. With the addition of GMA-comp (image-3), LDPE partially adheres on to the WF surface, and small gaps are observed at the interface in accordance with the poor performance of GMA as a compatibilizer. The preimpregnation increases the adhesion between WF and LDPE for both compatibilizers (image 4 and 5), because the matrix material still covers the surface of WF after fracture. It is noticed at the

magnified SEM image of LDPE–WF-pre 10 MA (image-6), LDPE penetrates into the cavities on WF surface that promotes mechanical interlocking. Mechanical properties of corresponding composites also support this conclusion.

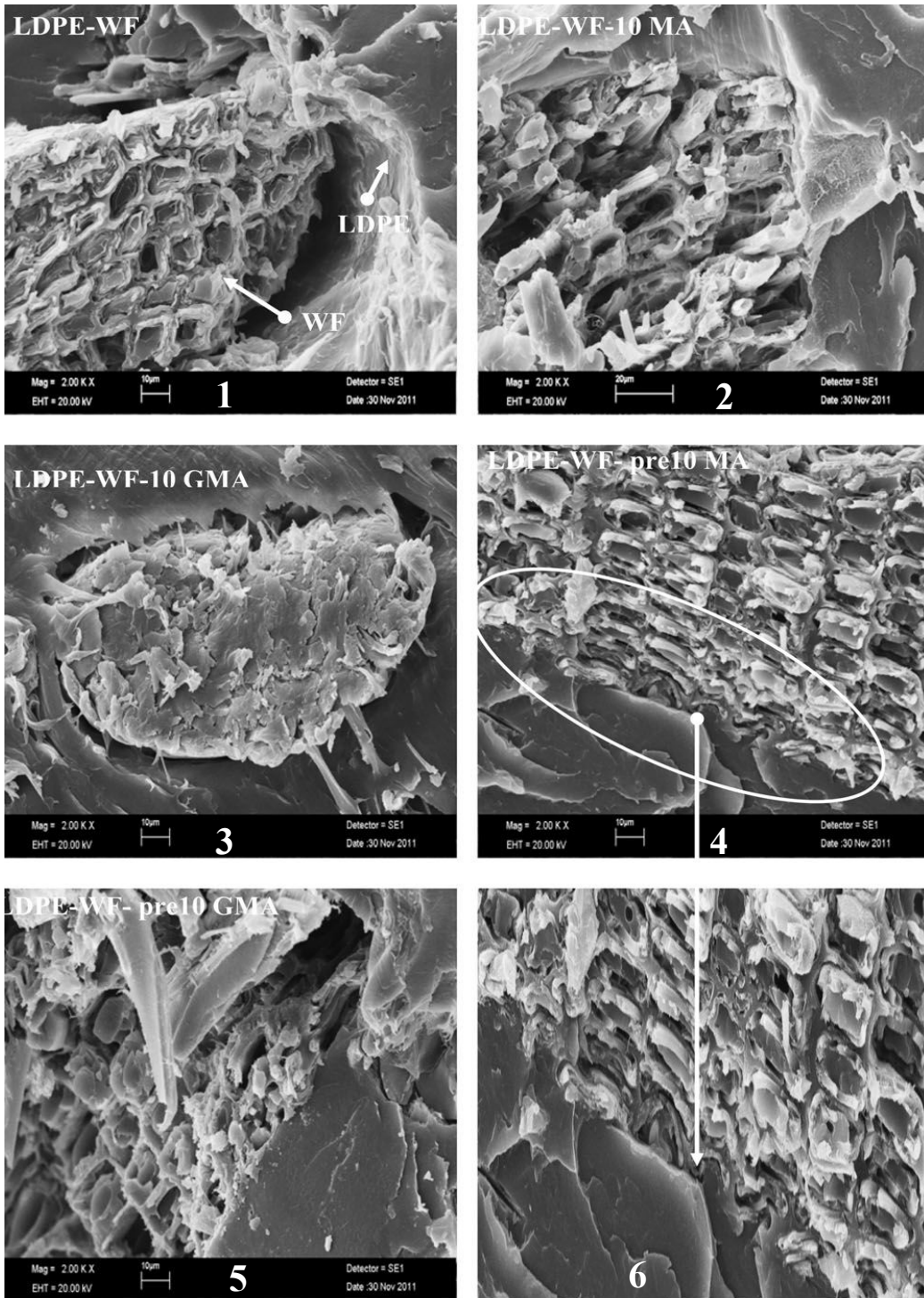


**Figure 4. 2** SEM images of freeze-fractured surfaces of selected composites

In this study, the effect of compatibilizers to WF ratio in extrusion and also the effect of preimpregnation on the mechanical properties of the composites are investigated. The results are given in Table 4.1.

**Table 4. 1** The Mechanical Properties of LDPE-WF Composites

<b>Sample Code</b>	<b>Tensile Strength (MPa)</b>	<b>Percentage Strain at break (%)</b>	<b>Modulus (GPa)</b>	<b>Impact Energy (J/m)</b>
<b>LDPE-WF</b>	11.3±0.2	9.7±1.0	0.38±0.03	40.6±1.6
<b>LDPE-WF- 3 MA</b>	12.1±0.6	10.6±0.9	0.46±0.06	43.0±4.6
<b>LDPE-WF- 5 MA</b>	12.8±0.2	9.5±0.8	0.48±0.05	43.4±3.6
<b>LDPE-WF- 10 MA</b>	13.0±0.3	10.8±0.3	0.68±0.08	47.3±5.3
<b>LDPE-WF- 15 MA</b>	12.6±0.4	12.2±1.5	0.57±0.02	51.3±3.9
<b>LDPE-WF- pre 10 MA*</b>	14.4±0.4	10.8±0.3	0.76±0.07	56.3±8.6
<b>LDPE-WF- 3 GMA</b>	10.1±0.5	11.4±1.8	0.32±0.05	38.5±4.5
<b>LDPE-WF- 5 GMA</b>	10.2±0.6	10.7±0.5	0.34±0.07	41.4±2.1
<b>LDPE-WF-10 GMA</b>	9.6±0.3	10.8±1.0	0.30±0.08	41.7±3.8
<b>LDPE-WF-15 GMA</b>	9.9±0.4	11.6±0.9	0.32±0.04	43.4±7.3
<b>LDPE-WF- pre 1 GMA</b>	11.5±0.2	10.1±0.4	0.38±0.03	41.4±3.2
<b>LDPE-WF- pre 3 GMA</b>	12.2±0.4	10.9±0.9	0.48±0.05	45.4±4.5
<b>LDPE-WF- pre 5 GMA</b>	11.1±0.0	10.8±0.4	0.38±0.04	45.5±4.3

pre represents preimpregnated WF were used, and number shows the compatibilizer WF ratio (wt %)

When compatibilizers are directly used, the MA-comp generally has a positive effect on the maximum tensile strength, impact strength, and modulus values of LDPE–WF composites. No improvement is observed for GMA-comp containing composite samples. The tensile strength and modulus values of composites increase with the increasing amount of MA-comp ratio and reach their maximum level at 10 wt %. It is well known that the usage of maleated coupling agents in WPCs improves the interfacial adhesion between WF and matrix [109-112]. In the case of MA-comp, the interaction between MA part of coupling agent and the WF, and the diffusion of the ethylene part of the coupling agent into LDPE promotes establishment of strong interactions. Further addition of MA-comp (15 wt %) does not improve tensile

strength and modulus values. Excessive use of compatibilizer results in the formation of a weak elastomeric phase that starts to deteriorate the composite's mechanical properties. The preimpregnation ratio is therefore chosen as the optimum value of 10 wt % for the MA compatibilizer. The preimpregnation further increased the tensile strength and modulus values by 27 and 100%, respectively, compared to LDPE-WF due to the better mechanical interlocking that increases the dispersion of WF particles [113,114]. The preimpregnation of GMA-comp is also used to WF at amounts of 1, 3, and 5 wt % of WF. When GMA-comp is used directly without preimpregnation, no improvement in mechanical properties was observed. With GMA-comp at 3 wt % preimpregnated sample some amount of improvement is obtained. As in MA-comp, increased interaction between the matrix and WF is responsible for the observed increase in tensile strength and modulus values. One possible explanation for poor performance of the epoxy functionalized compatibilizer can be polymer bridging.

It is well known in the surface science that the bridging of the particles by multifunctional compatibilizer polymer molecules is possible [115]. Polymer bridging eventually can give rise to flocculation of WF. The poor performance of GMA as a compatibilizer is probably due to the poor dispersion of WF due to bridging and formation of WF flocs.

The impact strength for notched samples is governed by crack propagation of fracture initiated at the predominant stress concentration at the notch tip [116]. The degree of WF dispersion and the interfacial bonding between the WF and matrix are the main parameters determining the amount of absorbed energy during fracture propagation [116-118]. Almost the same trend is observed between impact and tensile test results due to the same factors governing mechanical properties of the composites. The WF agglomeration increases the regions of stress concentration that

require less energy to break [119]. Poor adhesion between WF and matrix results the formation of microvoids that reduce efficient stress transfer from continuous polymer matrix to the dispersed WF and cause the material to absorb less energy [116-119].

All notched samples are completely broken during the test, and the results are listed in Table 4.1. The impact strength increases as the amount of MA-comp increases, and the highest value is obtained at 15 wt % when directly extruded. Although the tensile strength is reduced at 15 wt % loading, the impact strength increases, as the excess amount of MA-comp may increase the toughness of the matrix. The preimpregnation with MA-comp further increased the impact strength of the composite due to better WF dispersion and good adhesion between matrix and WF by mechanical interlocking. The impact strength of the GMA-comp, which is widely used as impact modifier, containing composites with direct extrusion are slightly higher than LDPE–WF. The preimpregnation further increased the impact strength of the composites due to the better WF dispersion and good adhesion between matrix and WF and the maximum impact strengths obtained at concentrations of 3 and 5 wt %.

#### **4.1.4 Water Uptake**

Water uptake in WPCs is mainly related to hydrogen bonding of water molecules to the hydroxyl groups present on wood surface [120-122]. One other effect is the lack of adhesion between the PE and WF that gives rise to capillaries (pores) in the WPC structure. Good adhesion between PE and WF in the presence of compatibilizer reduces number of capillaries and water uptake (suction). Figure 4.3 and Figure 4.4 show the effect of compatibilizer type and ratio on water uptake values of composites. The highest water uptake is obtained in the case where no compatibilizers are used. The addition of compatibilizer regardless of its kind and



ratio reduces the water uptake of composites, and the lowest water uptake value for both compatibilizers is obtained at a concentration of 5 wt % of WF, which seems to be the best composition that optimizes both effects (hydrogen bond and capillary formation). It turns out that due to multitude of effects MA-comp absorbs slightly less amount of water compared to GMA-comp. It may be due to dispersion effect, sizes of capillaries and amount of polymer bridging to count a few.

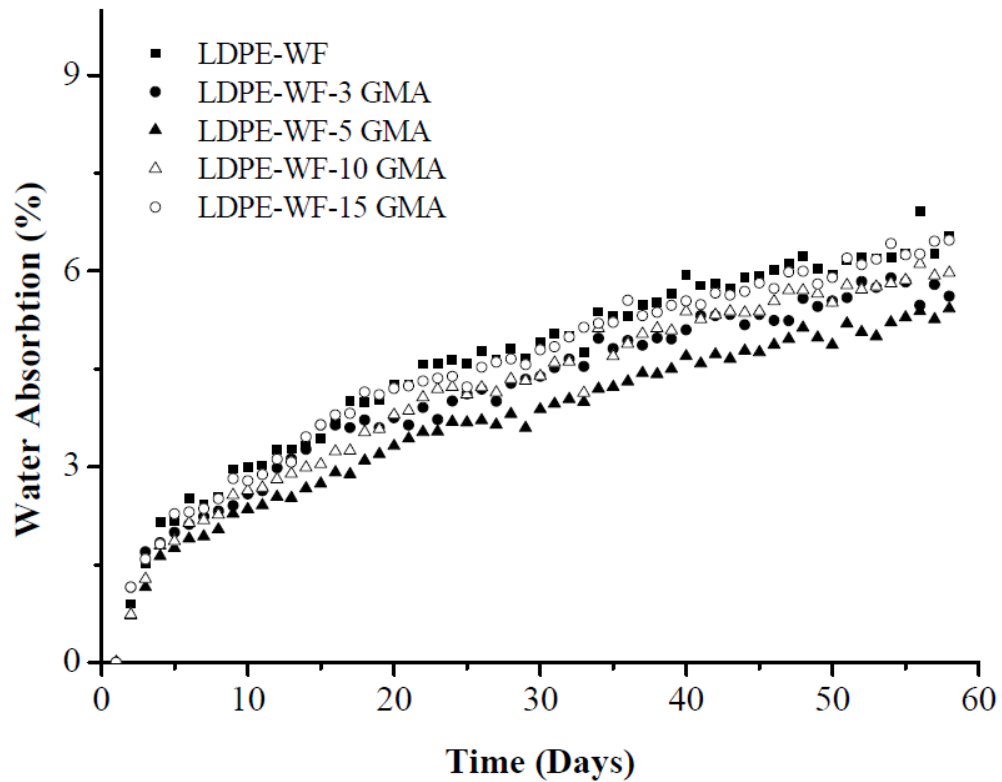


**Figure 4. 3** The effect of GMA compatibilizer ratio on water uptake values of LDPE-WF composites

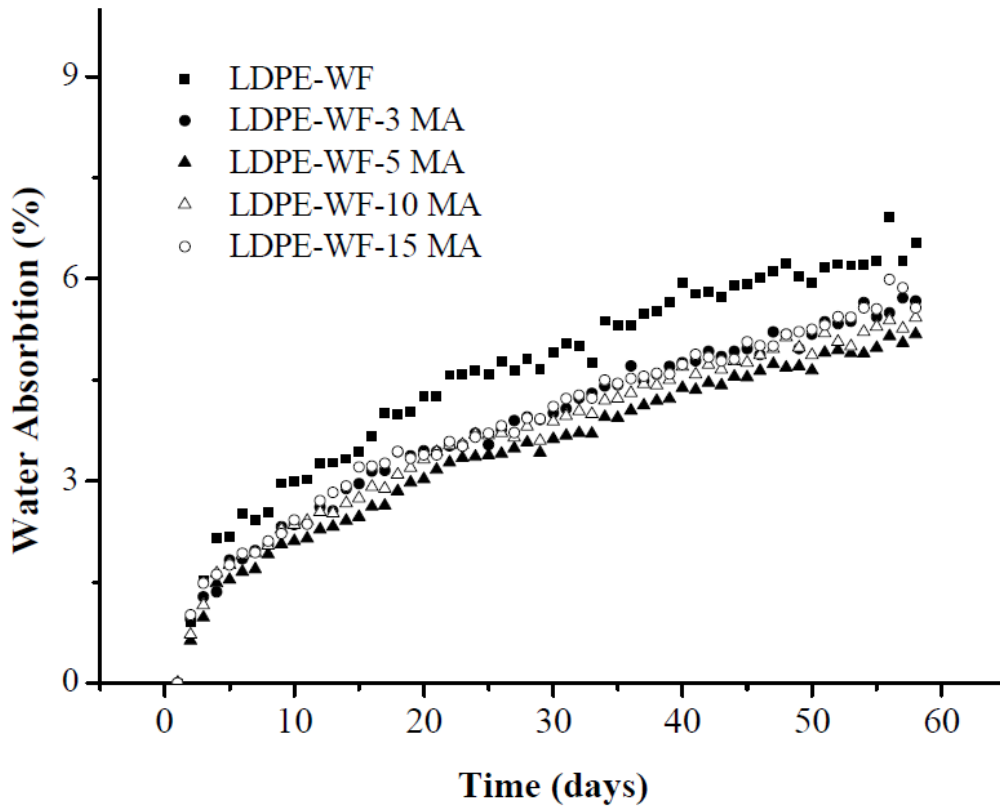


**Figure 4. 4** The effect of MA-compatibilizer ratio on water uptake values of LDPE-WF composites

Figure 4.5 shows the effect of preimpregnation on water uptake property of the composites. It becomes clear that preimpregnation has no effect on water absorption values of composites, and they absorb approximately the same amount of water at the end of 60 days.

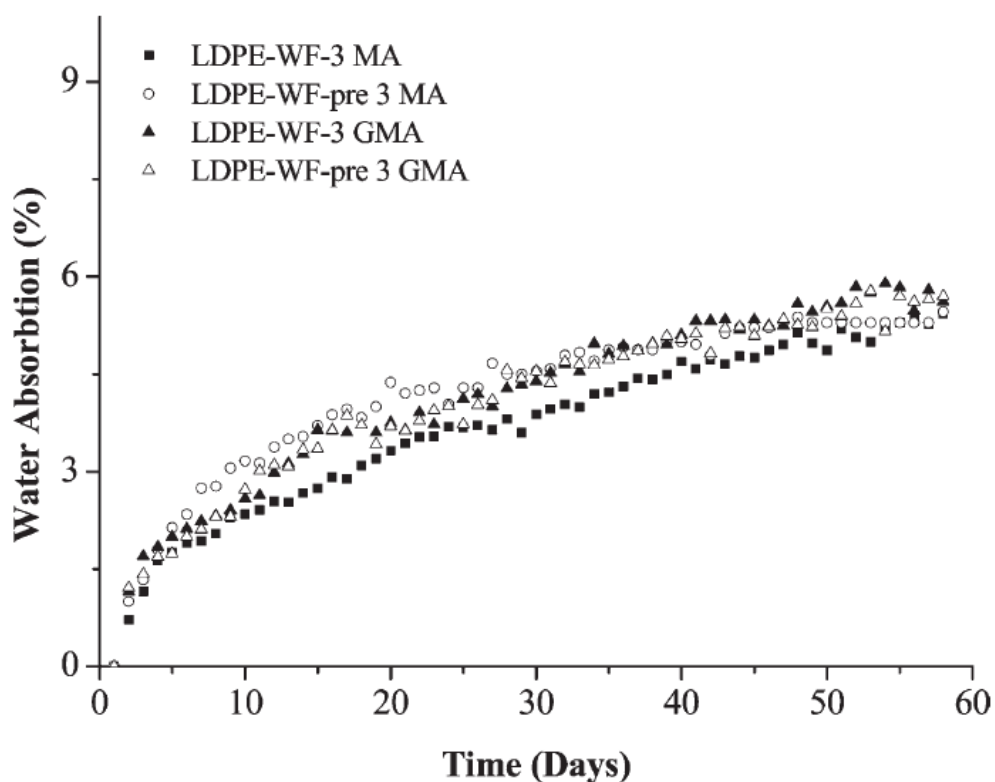


**Figure 4. 5** The effect of preimpregnation on water uptake property of the composites

#### 4.2 Effect of Alkaline Treatment and Pre-impregnation on Mechanical and Water Uptake Properties of WF-PLA Biocomposites

Different ratios of WF were used to prepare the composites. The compositions and the mechanical properties of the composites are shown in Table 4.2.

##### 4.2.1 FTIR Analysis

The FTIR spectra of PLA, aWF and pre-impregnated aWF with dilute solution of PLA are shown in Figure 4.6. The spectrum of PLA shows a pair of absorption bands at 2940 and 2997  $\text{cm}^{-1}$  due to symmetrical and asymmetrical  $-\text{CH}_2-$  stretching vibrations. The absorption bands at 1140, 1098 and 1043  $\text{cm}^{-1}$  arise from  $-\text{C}-\text{O}-$  stretching. A single absorption band at 1750  $\text{cm}^{-1}$  arises from carbonyl stretching in the ester bond. The absorption band at 1454  $\text{cm}^{-1}$  results from  $-\text{CH}_3$  bending [123].

The presence of PLA adsorbed on aWF is confirmed by the characteristic peak of PLA at  $1750\text{ cm}^{-1}$  which is not present at FTIR spectrum of aWF and the other characteristic peaks of PLA are masked with those of aWF peaks [5].

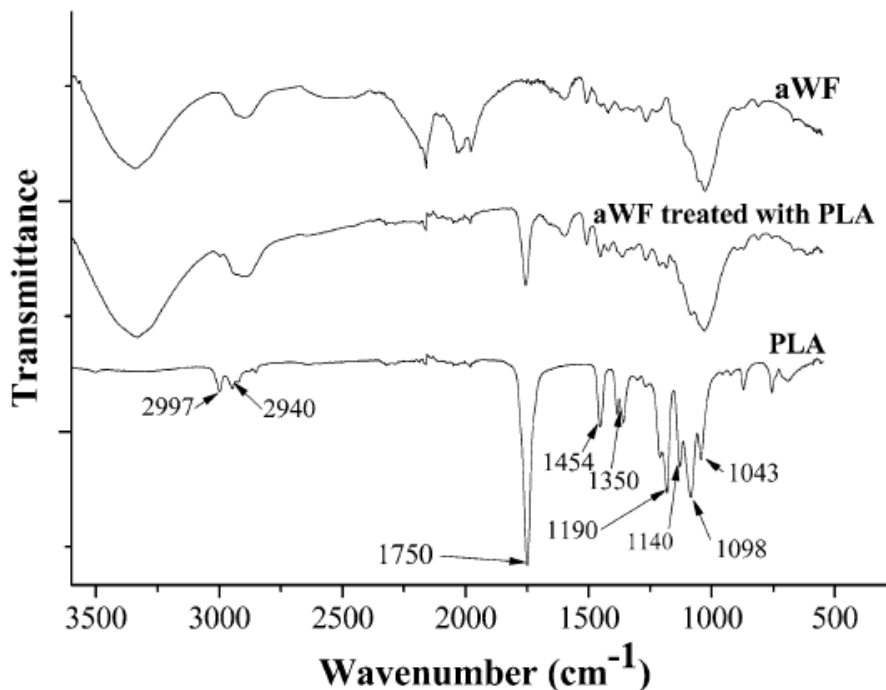


**Figure 4. 6** FTIR spectra of aWF, PLA and pre-impregnated aWF

#### 4.2.2 SEM Analysis

The effect of alkaline treatment and pre-impregnation on the morphology of the composites is studied by SEM. Representative SEM micrographs of fracture surfaces of selected composites are shown in Figure 4.7. From SEM image of PLA- 30 WF (image 1), there is a gap observed around WF after fracture indicating poor adhesion. However, the alkaline treatment greatly improves the interfacial adhesion between aWF and PLA since the PLA still covers on aWF surface after fracture (image 2 and image 3). It is also observed that most of the aWFs are broken during fracturing due

to the good stress transfer between matrix and aWF [124]. These findings provide qualitative evidence for the existence of adhesive bonds between surfaces. The pre-impregnation with dilute PLA solution (image 4) filling the cavities of aWF with matrix material further increases the adhesion between aWF and PLA by promoting mechanical interlocking. The mechanical tests results also support this conclusion [5].

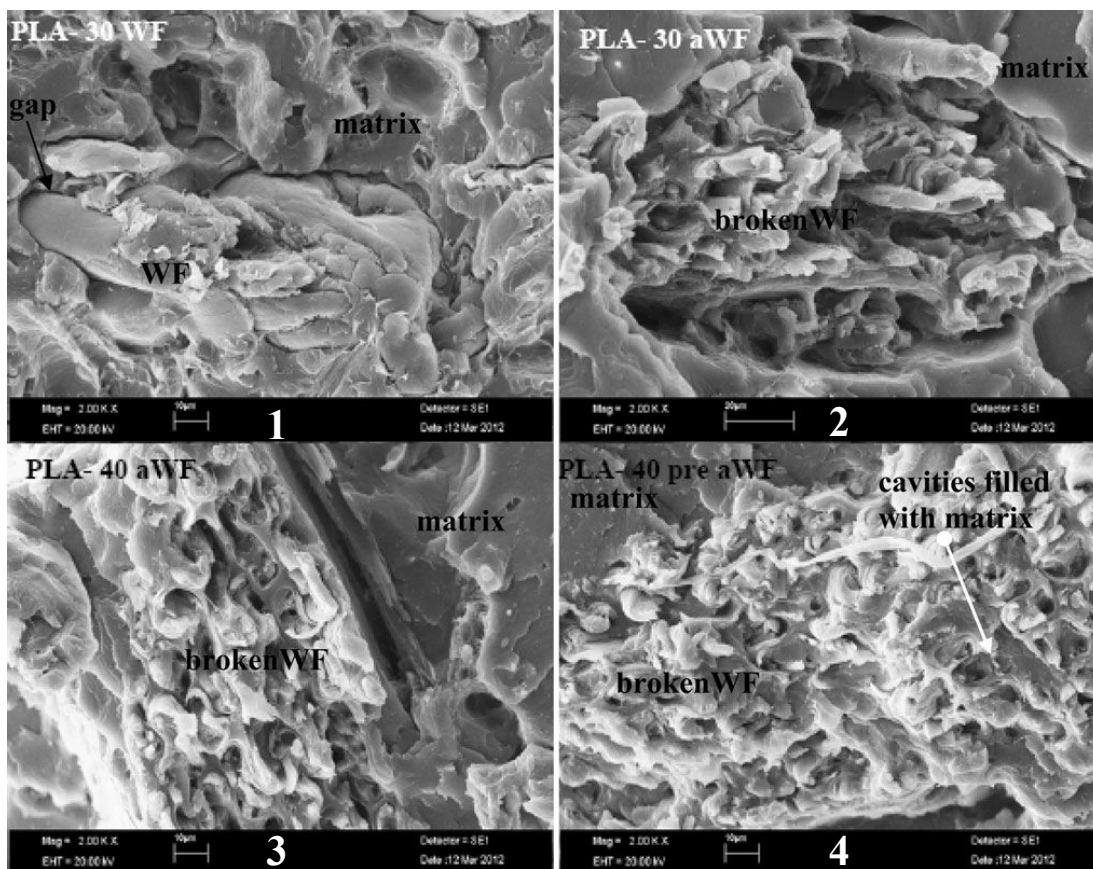


**Figure 4.7** SEM micrographs of fracture surfaces of selected composites

### 4.2.3 Mechanical Properties

The stress–strain curves of WF containing PLA green composites are shown in Figure 4.8 and the relevant mechanical data are reported in Table 4.2. PLA exhibits necking and undergoes stress whitening arising from crazing during tensile test. With the inclusion of WF, the type of stress– strain curve changes to brittle failure and the toughness of the composites reduce due to WF particles which act as stress concentrators, similar to previous studies [125-127].

**Table 4. 2** The compositions and the mechanical properties including tensile and impact strength of composites

Sample Code	Tensile Strength (MPa)	Percentage Strain at break (%)	Modulus (GPa)	Impact Strength (kJ/m <sup>2</sup> )
PLA	61.2±2.1	2.5±0.1	2.8±0.2	10.0±1.6
PLA-30 WF	33.3±1.1	0.98±0.1	3.7±0.2	5.2±0.3
PLA-30 aWF	56.9±0.3	1.45±0.1	4.1±0.3	6.1±0.9
PLA-40 aWF	59.8±2.0	1.38±0.1	4.4±0.3	5.9±0.4
PLA-50 aWF	66.2±2.0	1.28±0.1	5.4±0.2	6.0±0.2
PLA-40 pre aWF	63.2±2.2	1.38±0.1	4.8±0.2	7.0±0.5

Number shows the WF ratio (wt%)

aWF, alkaline treated WF; pre, pre-impregnated WF

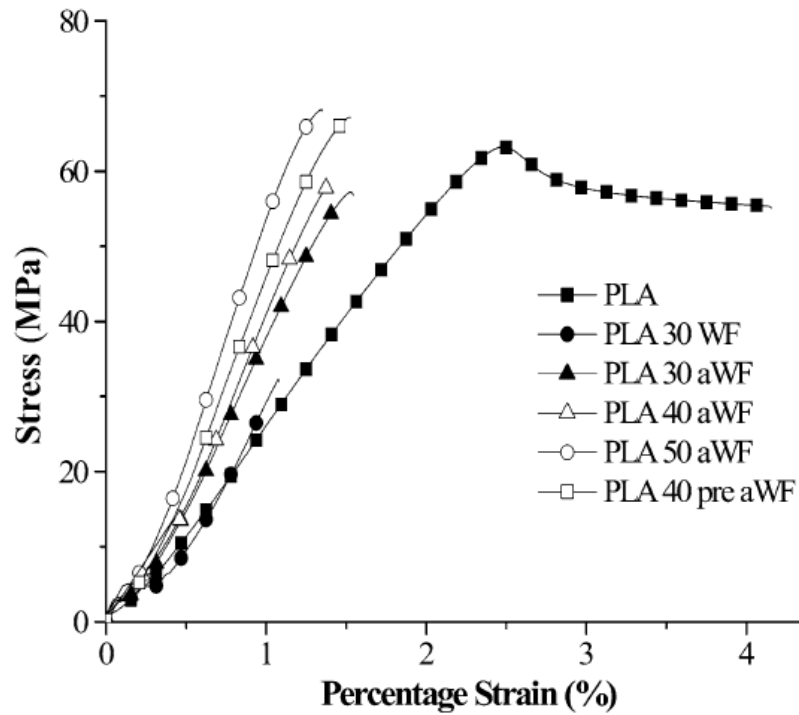


**Figure 4. 8** The stress–strain curves of WF containing PLA composites

The tensile modulus values of all composites containing WF are higher than the pure PLA. As the amount of aWF is increased, the tensile modulus values are further increased. The previous studies show that the filler with higher stiffness than the matrix can increase the tensile modulus of the composites and further increase as the amount increase as a rule of mixture [127-129]. The other factors affecting the tensile modulus of composites are the state of filler dispersion and polymer-particle interfacial area. Alkaline treatment further increases the tensile modulus values of the composites due to the higher polymer-particle interfacial area which restricts the inter and intra chain mobility. Pre-impregnation also further increases the tensile modulus values of the composites due to better WF dispersion arising from PLA coating.

The tensile strength and percentage elongation at break are sharply reduced with the addition of 30 wt% WF due to the weak interfacial adhesion [130]. Both the tensile strength and percentage strain at break values increase with alkaline treatment with respect to non-alkaline treated one but still lower than the pure PLA. The increase in tensile strength is an indication of good stress transfer between PLA matrix and WF particle. As the filler loading is increased, the percentage strain at break values are reduced owing to reduced deformability of the matrix material arising from the rigid WF particles. The tensile strength of the composite increases as the amount of aWF increases and exceeds that of PLA when the amount of aWF reaches 50 wt%. The pre-impregnation further increases the tensile strength of the composites due to the penetration of PLA into the cavities of aWF enabling better mechanical interlocking.

Izod impact strengths of the composites are listed in Table 4.2. The impact strength of unnotched samples is governed by crack initiation and crack propagation [124]. There is a relationship observed between the area under the stress strain curve (toughness) and the impact strength of composites. The impact strength of PLA is highly reduced with the inclusion of WF regardless of its amount and surface treatment. The alkaline treatment increases the impact strength with respect to untreated one due to the good adhesion between PLA and WF. Previous studies show that poor adhesion between WF and matrix results in the formation of micro voids that reduce efficient stress transfer from continuous polymer matrix to the dispersed WF and cause the material to absorb less energy [124,127,131]. There is no significant difference observed in impact strength of the composites with the increasing amount of aWF. The preimpregnation of aWF with dilute PLA solution further increased the impact strength of the composite due to the improved WF dispersion and good adhesion between matrix and WF by mechanical interlocking.



#### 4.2.4 Dynamic Mechanical Analysis

The dynamic storage modulus and  $\tan \delta$  values of PLA composites as a function of temperature are shown in Figure 4.9 and 4.10 respectively. As seen in Figure 4.9, a general declining trend is observed as the temperature increases and sharp reduction is observed when composites reach their glass transition temperature, corresponding to 60–64 °C depending on composition.

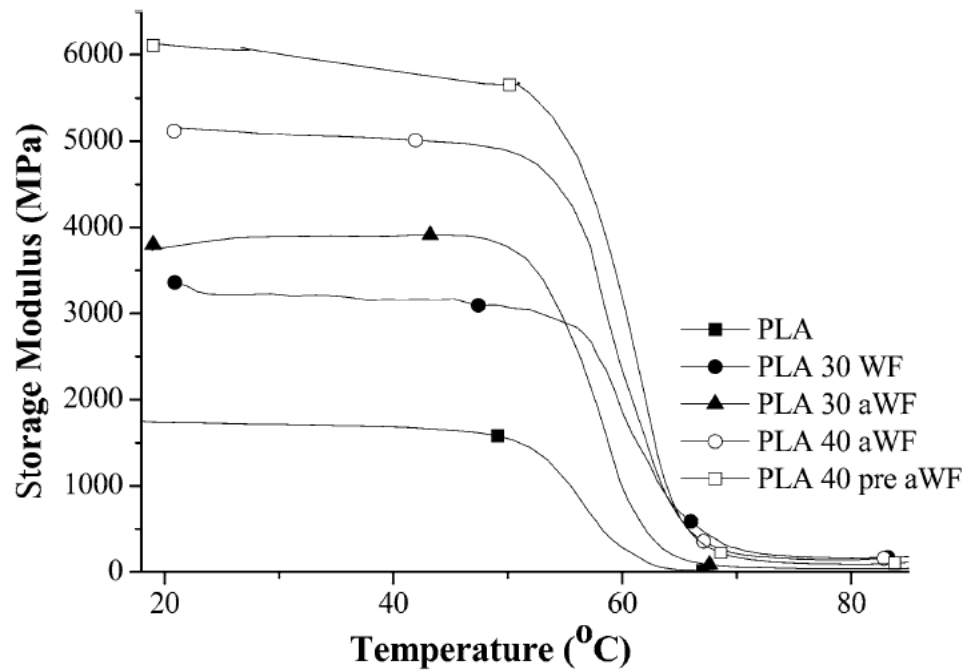


**Figure 4. 9** The dynamic storage modulus of PLA composites as a function of temperature

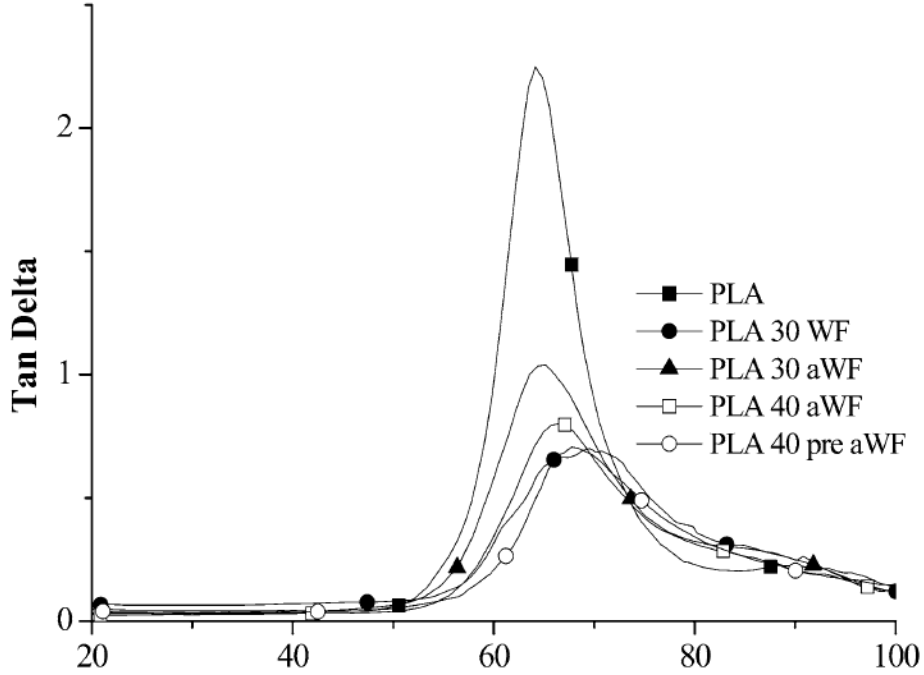


**Figure 4. 10** tan  $\delta$  values of PLA composites as a function of temperature

The  $T_g$  of the composites shifts to a bit higher temperatures due to the restricted molecular motion arising from strong interaction between the matrix and WF [132]. The highest increase obtained in the case of pre-impregnated WF since the dilute PLA solution fills the cavities of WF and PLA gets absorbed on WF surface, increases the effective volume of the filler. The study of Huda [135] showed that the glass transition temperature increases with increasing amount of WF. It is found that the addition of WF into PLA increases storage modulus. The alkaline treatment and the preimpregnation have further improved the storage modulus of composites at same amount of WF loading level. The results are in accordance with the tensile modulus results. The peak tan  $\delta$  decreases and the curve gets broadened with the addition of WF regardless of its amount and the surface treatment. Tan  $\delta$  broadens and the peak position shifts if there is an interaction between the matrix polymer and the filler/reinforcement [132-134]. The highest reduction at tan  $\delta$  value is obtained

when pre-impregnated aWF is used due to the restriction of the movement of PLA polymer chains adsorbed on WF [124].

#### 4.2.5 Water Uptake of PLA-WF Composites

Water uptake in WPCs is partly related to hydrogen bonding of water molecules to the hydroxyl groups present on wood surface [131,136,137]. The second factor in water uptake is the pore volume of the WF. The water uptake behavior of the composites are shown in Figure 4.11. It becomes clear that alkaline treatment has no effect on water absorption values of composites and they absorb approximately the same amount of water at the end of 40 days. The water absorption increases as the amount of WF increases due to high hydrophilic character. The preimpregnation made with dilute solution of PLA enables the penetration of PLA into the WF structure and reduces number of capillaries (pores) and water uptake (suction).

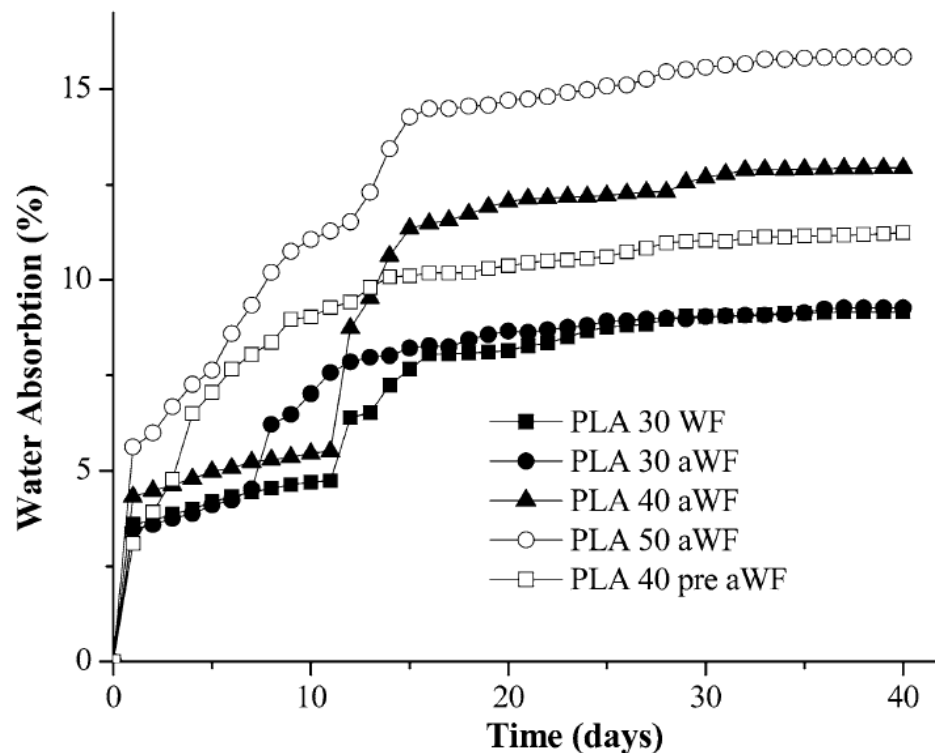


Figure 4. 11 The water uptake behavior of the PLA-WF composites

### 4.3 The Effect of Treatment of WF with Flame Retardant Solutions on the Flame Retardancy of LDPE-WF Composites Containing APP

In the previous studies it is mentioned that treatment of WF with a flame retardant solution increases the char yield so that this creates flame retardancy of the composite [103,104]. In the light of those studies, it is predicted that treatment of WF with a flame retardant solution shows higher LOI values and better UL-94 results than those of LDPE-WF composites.

WF was treated with DFP, DFAP, UDFP, and THPS solutions. After all treatments of WF, the amount of flame retardant material that had been impregnated, was determined. The amount of impregnated flame retardant was subtracted from the total amount of flame retardant (30 wt %) and the rest amount of APP was added to all compositions. The composition of formulations, LOI values and UL-94 ratings are given in Table 4.3.

**Table 4. 3** The composition of formulations, LOI values and UL-94 ratings

SAMPLE	LDPE (%wt)	APP (%wt)	WF + impregnated FR (%wt)	UL-94	LOI
PE-1	70	-	30+0	BC	17.5
PE-2 (Untreated )	40	30	30+0	BC	24.3
PE-7 (THPS)	40	25.90	30+4.1	BC	24.8
PE-8 (DFP)	40	24.14	30+5.86	BC	24.6
PE-9 (DFAP)	40	15.50	30+14.5	BC	23.3
PE-10 (UDFP)	40	25.22	30+4.88	BC	24.2

B.C: Burn to clamp

FR: Flame retardant

#### 4.3.1 LOI and UL-94

According to LOI and UL-94 tests, neither the LOI value nor UL-94 ratings change very much. When compared with the untreated sample result, treatment of WF with

DFP, UDFP and THPS solutions do not increase the LOI values; also treatment with DFAP solution even causes to observe decrease in LOI value of the composite. For this reason, only two selected samples which are DFP and THPS are examined in detail with TGA analysis and cone calorimeter.

#### **4.3.2 Thermogravimetric Analysis (TGA)**

Decomposition characteristics of LDPE-WF composites and flame retardant treated WF are studied by TGA. TGA graphs of flame retardant treated WF and untreated WF are demonstrated in Figure 4.12 and 4.13.

It is well known fact that wood thermally decomposes between 170-550 °C as a result of having hemicellulose (decomposes between 150-350 °C), cellulose (decomposes between 275-350 °C) and lignin (decomposes between 250-500 °C) constituents [138]. That is why, it is observed that untreated wood flour mainly decomposes at a maximum degradation temperature of 364 °C. DFP and THPS treated WF have lower maximum decomposition temperature at about 295 and 304 °C respectively. The reduction of maximum decomposition temperature for both treatments of WF arises from the containment of phosphorus in both flame retardants. The flame retardants containing phosphorous minimizes the formation of levoglucosan which is a tarry mixture, cellulose decomposes into at higher temperatures [139-140]. Minimization of levoglucosan is performed by reducing the decomposition temperature of cellulose and increasing the char formation by catalyzing dehydration and decomposition reaction [141-143]. The treatments of DFP and THPS enhance the residue of untreated WF from 10.6 % to 29.6 % and 31.2 % respectively. The increase in residue is due to the change in degradation pathway of cellulose. In the presence of phosphoric acid, cellulose is phosphorylated predominantly at C6 hydroxyl groups rather than depolymerization [144].

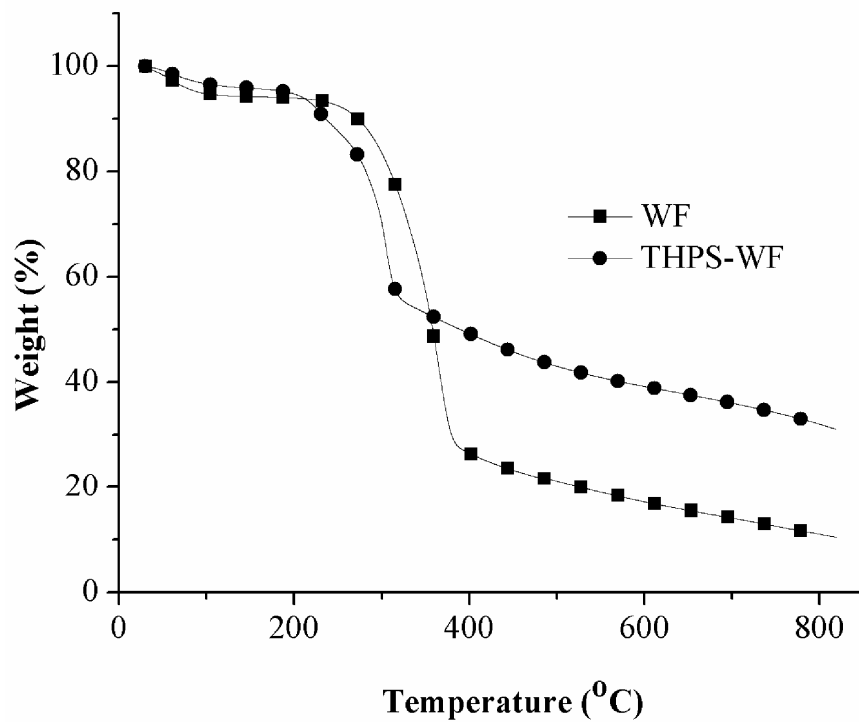


**Figure 4.12** TGA results of untreated WF and THPS treated WF

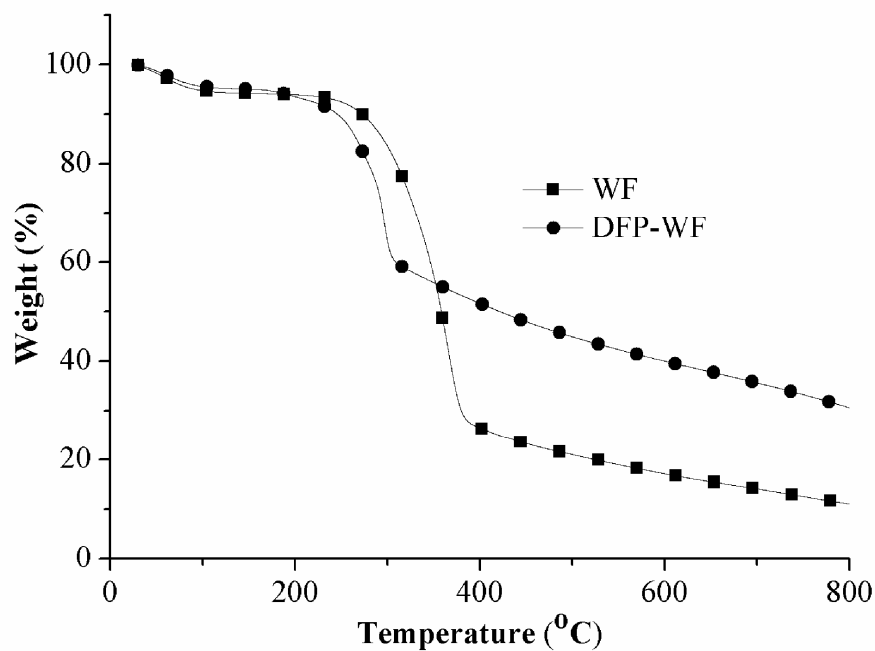


**Figure 4.13** TGA results of untreated WF and DFP treated WF

**Table 4. 4** TGA data of flame retardant treated WF-LDPE composites

SAMPLE	T <sub>5%</sub> (°C) <sup>a</sup>	T <sub>max</sub> (°C) <sup>b</sup>		Residue (%) <sup>c</sup>	
		1 <sup>st</sup> step	2 <sup>nd</sup> step	600 °C	800 °C
PE-1	314	361	488	5.1	2.9
PE-2	275	309	490	27.9	24.5
PE-7 (THPS)	235	298	478	31.3	26.9
PE-8 (DFP)	241	287	475	31.2	27.7

a: Temperature at 5% weight loss

b: The maximum rate degradation temperature c: Residue at 600 and 800 °C

Figure 4.14 and Table 4.4 show the TGA curves and data of all composites, respectively. All samples decompose in two degradation steps. First step arises from the degradation of WF and the second step arises from the decomposition of LDPE. The residue of PE-1 (30wt % WF) is found as 5.1 % at 600 °C that is due to the decomposition products of WF remained in the condensed phase. The residue decreases at about 43% at 800 °C, due to the degradation of low thermal stability decomposition products of WF. The addition of 30 wt % of APP (PE-2) decreases T<sub>5%</sub> and T<sub>max</sub> (first step) at about 40 and 50 °C, respectively. The decomposition product of APP which is polyphosphoric acid, causes the phosphorylation of cellulose. This results in the reduction of T<sub>5%</sub> and T<sub>max</sub> (first step) [145,146]. The addition of 30 wt % APP enhances the residue from 5.1 to 27.9 % at 600 °C due to the formation of thermally stable char arising from the carbonization reaction that occurs between the constituents of IFR system and favoring the char formation of WF by catalyzing effect of polyphosphoric acid. The samples containing APP and flame retardant treated WF (PE-3 and PE-4) have about 35 °C and 10 °C less T<sub>5%</sub> and T<sub>max</sub> (first step) respectively than PE-2 because of the reasons mentioned before. The char yield at 600 and 800 °C increases about 3% when APP and DFP or THPS treated WF is used. The presence of APP enhances the charring process for the composites and the materials treated with flame-retardant chemicals produce fewer

flammable gases and more chars and water which eventually cause dehydration and charring of cellulose [145,147]. In addition it is proposed that the temperatures above 400 °C, the matrix and the intumescent component begin to fully develop a bonded char structure [145,148]. As a result of these, the char yield increases at 600 and 800°C when APP and DFP or THPS treated WF is used.

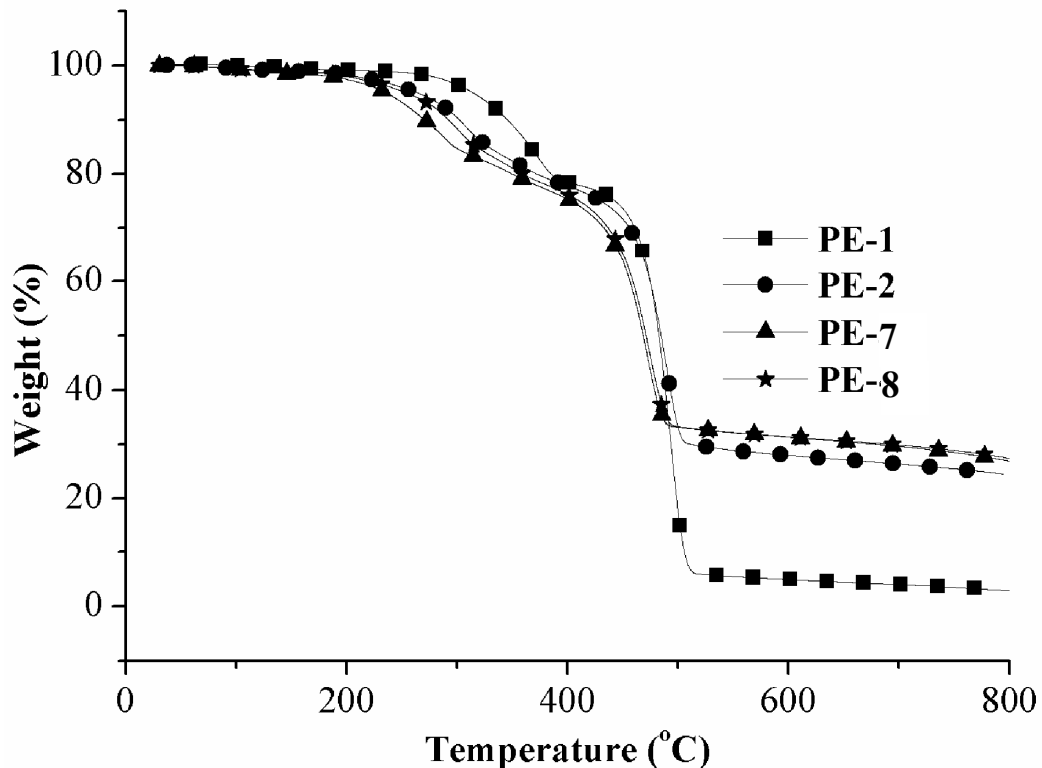


Figure 4. 14 The graph of TGA results

#### 4.3.3 Cone Calorimeter

Cone calorimeter is used to monitor heat release rate (HRR) during combustion. The HRR is recognized to be the most important parameter to evaluate the developing, spreading, and intensity of fires [149]. Low values of peak heat release rate (pHRR) and total heat evolved (THE) normally indicate improved flame retardancy. Figure



4.15 and Table 4.5 show the HRR curves and cone calorimeter data of all compositions at a heat flux of  $35 \text{ kWm}^{-2}$ .

According to Figure 4.15, it is noteworthy that the sample without flame retardant (PE-1) burns very fast after ignition and the pHRR value appears at  $432 \text{ kWm}^{-2}$  with one sharp peak. When mAPP is inserted into WF-LDPE matrix (PE-2), the HRR curves become more plateau like with extended burning time owing to barrier effect of foamed char. When APP is added (PE-2), the pHRR, average HRR and THE values decrease at about 62.5, 47.6 and 29.7 % with respect to the sample without any flame retardant (PE-1), respectively. The addition of THPS treated WF (PE-3) decreases the pHRR, average HRR and THE values more at about 4%, 36%, 17% with respect to PE-2 sample and 64 %, 67%, 48% with respect to PE-1 sample respectively. The more decrease in pHRR, average HRR and THE values is observed when DFP treated WF (PE-4) is added. The pHRR, average HRR and THE values decrease about 21 %, 36%, 27% with respect to PE-2 and 70%, 67%, 48% with respect to PE-1 sample respectively. In the view of these results, the high reduction in pHRR values shows that there is an enhancement in the fire performance with the use of THPS or DFP treated WF together with mAPP due to the increase in the amount of foamed char providing barrier effect.

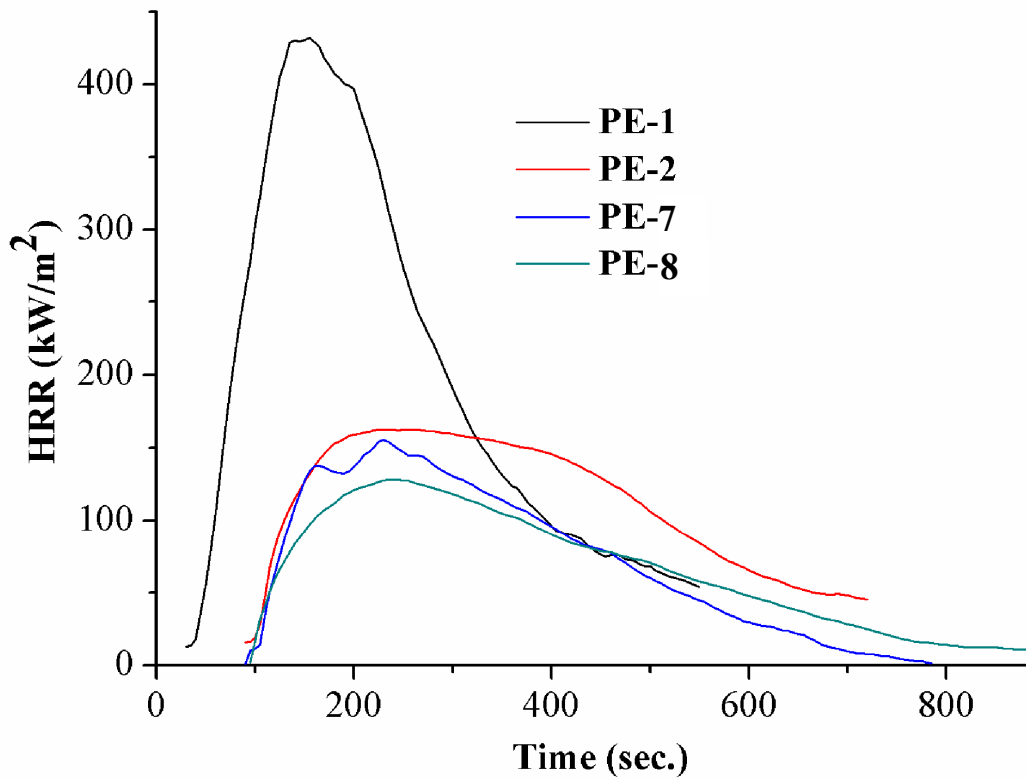


**Figure 4. 15** The graph of cone calorimeter results

**Table 4. 5** Mass loss calorimeter results of the composites

Samples	TTI (sec.)	pHRR (Kw.m <sup>-2</sup> )	Av. HRR (Kw.m <sup>-2</sup> )	THE (MJ.m <sup>-2</sup> )	Residue (%)
PE-1	37	432	225	98.1	6.3
PE-2	91	162	118	68.9	41.7
PE-7 (THPS)	99	155	75	51.2	43.6
PE-8 (DFP)	94	128	75	50.6	45.8

TTI: Time to ignition, pHRR: Peak Heat Release Rate, Av. HRR: Average HRR, THE: Total Heat Evolved, TML: Total Mass Loss

#### 4.4 The Effect of Direct Mixing of Flame Retardants on the Flammability and Thermal Characteristics of WF-LDPE Composites

Red phosphorus (RP) was used to improve the flame retardancy of WF-LDPE composites containing APP.

##### 4.4.1 LOI and UL-94

The flammability characteristics of composites were determined by LOI and UL-94 rating. As seen from Table 4.6, the LOI value and UL-94 rating of WF containing PE (PE-1) are 17.5 % and burn to clamp (BC), respectively. The addition of 30 wt% APP (PE-2) increases LOI value to 24.2 % with due to formation of foamed char structure which protects the underlying material [150-152]. However, the UL rating is remained same (BC). The addition of 5 wt% RP (PE-6) increases the LOI value to 20.5% and UL-94 rating increases to V2. With the partial substitution of RP with APP (PE-3, PE-4, PE-5), the composites have the highest UL-94 rating of V0. The highest LOI value, 27.2 %, is obtained when APP (25 wt%) and (5 wt %) RP is used together (PE-4). It is thought that the RP shows its adjuvant effect due to flame inhibition arising from gas phase mechanism of RP.

**Table 4. 6** Formulations of composites, LOI values and UL-94 ratings

Sample	LDPE	WF	AP 750	RP	LOI	UL-94
PE-1	70	30	-	-	17.5	BC
PE-2	40	30	30	-	24.2	BC
PE-3	40	30	27	3	26.3	V0
PE-4	40	30	25	5	27.2	V0
PE-5	40	30	20	10	26.8	V0
PE-6	65	30	-	5	20.5	V2

BC: Burn to clamp, NC: No clay

#### 4.4.2 Thermogravimetric Analysis

Decomposition characteristics of WPC are studied by TGA. Figure 4.16 and Table 4.7 show the TGA curves and data of all samples, respectively. All samples decompose in two degradation steps. First step arises from the degradation of WF and the second step arises from the decomposition of LDPE. The addition of 30 wt % WF (PE-1) increases residue to 5.1 % at 600 °C due to the decomposition products of WF remained in the condensed phase. Further heating to 800 °C, the char residue reduces at about 43% due to the degradation of low thermal stability decomposition products of WF. The inclusion of 30 wt% APP (PE-2) reduces  $T_{5\%}$  and  $T_{max}$  (first step) at about 40 and 50 °C, respectively. It arises from the phosphorylation of cellulose by polyphosphoric acid which is the decomposition product of APP [153,154]. The addition of 30 wt % APP increases residue from 5.1 to 27.9 % at 600 °C due to the formation of thermally stable char arising the carbonization reaction that occurs between the constituents of IFR system and favoring the char formation of WF by catalyzing effect of polyphosphoric acid.  $T_{max}$  of second step is slightly higher in all APP containing composites (PE-2, PE-3, PE-4 and PE-5) than only WF containing one owing to the formation of foamed char which protects the underlying material.

**Table 4. 7** TGA data of LDPE-WF composites

SAMPLE	$T_{5\%}$ (°C) <sup>a</sup>	$T_{max}$ (°C) <sup>b</sup>		Residue (%) <sup>c</sup>	
		1 <sup>st</sup> step	2 <sup>nd</sup> step	600 °C	800 °C
PE-1	314	361	488	5.1	2.9
PE-2	275	309	490	27.9	24.5
PE-3	275	309	492	27.5	23.9
PE-4	278	309	490	26.9	23.1
PE-5	279	309	491	26.4	22.9
PE-6	300	276	484	8.4	7.1

a: Temperature at 5% weight loss

b: The maximum rate degradation temperature c: Residue at 600 and 800 °C

Similar trend (reduction in  $T_{max}$  of first step and increase in residue) is observed with the addition of 5 wt % RP (PE-6) due to formation of phosphoric acid which catalyzed the dehydration of WF and increases the char yield [155-157]. The partial substitution of RP with APP does not change the shape of TGA curve. The slight increase in  $T_{5\%}$  and reduction in residue is observed as the added amount of RP increases.

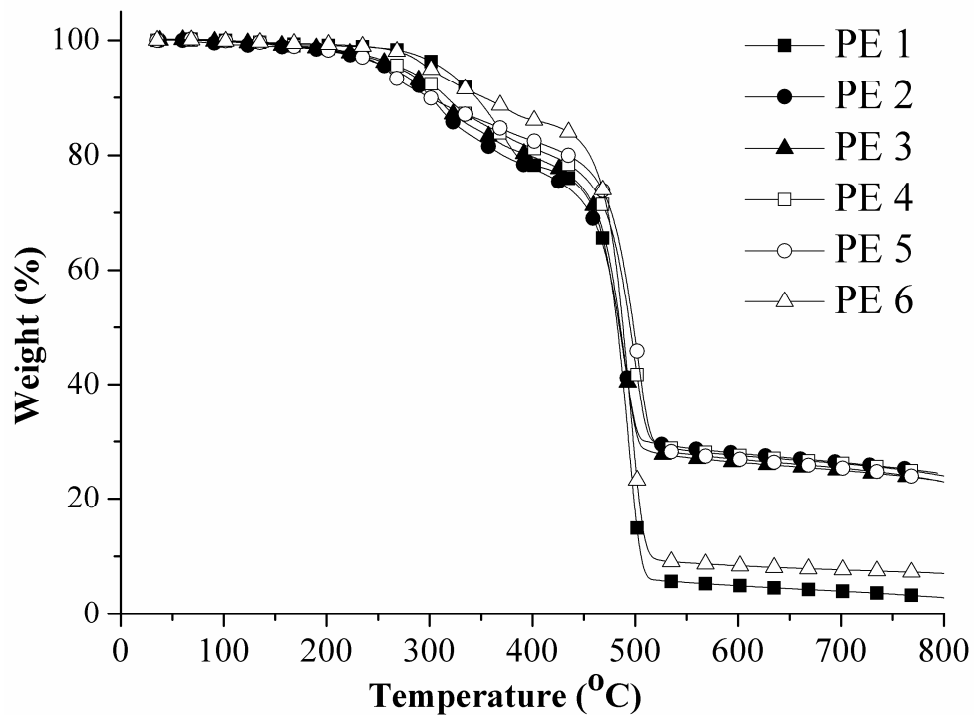


**Figure 4. 16** TGA graph of LDPE-WF composites

#### 4.4.3 Cone Calorimeter

Cone calorimeter is used to monitor heat release rate (HRR) during combustion. Low values of peak heat release rate (pHRR) and total heat release (THE) normally indicate improved flame retardancy. Figure 4.17 and Table 4.8 show the HRR curves and cone calorimeter data of selected compositions at a heat flux of  $35 \text{ kWm}^{-2}$ .

According to Figure 4.17, WF containing composite (PE-1) burns very fast after ignition and one sharp HRR peak appears with a heat release peak of  $432 \text{ kWm}^{-2}$ . With the addition of APP (PE-2, PE-4), HRR curves become more plateau like with extended burning time due to the barrier effect of foamed char. When APP is added (PE-2), the pHRR, average HRR and THE decrease at about 62.5, 47.6 and 29.7 % with respect to solely WF containing composite (PE-1), respectively. With the partial substitution of RP with APP (PE-4), the pHRR, average HRR and THE decrease at about 57.9, 43.1 and 26.7 % with respect to PE-1. In the view of these results, it is concluded that the addition of RP slightly reduces the barrier effect of char due to the reduction in the amount of foamed char.

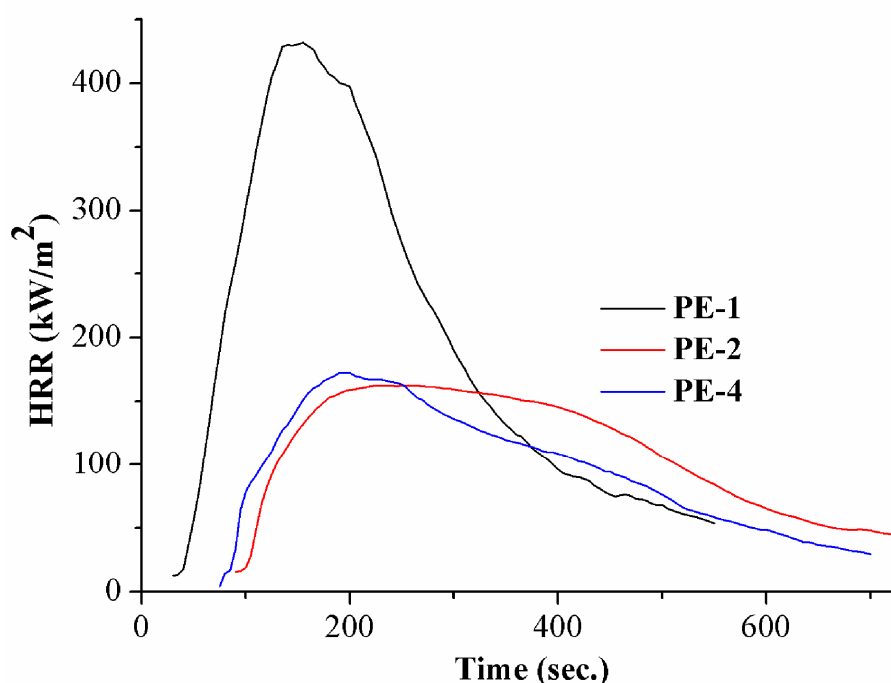


**Figure 4. 17** Cone calorimeter results of selected compositions

Total heat evolved to total mass loss ratio (THE/TML) is a measure for the effective heat of combustion and a reduction of this value indicates that the flame retardant additive shows its effect in the gas phase by flame inhibition [158]. The THE/TML

ratio remains almost same with the addition of APP. The reduction at THE/ TML value by 9.3 % is observed with the partial substitution 5 wt % RP because of the gas phase flame retardant action of RP. It is shown in the previous studies that RP also shows its flame retardant action in the gas phase due to the formation of PO radicals whose several hundred ppm in the flaming zone is enough to trap active radicals in the gas phase [159,160]. With the reduction at THE/TML value, it can be clearly seen that RP shows its adjuvant effect in the gas phase.

**Table 4. 8** Mass loss calorimeter data of selected compositions

<b>Samples</b>	<b>TTI</b> (sec.)	<b>pHRR</b> ( Kw.m <sup>-2</sup> )	<b>Av. HRR</b> (Kw.m <sup>-2</sup> )	<b>THE</b> (MJ. m <sup>-2</sup> )	<b>THE/TML</b> (MJ. m <sup>-2</sup> g <sup>-1</sup> )	<b>Residue</b> (%)
<b>PE-1</b>	37	432	225	98.1	2.96	6.3
<b>PE-2</b>	91	162	118	68.9	2.90	41.7
<b>PE-4</b>	74	172	128	71.9	2.63	37.4

**TTI:** Time to ignition, **pHRR:** Peak Heat Release Rate, **Av. HRR:** Average HRR, **THE:** Total Heat Evolved, **TML:** Total Mass Loss

#### **4.5 Flammability and Thermal Degradation Behavior of Flame Retardant Treated Jute Fabric Reinforced PLA**

The aim was to investigate and compare the flame retardant treatments of jute fabric made with ADP and GDP on flammability and thermal properties of PLA based biocomposites.

##### **4.5.1 LOI and UL-94**

The flammability properties of composites are evaluated by LOI and UL-94 tests and the relevant data are given in Table 4.9. The pure PLA composite has a LOI of 23 % and burns to clamp by melt dripping during UL-94 test. The incorporation of pure jute fabric in PLA reduces the LOI value to 19.7 % due to the candlewick effect of jute fibers. The composites containing flame retardant treated jute fabric have higher

LOI value than that of pure jute fabric containing one due to the increase in char residue. ADP treated jute fabric containing composite shows highest UL-94 rating (V0). It is thought that the flame retardant treatments exert dual flame retardant effect shown in gas and condensed phase. The increase in residue causes reduction in the amount of the combustible gases (gas phase) and the increment of barrier effect which limits the transfer of oxygen and fuel transfer between condensed and gas phase of char as the amount of char increases (condensed phase).

**Table 4. 9** LOI, UL-94 and TGA data of all composites

<b>SAMPLE</b>	<b>T<sub>5%</sub> (°C)<sup>a</sup></b>	<b>Residue (%)<sup>b</sup></b>	<b>UL-94</b>	<b>LOI (%)</b>
<b>PLA</b>	332	0	NR <sup>c</sup>	23.0
<b>PLA/JF</b>	261	5.0	BC	19.7
<b>PLA/JF-ADP</b>	224	18.2	V0	26.5
<b>PLA/JF-GDP</b>	247	17.7	BC	26.0

a: Temperature at 5% weight loss b: Residue at 800 °C c: Not rated

#### 4.5.2 Thermogravimetric Analysis

Thermal degradation properties of flame retardants, flame retardant treated jute fabrics and biocomposites are investigated by TGA under nitrogen atmosphere. TGA graphs of flame retardants, jute fabric and flame retardant treated jute fabrics are shown in Figure 4.18. It is observed that pure jute fabric mainly decomposes at maximum degradation temperature of 361 °C due to the decomposition of cellulosic substance such as hemicellulose and  $\alpha$ -cellulose [161]. The treatments of jute fabric with GDP and ADP lower the main decomposition temperature of jute fabric at about 92 and 109 °C due to the formation of phosphoric acid during the decomposition of both flame retardants. It is well known fact that the acids catalyze the decomposition of cellulose via hydrolysis [162-164]. The residue of pure jute fabric increases from 4.5 % to 32.7 and 35.5 % with the treatment of GDP and ADP,



respectively. The enhancement in residue arises from the changing in degradation pathway of cellulose. In the presence of phosphoric acid, the phosphorylation of cellulose occurs predominantly at C6 hydroxyl groups rather than depolymerization [165].

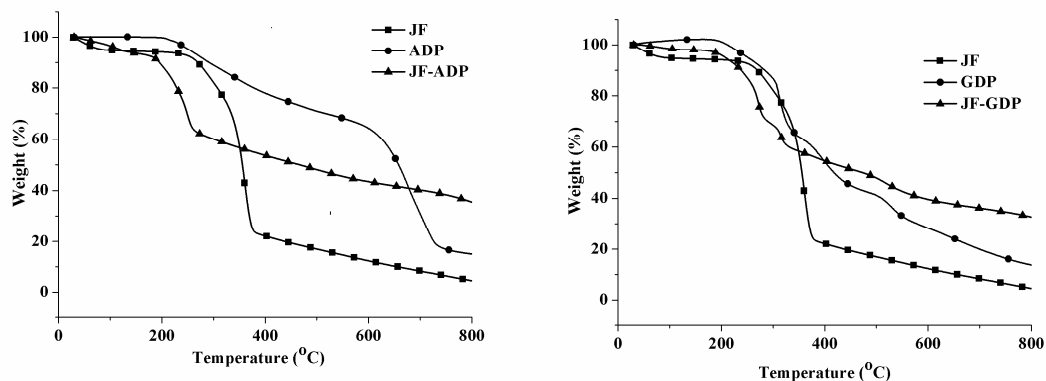


**Figure 4. 18** TGA graphs of pristine jute fiber and ADP or GDP treated jute fiber

TGA data and graphs of pure PLA and composites are given in Table 4.9 and Figure 4.19, respectively. The weight loss of PLA takes place at a single step with a maximum rate of weight loss at 374 °C with no char residue. The weight loss step of pure jute fabric containing composite also takes place in single step due to the approximately similar  $T_{max}$  values of jute fabric and PLA. Flame retardant treated jute fabrics containing composites degrade into two steps. First step is attributed to degradation of jute fabric and second step is attributed to the degradation of PLA. The addition of pure and flame retardant jute fabric reduces the  $T_{5\%}$  and increases the residue due to the reasons as stated before.

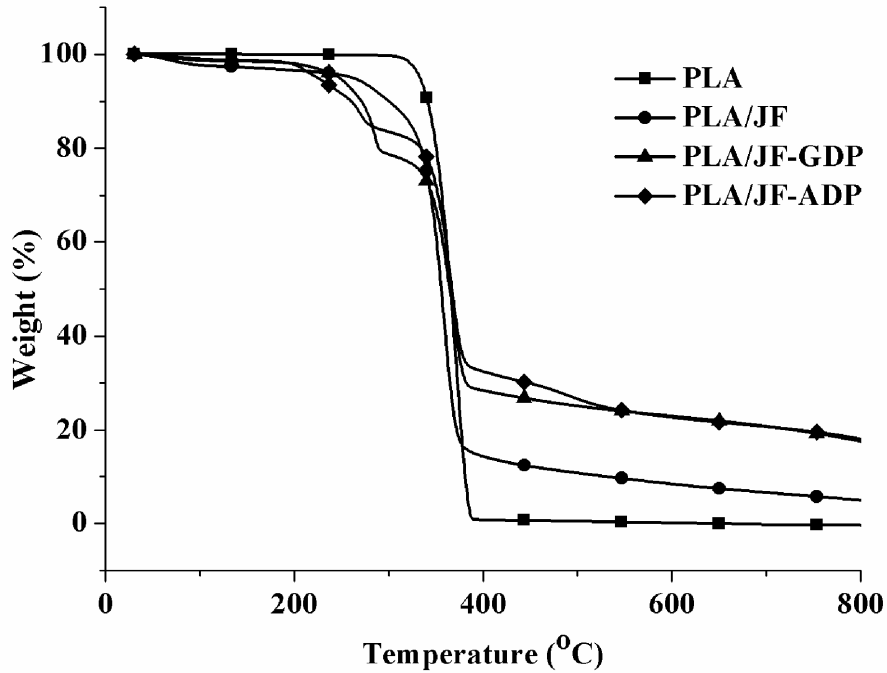
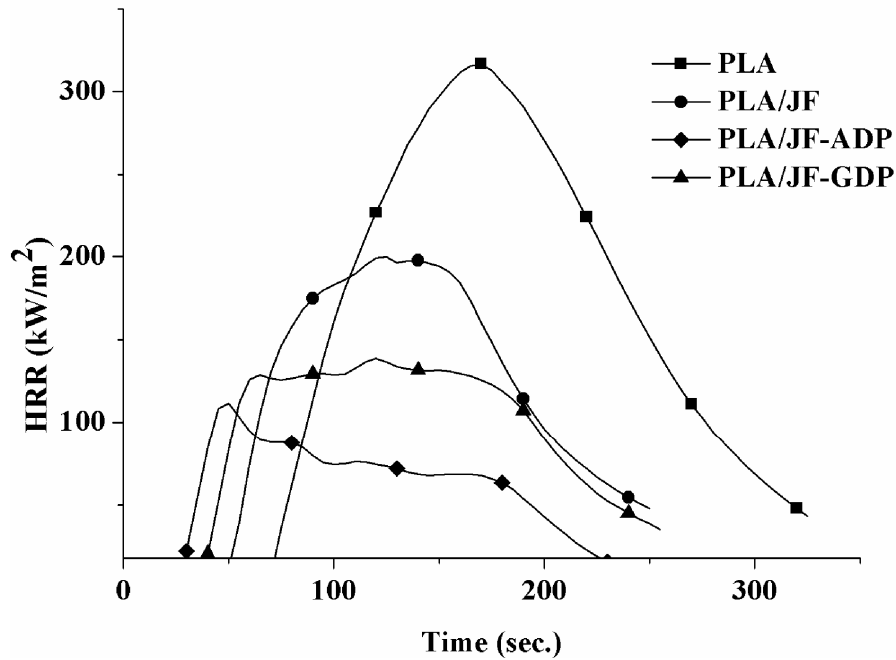


Figure 4. 19 TGA graph of all PLA-jute composites

#### 4.5.3 Cone Calorimeter

Mass loss calorimeter is used to monitor heat release rate (HRR) during combustion. Low values of peak heat release rate (pHRR) and total heat release (THE) normally indicate improved flame retardancy. Figure 4.20 and Table 4.10 show the HRR curves and mass loss calorimeter data of composites at a heat flux of  $35 \text{ kWm}^{-2}$ . According to Table 4.10 the incorporation of jute fabric in PLA matrix reduces the TTI value of pure PLA due to lower degradation temperature of jute fabric with respect to PLA. Similar results are found with the addition of natural fibers in different polymers [166,167]. The addition of flame retardant treated of jute fabric with GDP ( $T_{\text{max}}$ :  $269 \text{ }^{\circ}\text{C}$ ) and ADP ( $T_{\text{max}}$ :  $252 \text{ }^{\circ}\text{C}$ ) further reduces the TTI due to the reduction in  $T_{\text{max}}$  of pure jute fabric. The lowest TTI value is achieved in the case of ADP treated jute fabric which has the lowest  $T_{\text{max}}$  value according to TGA results.



**Figure 4. 20** Cone calorimeter graph of PLA-jute fiber composites

According to Figure 4.20, PLA burns very fast after ignition and one sharp HRR peak appears with pHRR and THE of  $316 \text{ kWm}^{-2}$  and  $46.6 \text{ MJ. m}^{-2}$ , respectively. HRR curves become plateau like with the incorporation of both pure and flame retardant jute fabrics due to the barrier effect of jute fabric residue. The pHRR, average HRR and THE values decrease at about 37, 28 and 40 % with the incorporation of jute fabric, respectively. The incorporation of GDP treated jute fabric further reduces the pHRR, average HRR and THE values at about 31, 21, 16 % with respect to those of pure jute fabric containing one, respectively. The lowest pHRR, average HRR and THE values are achieved with the addition of ADP treated jute fabric which has the highest char yield. It is observed that there is a correlation between char yield and fire performances of composites. As the amount of char increases, the amount of combustible material reduces and the barrier effect of char increases. Thus, the composite which has the highest char yield exhibits the best fire performance results.

**Table 4. 10** Cone calorimeter data of selected compositions of PLA-jute fiber composites

Sample	TTI (sec.)	pHRR ( Kw.m <sup>-2</sup> )	Av. HRR (Kw.m <sup>-2</sup> )	THE (MJ. m <sup>-2</sup> )	Residue (%)
PLA	72	317	184	46.6	-
PLA/JF	52	200	132	27.8	11.6
PLA/JF-ADP	33	112	61	13.8	32.5
PLA/JF-GDP	43	139	104	23.2	25.3

**TTI:** Time to ignition, **pHRR:** Peak Heat Release Rate, **Av. HRR:** Average HRR, **THE:** Total Heat Evolved

#### 4.5.4 SEM and ATR- FTIR Analysis

The char residues remained after cone calorimeter test are characterized by SEM and ATR- FTIR analysis. SEM images of char residues are presented in Figure 4.21. According to Figure 4.21, the morphology of charred fibers remains intact and no drastic changes in the surface characteristics are observed with flame retardant treatments after cone calorimeter test. The surfaces of flame retardant treated jute fabrics are irregularly covered with inorganic residue remained after decomposition of fire retardant additives. Figure 4.22 shows the ATR – FTIR spectra of char residues. ADP and GDP treated jute fabrics show additional peaks at 1090 cm<sup>-1</sup> and 1580 cm<sup>-1</sup>. The peak seen at 1090 cm<sup>-1</sup> arises from the stretching vibrations of P-O-P and C-O-P groups which mask each other [168,169]. The presence of these peaks supports that the cellulose phosphate ester formation via the reaction of hydroxyl groups of cellulose with phosphoric acid and the presence inorganic residues remained decomposition of flame retardant additives on fiber surfaces. The peaks seen at 1580 cm<sup>-1</sup> arises from C=C groups owing to the formation of stable conjugated structures during burning process. According to study made by Liodakis et al., cellulose phosphate ester forms conjugated structures via elimination reactions during burning process [170].



Figure 4. 21 SEM results of PLA-jute fiber's char residues

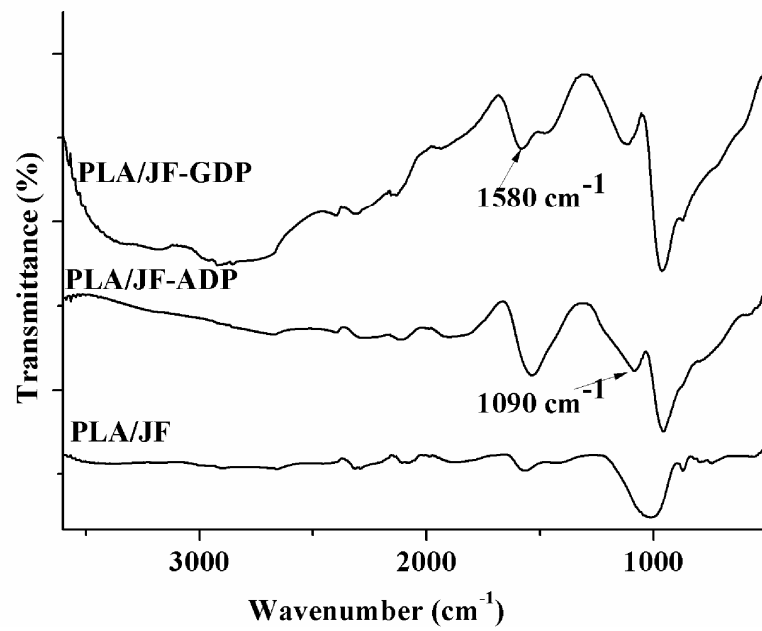


Figure 4. 22 ATR-FTIR results of PLA-jute fiber char residues



## CHAPTER 5

### CONCLUSIONS

#### **5.1 Comparative Study of MA and GMA Functionalized Terpolymers as Compatibilizers for LDPE-WF Composites**

The possibility of using two terpolymers, MA and GMA functionalized, as compatibilizers for LDPE–WF composites is investigated. The effect of preimpregnation is also studied. FTIR results show that both compatibilizers adhere on WF surface after preimpregnation.

It is observed that MA-comp increases tensile and impact strengths when it is directly used. It shows the highest value at a concentration 10 wt % of WF. The preimpregnation with MA-comp further increases tensile and impact strength. In addition MA-comp increases the adhesion between LDPE and WF as suggested by SEM results. Compared to MA-comp, the GMA-comp does not increase the tensile strength as much and slightly increases the impact strength. Compared to pristine WF composite, the preimpregnation with GMA-comp increases both tensile strength and impact strength.

The use of both type of compatibilizer reduces the water uptake value of the LDPE–WF composite, and the lowest value is obtained at a compatibilizer concentration of 5 wt % of WF. MA-comp containing composites show lower water uptake values than the GMA-comp ones. It is also observed that preimpregnation has no effect on final water uptake value of composites at the end of 60 days. Finally, it can be

concluded that MA-comp is more effective than GMA-comp as a compatibilizer in LDPE–WF composites.

## **5.2 Effect of Alkaline Treatment and Pre-impregnation on Mechanical and Water Uptake Properties of WF-PLA Green Composites**

In the current study, the effect of alkaline treatment, WF ratio and pre-impregnation on mechanical properties including tensile, impact and DMA and water absorption properties of WF containing PLA based composites are investigated. It is concluded that alkaline treatment and pre-impregnation are effective methods to increase the mechanical properties including tensile modulus, tensile and impact strength of PLA-WF composites. Alkaline treatment one can speculate increases the interfacial interactions between WF and PLA by creating functional groups at the interface. Apparently porosity remains unchanged so the water uptake remains constant. Pretreatment of WF with PLA on the other hand reduces porosity by impregnating WF. DMA analysis reveals that the T<sub>g</sub> of the composites shifts to a bit higher temperatures with the addition WF and the highest increase is obtained in the case of pre-impregnated WF. This observation can be explained by the hindrance of polymer chain motions due to increased interaction with adhered polymer segments. Alkaline treatment has no effect on water uptake properties but pre-impregnation is effective by reducing the pore volume and the water sensitivity of the composite.

## **5.3 The Effect of Treatment of WF with Flame Retardant Solutions on the Flame Retardancy of LDPE-WF Composites Containing APP**

WF is treated with DFP, DFAP, UDFP, and THPS solutions and LOI and UL-94 tests are performed. When compared with the untreated sample result, treatment of WF with DFP, DFAP, UDFP and THPS solutions does not increase the LOI values and all UL-94 ratings are BC. For this reason, only two selected samples which are DFP and THPS, are examined in detail with TGA analysis and cone calorimeter. As a conclusion, the combined use of THPS or DFP treated WF with APP increases the



fire performance of composites as the 70% of increase in pHRR value with respect to sample without flame retardant (PE-1) owing to the increase in the amount of foamed char providing barrier effect.

#### **5.4 The Effect of Direct Mixing of Flame Retardants on the Flammability and Thermal Characteristics of WF-LDPE Composites**

The combustion and thermal properties of WF- LDPE composites containing APP with and without RP are investigated. The addition of 30 wt % APP increases the LOI value from 17.5 to 24.2 and BC rating is obtained from UL-94 test. The combined use of APP and RP shows adjuvant effect. The maximum adjuvant effect is seen at a ratio of 5:1 (APP: RP). Although the addition of RP reduces barrier effect of char, the RP increases the gas phase action.

#### **5.5 Flammability and Thermal Degradation Behavior of Flame Retardant Treated Jute Fabric Reinforced PLA**

It is investigated and compared the effect flame retardant finishing of jute fabric with two phosphorus based flame retardants, ADP and GDP, on flammability and fire performances of PLA based biocomposites. According to TGA and ATR-FTIR results, both flame retardant treatments favor the char formation by changing the degradation pathway of jute fabric. The increase in char yield is the main flame retarding effect of both flame retardant additives. The increment in char residue causes the reduction in combustible gases arising from the degradation jute fabric and increases the barrier effect of formed char. Accordingly, ADP treated jute fabric containing composite shows better flammability and fire performance than GDP containing one. According flammability and fire performance test results, ADP is more effective than GDP.

## **5.6 Overall Evaluation of Compatibilizers and Processing Methods on the Mechanical and Flame Retardancy Properties**

WF and jute fiber are abundant, natural fibers. Thus, they are mostly used as fillers in composites to decrease the cost. However, when they are used in composites, the mechanical properties of the composites decrease after some extent. In addition, the flammability of the composites increases with the use of WF. Therefore, the mechanical properties and the flammability of the composites should be considered and improved somehow.

In the scope of this study, the mechanical properties of WF-LDPE composites are improved with MA-functionalized compatibilizer. In addition, alkaline treatment and pre-impregnation are effective methods to increase the mechanical properties of the LDPE-WF composites. In PLA-WF composites, alkaline treatment and preimpregnation of WF with dilute solution of PLA increases the tensile strength of the composites. In the light of these results the researchers who want to improve the mechanical properties of WF-plastic composites should focus on alkaline treatment of WF and preimpregnation of WF with dilute solution of compatibilizer or matrix polymer.

The flammability of WF-LDPE and PLA-jute composites, different kinds of approaches are applied. Better results are obtained with decreasing the flammability of matrix when combined use of APP and RP. They showed adjuvant effect in LDPE-WF composites. It is concluded that phosphorous containing flame retardants are effective for decreasing the flammability of LDPE-WF composites. The flammability of both WF and LDPE is decreased with the treatment of WF with phosphorous containing flame retardant solutions in addition to mixing with APP. However, this application does not decrease the flammability of the composites as much as direct mixing of the flame retardants with WF and LDPE. These results

show that phosphorous containing flame retardants are effective in LDPE-WF composites especially direct mixing of flame retardants with the matrix and the fiber.

The flammability of PLA-jute composites are decreased with the approach of decreasing the flammability of the jute fabric. Treatment of jute fabric in phosphorous containing flame retardant solutions gives promising results in terms of flammability and the fire performances of the biocomposites for future studies.



## REFERENCES

- [1] Mohanty A K, Misra M, Drzal L T, 'Natural Fibers, Biopolymers and Biocomposites' Taylor&Francis Group, 2005.
- [2] Vilaplana F, Strömberg E, Karlsson S, Polym Degrad Stab, 95, 2010, 2147-2161.
- [3] Mohanty A K, Misra M, Hinrichsen G, Macromol Mater Eng 276/277, 2000, 1–24.
- [4] Sreekumar, P. A. Matrices for natural-fibre reinforced composites. In K. L. Pickering (Ed.),UK: Brimingham, Woodhead Publication Limited, 2008.
- [5] Altun Y, Doğan M, Bayramlı E, Polym Environ, 21, 2013, 850–856.
- [6] George J, Sreekala M S, Thomas S A, Polym Eng Sci, 41, 2001,1471.
- [7] Saheb D N, Jog J P, Adv Polym Sci,18, 1999, 351.
- [8] Herrera-Franco PJ, Valadez-Gonzalez A, Compos Part B Eng 36, 2005, 597.
- [9] Aydın M, Tozlu H, Kemaloğlu S, Aytaç A, Özkoç G, J Polym Environ,19, 2011,11.
- [10] Huda M S, Drzal M T, Mohanty A K, Misra M., Compos Sci Technol 68, 2008, 424.

- [11] Bogoeva-Gaceva G, Avella M, Malinconico M, Buzarovska A, Grozdanov A, Gentile G, Errico ME, Polym Compos 28, 2007, 98.
- [12] Doğan M. ‘Production and Characterization of Boron Containing Flame Retardant Polyamide-6 and Polypropylene Composites and Fibers’, PhD Tesis, METU, 2011.
- [13] Altun Y, Doğan M, Bayramlı E, J. Appl Polym. Sci., 127, 2013, 1010-1016.
- [14] Fowler PA, Hughes J M, Elias RM, J Sci Food Agric, 86, 2006, 1781-1789.
- [15] [http://en.wikipedia.org/wiki/Composite\\_material](http://en.wikipedia.org/wiki/Composite_material) last accessed on 05/06/2013.
- [16] Kabir M M, Wang H, Lau K T, Cardona F, Compos Part B, 43, 2012, 2883-2892.
- [17] Vilaplana F, Strömberg E, Karlsson S, Polym Degrad Stabil, 95, 2010, 2147-2161.
- [18] Bismarck A, Baltazar-Y-Jimenez A, Sarlkakis K, Environ Dev Sustainability, 8 (3), 2006, 445–463.
- [19] Kim J P, Yoon T H, Mun S P, Rhee J M, Lee J.-S., Bioresour Technol, 97 (3), 2006, 494–499.
- [20] Bledzki A K, Gassan J, Prog Polym. Sci, 24, 1999, 221.
- [21] Li K, Zadorecki P, Flodin P, Polym Compos, 8, 1987, 199.

- [22] Satyanarayana K G, Arizaga G G G, Wypych F, *Prog Polym Sci*, 34, 2009, 982-1021.
- [23] Li X, Tabil L G, Panigrahi S, *Polym Environ*, 15(1), 2007, 25–33.
- [24] Mwaikambo L Y, Tucker N, Clark A J, *Macromol Mater Eng*, 292(9), 2007, 993–1000.
- [25] Ray D, Sarkar B K, Rana A K, Bose N R, *Bull Mater Sci*, 24(2), 2001, 129–35.
- [26] Lu J Z, Wu Q, McNabb H S, *Wood and Fiber Sc*, 32 (1), 2000, 88–104.
- [27] Kalia S, Kaith B S, Kaur I, *Polym Eng Sci*, 49(7), 2009, 1253–1272.
- [28] Xie Y, Hill C A S, Xiao Z, Militz H, Mai C, *Composites Part A* 41(7), 2010, 806–819.
- [29] Xanthos M, *Funct Fillers Plast*, Wiley VCH, Germany, 2005.
- [30] Miller R B, "Structure of Wood", Chapter 2 in the *Wood Handbook: Wood as an Engineering Material*, General Technical Report, FPL-GTR-113, USDA Forest Service, Forest Products Laboratory, Madison, WI, USA, 1999.
- [31] Panthapulakkal S, Zereshkian, A, Sain, M, *Bioresour Technol*, 97 (2), 2006, 265–272.
- [32] Bengtsson, Magnus, Oksman K, *Compos Sci Technol*, 66, 2006, 2177–2186.
- [33] English BW, Falk P, *Forest Products Society, Proceedings*, 7293, 1995, 189-94.

- [34] Nielsen LE, Landen RF, Mechanical Properties of Polymer and Composite, New York, NY: Marcel Dekker, Inc; 1994.
- [35] Plueddemann EP. Silane coupling agents, New York, NY: Plenum Press; 1982, 1–28.
- [36] Verhey A S, Lacks E P, Richter L D, Keranen D E, Larkin M G., Forest Products Journal, 53(5), 2002, 67–74.
- [37] <http://briencounter.wordpress.com/2012/09/24/jute-harvesting-and-basic-processing/> last accessed on 12/07/2013.
- [38] <http://shreebalajiexports.co.in/products4/> last accessed on 12/09/2012.
- [39] Malpass D.B., Introduction to Industrial Polyethylene, Jon Wiley and Sons, USA, 2010.
- [40] [http://en.wikipedia.org/wiki/Low-density\\_polyethylene/](http://en.wikipedia.org/wiki/Low-density_polyethylene/) last accessed on 15/03/2014.
- [41] <https://moodle.fp.tul.cz/mod/page/view.php?id=11707/> last accessed on 16/10/2014.
- [42] Bajpai P K, Singh I, Madaan J, J Thermoplast Compos Mater, 2012,1-30.
- [43] Bourbigot S, Fontaine G, Polym. Chem., 1, 2010, 1413-1422.
- [44] Garcia Z F, Martinez E, Alvarez C A, Castano V M, J Reinf Plast Compos 1995, 14, 641.



- [45] Tobias B C, Proceedings of the International Conference on Advanced Composite Materials; Minerals, Metals & Materials Society (TMS), Warrendale, PA, 1993, p 623.
- [46] Vollenberg P H Th, Heiken D, Polymer 1990, 30, 1652.
- [47] Felix J M, Gotenholm P, Schreiber H P, Polym Compos 1993, 14, 449.
- [48] Mukharjea R N, Pal S K, Sanyal S K, Phani D K, J Polym Mater 1984, 1, 69.
- [49] Calamari T A, Harper R J, "Flame Retardants for Textiles", Kirk-Othmer Encyclopedia of Chemical Technology, 2000.
- [50] Grand A F, Wilkie A C, "Fire Retardancy of Polymeric Materials", Marcel Dekker, Inc., New York, 2000.
- [51] Lewin M, Atlas S M, Pearce E M, "Flame Retardant Polymeric Materials", Plenum Press, New York and London, 1975.
- [52] Lomakin S M, Zaikov G E, "Modern Polymer Flame Retardancy", VSP, Boston, 2003.
- [53] Pearce M E, Liepins R, "Flame Retardant, Environmental Health Perspectives", 11, 59-69, 1975.
- [54] Kuryla W C, Papa A J, "Flame Retardancy of Polymeric Materials", 2, Marcel Dekker, New York, 1973.
- [55] Morgan A B, Wilke C A, "Flame Retardant Polymer Nanocomposites", John Wiley & Sons, New Jersey, 2007.

- [56] [www.fitfibers.com/files/PLA%20Fibers.doc](http://www.fitfibers.com/files/PLA%20Fibers.doc)/last accessed on 02/002/2014.
- [57] Tsafack M J, Levalois-Grützmacher J, *Surf Coat Technol*, 200, 2006, 3503-3510,
- [58] Mouritz A P, Gibson A G, "Fire Properties of Polymer Composite Materials", Springer, Dordrecht, 2006.
- [59] Lu S, Hamerton I, *Prog Polym Sci*, 27, 2002, 1661-1712.
- [60] Xanthos M, "Funtional Fillers for Plastics", Wiley-VCH, Weinheim, 2005.
- [61] Li Q, Pingkai J, Wei P, *Macromol Mater Eng*, 290, 2005, 912-919.
- [62] Bourbigot S, Le Bras M, Duquesne S, Rochery M., *Macromol Mater Eng*, 289, 2004, 499-511.
- [63] Xie F, Wang Y, Yang B, Liu Y, *Macromol Mater Eng*, 291, 2006, 247-253,
- [64] Doğan M, Bayramli E, *Polym Advan Technol*, 22, 2011, 1628-1632.
- [65] (Melamine based flame retardants mechanism of action), <http://www.specialchem.com/4polymers.com/tc/melamine-flame-retardants/index.aspx?id=4005>, last accessed on 05/05/2014.
- [66] Zhang S, Horrocks A R, *Prog Polym Sci*, 28, 2003, 1517-1538.
- [67] Levchik V S, Weil E D, *Polym Int*, 49, 2000, 1033-1073.

- [68] ChemWiki,[http://chemwiki.ucdavis.edu/Inorganic\\_Chemistry/Descriptive\\_Chemistry/Main\\_Group\\_Elements/Group\\_15:\\_The\\_Nitrogen\\_Family/The\\_Chemistry\\_of\\_Phosphorous#Red\\_Phosphorus\\_and\\_Violet\\_Phosphorus](http://chemwiki.ucdavis.edu/Inorganic_Chemistry/Descriptive_Chemistry/Main_Group_Elements/Group_15:_The_Nitrogen_Family/The_Chemistry_of_Phosphorous#Red_Phosphorus_and_Violet_Phosphorus), last accessed on 05/05/2014.
- [69] Liu Y, Wang Q, Polym Degrad Stabil, 91, 2006, 3103-3109.
- [70] Wang H, Meng X, Wen B, Gao X, Zhang S, Yang M, Mater Lett, 62, 2008, 3745-3747.
- [71] Weil E D, Levchik S, J Fire Sci, 22, 2004, 251-264.
- [72] Wang H, Meng X, Wen B, Gao X, Zhang S, Yang M, Mater Lett, 62, 2008, 3745-3747.
- [73] Davis J, Huggard M, J Vinyl Add Tech, 2, 1996, 69-75.
- [74] Wang J, Tu H, Jiang Q, J Fire Sci, 13, 1995, 261-280.
- [75] Giraud S, Bourbigot S, Rochery M, Vroman I, Tighzert L, Delobel R, Poutch F, Poly Degrad Stab, 88, 2005, 106-113.
- [76] Davies P J, Horrocks A R, Alderson A, Poly Degrad Stab, 88, 2005, 114-122.
- [77] Ammoniumpolyphosphate,[http://www.ul.ie/~childsp/CinA/Issue65/Images/TO\\_C34\\_8.gif](http://www.ul.ie/~childsp/CinA/Issue65/Images/TO_C34_8.gif), last accessed on 05/05/2014.
- [78] Bourbigot S, Duquesne S, J Mater Chem, 17, 2007, 2283-2300.

- [79] Le Bras M, Bourbigot S, Delporte C, Siat C, Le Tallec Y, Fire Mater, 20,1996, 191-203.
- [80] Camino G, Costa L, Trossarelli L, Poly Degred Stab,6, 1984, 243-252.
- [81] Camino G, Costa L, Trossarelli L, Poly Degred Stab,7, 1984, 25-31.
- [82] Jegatheesan A, Neelakantaprasad B, Murugan J, Rajarajan G, Int J Comput Appl, 53, 2012, 15-18.
- [83] [http://en.wikipedia.org/wiki/ABC\\_Dry\\_Chemical](http://en.wikipedia.org/wiki/ABC_Dry_Chemical) last accessed on 05/05/2014.
- [84] GÜthner T, Mertschenk B, Schulz B, Ullmann's Encyclopedia of Industrial Chemistry, 17, 2006, 175-189.
- [85] [http://en.wikipedia.org/wiki/Scanning\\_electron\\_microscope/](http://en.wikipedia.org/wiki/Scanning_electron_microscope/)last accessed on 05/05/2014.
- [86] Fried J R, Polymer Science and Technology, Prentice Hall PTR, USA, 2003.
- [87] Kılınç, M, Processing and Characterization of Poly(ethylene terephthalate) Based Composites, M.S., Middle East Technical University, Ankara, 2004.
- [88] Annual Book of ASTM Standards, ASTM D 638 M Standard Test Method for Tensile Properties of Plastics, 08.01, Philadelphia, 1993.
- [89] Özkoç G, "Abs/Polyamide-6 Blends, Their Short Glass Fiber Composites and Organoclay Based Nanocomposites: Processing and Characterization" PhD Thesis, METU, 2007.

- [90] Seymour R B, Carraher C E, Structure-Property Relationships in Polymers, Plenum Press, New York, 1984.
- [91] Annual Book of ASTM Standards, ASTM D 256-92: Standard Test Methods for Impact Resistance of Plastics and Electrical Insulating Materials, 08.01, Philadelphia, 1993.
- [92] Menard K, Dynamic mechanical analysis: A practical introduction, CRC press, New York, 1999.
- [93] Sinha S, Ray K, Okamoto M, Macromol, 36, 2003, 2355.
- [94] UL-94-Test for Flammability of Plastic Materials for Parts in Devices and Appliances, Northbrook, IL: Underwriters Laboratories Inc., 1997.
- [95] Kiliaris P, Papaspyrides C D, Prog Polym Sci, 35, 2010, 902- 958.
- [96] Laoutid F, Bonnaud L, Alexandre M, Lopez-Cuesta J.M., Dubois Ph., Mater Sci Eng R”, 63, 2009, 100-125.
- [97] Schartel B, Bartholmai M, Knoll U, Polym Degrad Stab, 88, 2005, 540-547.
- [98] Schartel B, Hull T R, Fire Mater, 31, 2007, 327-354.
- [99] [http://en.wikipedia.org/wiki/X-ray\\_photoelectron\\_spectroscopy/last](http://en.wikipedia.org/wiki/X-ray_photoelectron_spectroscopy/last) accessed on 05/05/2014.
- [100] Giles H F, Wagner J R, Mount E M, “Extrusion The Definitive Processing Guide and Handbook”, William Andrew Publishing, New York, 2005.

- [101] Strong A B, "Plastics Materials and Processing", Prentice Hall, New Jersey, 2006.
- [102] [http://en.wikipedia.org/wiki/Injection\\_molding/](http://en.wikipedia.org/wiki/Injection_molding/) last accessed on 05/05/2014.
- [103] Pan X , Sun C Y, Gao M, J Fire Sci, 21, 2003, 189-201.
- [104] Bagga S L, Jain R K, Gur I S, Bhatnagar H L, Br Polym J, 22, 1990, 107-120.
- [105] Li Q, Matuana L M, J. Appl. Sci., 88, 2003, 278.
- [106] Balasuriya P W, Ye L, Mai Y W, Wu J, J. Appl. Sci. 83, 2002, 2505.
- [107] Lai S M, Yeh F C, Wang Y, Chan H C, Shen H F, J. Appl. Polym. Sci. 87, 2003, 487.
- [108] Tserki V, Zafeiropoulos N E, Simon F, Panayiotou C, Compos. Part A: Appl. Sci., 36, 2005, 1110.
- [109] Oksman K, Clemons C, J. Appl. Sci. 67, 1998, 1503.
- [110] Oksman K, Lindberg H, J. Appl. Sci. 68, 1998, 1845.
- [111] Hristov V N, Krumova M, Vasileva St, Michler G H, J. Appl. Sci., 92, 2004, 1286.
- [112] Keener T J, Stuart R K, Brown T K, Compos. Part A: Appl. Sci., 35, 2004, 357.

- [113] Herrera-Franco P J, Valadez-Gonzalez A, Compos. Part B: Eng. 36, 2005, 597.
- [114] Herrera-Franco P J, Valadez-Gonzalez A, Compos. Part A: Appl. Sci., 35, 2004, 339.
- [115] Takamura K, Goldsmith H L, Mason S G J, Colloid Interface Sci., 82, 1981, 190.
- [116] Yang H, Wolcott M P, Kim H, Kim S, Kim H, Compos Struct, 79, 2007, 369375.
- [117] Roy S B, Ramanaj B, Shit S C, Nayak S K J Appl Sci 120, 2011, 3078.
- [118] Marcovich N E, Villar M A, J Appl Sci 90, 2003, 2775.
- [119] Nunez A J, Sturm P C, Kenny J M, Aranguren M I, Marcovich N E, Reboredo M M, J Appl Sci, 88, 2003, 1420.
- [120] Ichazo M N, Albano C, Gonzalez J, Perera R, Candal M V, Compos Struct 54, 2001, 207.
- [121] Nachtigall S M B, Cerveira G S, Rosa S M L, Polym Test, 26, 2007, 619.
- [122] Nitz H, Reichert P, Römling H, Mülhaupt R, Macromol Mater Eng 51, 2000, 276–277.
- [123] Garlotta D, J Polym Environ 9, 2001, 63.

- [124] Shah B L, Selke S E, Walters M B, Heiden P A, Polym Compos 29, 2008, 665.
- [125] Yang H, Wolcott M P, Kim H, Kim S, Kim H, Compos Struct 79, 2007, 369.
- [126] Nyambo C, Mohanty A K, Misra M, Biomacromolecules 11, 2010, 1654.
- [127] Pilla S, Gong S, O'Neill E, Rowell R M, Krzysik A M, Polym Eng Sci 48, 2008, 578.
- [128] Marcovich N E, Villar M A, J Appl Sci, 90, 2003, 2775.
- [129] Petinakis E, Yu L, Edward G, Dean K, Liu H, Scully A D, J Polym Environ, 17, 2009, 83.
- [130] Bengtsson M, Gatenholm P, Oksman K, Compos Sci Technol, 65, 2003, 1468.
- [131] Tserki V, Matzinos P, Panayiotou C, Compos Part A, 37, 2006, 1231.
- [132] Nunez A J, Sturm P C, Kenny J M, Aranguren M I, Marcovich N E, Reboredo M M, J Appl Sci 88, 2003, 1420.
- [133] Lai S, Yeh F, Wand Y, Chan H, Shen H, J Appl Sci 87, 2003, 487.
- [134] Nielsen L E, 'Mechanical properties of polymers and composites'. Marcel Dekker, 1974, New York.
- [135] Huda M S, Drzal M T, Mohanty A K, Misra M, Compos Sci Technol 68, 2008, 424.



- [136] Ichazo M N, Albano C, Gonzalez J, Perera R, Candal MV, Compos Struct 254, 2001, 207.
- [137] Nachtigall S M B, Cerveira G S, Rosa S M L, Polym Test, 26, 2007, 619.
- [138] Bodirlâu R, Teacă C A, Spiridon I, Rev Roum Chim, 52(1-2), 2007.
- [139] Kandola B K, Horrocks A R, Price D, Coleman G V, J. Macromol. Sci. Rev. Macromol. Chem. Phys., C36 (4), 1996, 721-794.
- [140] Gao M, Sun C Y, Zhu K, J Therm Anal Calorim, 75, 2004, 221-232.
- [141] Jain R K, Lal K, Bhatnagar H L, J Appl Polym Sci, 30, 1985.
- [142] Blasi C M, Branca C, Galgano A, Polym Degrad Stabil, 93, 2008.
- [143] Gao M, Zhu K, Sun Y J, Sun C, J Fire Sci, 22, 2004.
- [144] Joseph P, Ebdon J R, Fire Retardancy Polymeric Materials, Boca Raton, 2010.
- [145] Schumao L, Jie R, Hua Y, Tao Y, Weizhong Y, Polym Int, 59, 2010.
- [146] Chen D, Li J, Ren J, Polym Int, 60, 2011.
- [147] Hashim R, Sulaiman O, Kumar R N, Tamyez P F, Murphy R J, Alic Z, J. Mater Process Technol, 209, 2009.
- [148] Horrocks A R, Anand S C, Sanderson D, Polymer, 37, 1996.

- [149] Nie1 S, Hu1 Y, Song L, He Q, Yang D, Chen H, Polym Adv Technol, 19, 2008.
- [150] Le Bras M, Bourbigot S, Delporte C, Siat C, Le Tallec Y, Fire and Mater. 20, 1996, 191.
- [151] Camino G, Costa L, Trossarelli L, Polym Degrad Stabil 6, 1984, 243.
- [152] Camino G, Costa L, Trossarelli L, Polym Degrad Stabil 7, 1984, 25.
- [153] Shumao L, Ren J, Hua Y, Weizhong Y, Polym Int 59, 2010, 242.
- [154] Chen D, Li J, Ren J, Polym Int, 60, 2011, 599.
- [155] Mostashai S M, Fayyaz F, Chin J Chem, 26, 2008, 1030.
- [156] Mostashai S M, Bale S, J. Therm Anal Calorim, 99, 2010, 431.
- [157] Levchik G F, Vorobyova S A, Gorbarenko V V, Levchik S V, Weil E D, J. Fire Sci., 18, 2000; 172.
- [158] Braun U, Schartel B, Fichera M A, Jager C, Polym Degrad Stab, 92, 2007, 1528.
- [159] Granzow A, Cannelongo J. F, J Appl Polym Sci 20, 1976, 689.
- [160] Wu Q, Lu J, Qu B, Polym Int 52, 2003; 1326.
- [161] Kahn J A, Kahn M A, Islam R, Gafur A. Mater Sci Appl 1, 2010, 350-57.

- [162] Gao M, Sun C, Zhu K, *J Therm Anal Calorim* 75, 2004, 221-32.
- [163] Gao M, Ling B, Yang S, Zhao M, *J Anal Appl Pyrol* 73, 2005,151-56.
- [164] Blasi C M, Branca C, Galgano A, *Polym Degrad Stab*, 93, 2008, 335-46.
- [165] Joseph P, Ebdon J R, Phosphorus- based flame retardants. In: Wilkie CA, Morgan AB, editors. *Fire retardancy of polymeric materials*, Boca Raton: Taylor &Francis, 2010.
- [166] Kozłowski R, Władysław-Przybylak M, *Polym Adv Technol* 19, 2008, 446-53.
- [167] Dorez G, Tauget A, Ferry L, Lopez-Cuesta J M, *Polym Degrad Stab*, 98, 2013,87-95.
- [168] Zhan J, Song L, Nie S, Hu Y, *Polym Degrad Stab*, 94, 2009, 291-296.
- [169] Rupper P, Gaan S, Salimova V, Heuberger M, *J Anal Appl Pyrolysis*, 87, 2010, 93-98.
- [170] Liodakis S, Fetsis I K, Agiovlasis I P, *J Therm Anal Calorim*, 98, 2009, 285.



## APPENDIX

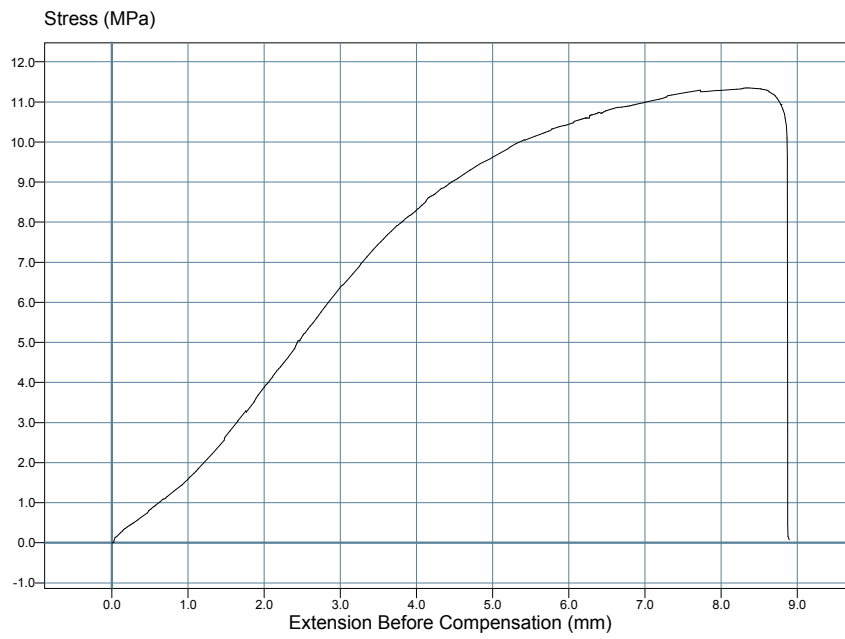


**Figure A. 1** Stress-Strain curve of LDPE-WF composition

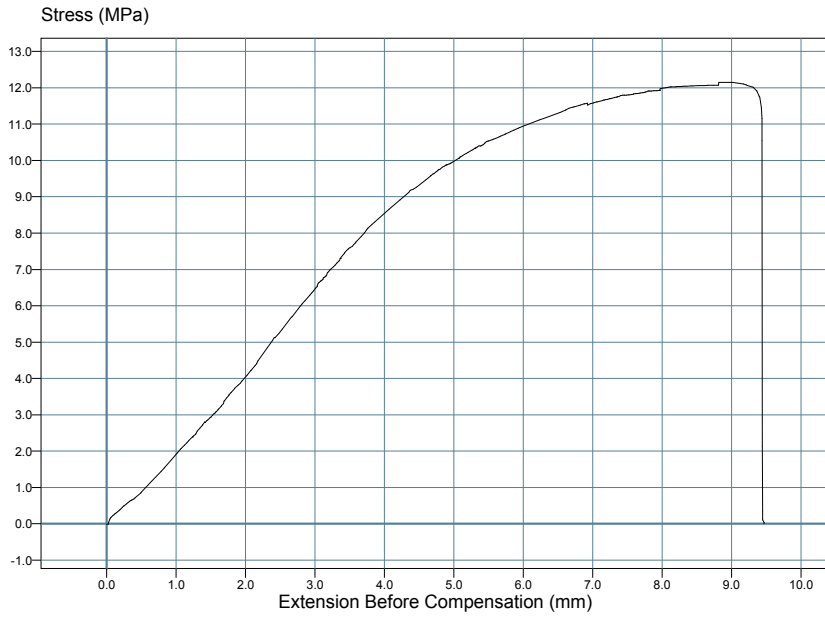


**Figure A. 2** Stress-Strain curve of LDPE-WF-3 MA composition

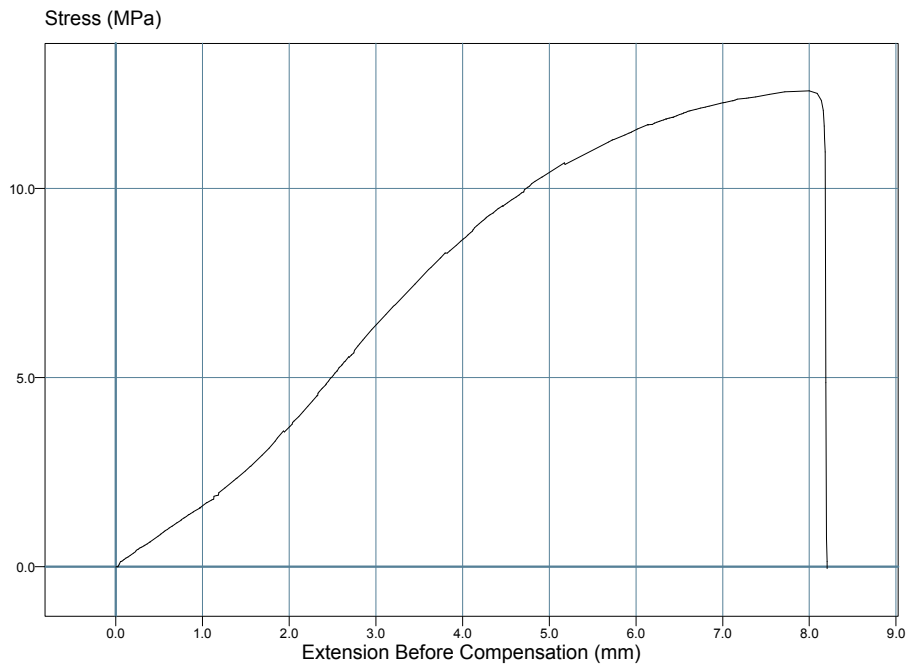


**Figure A. 3** Stress-Strain curve of LDPE-WF-5 MA composition

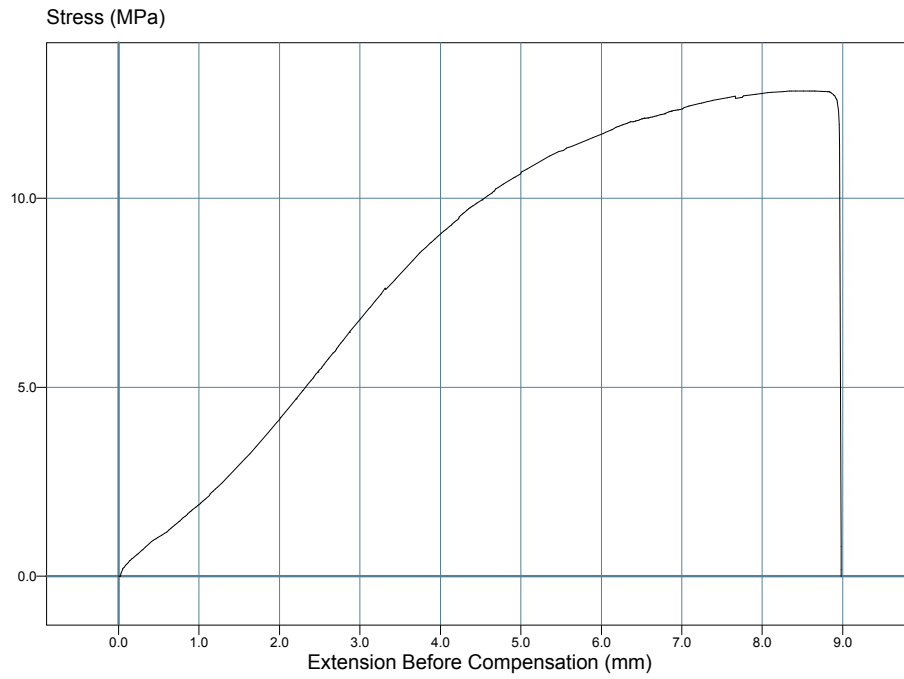


**Figure A. 4** Stress-Strain curve of LDPE-WF-10 MA composition

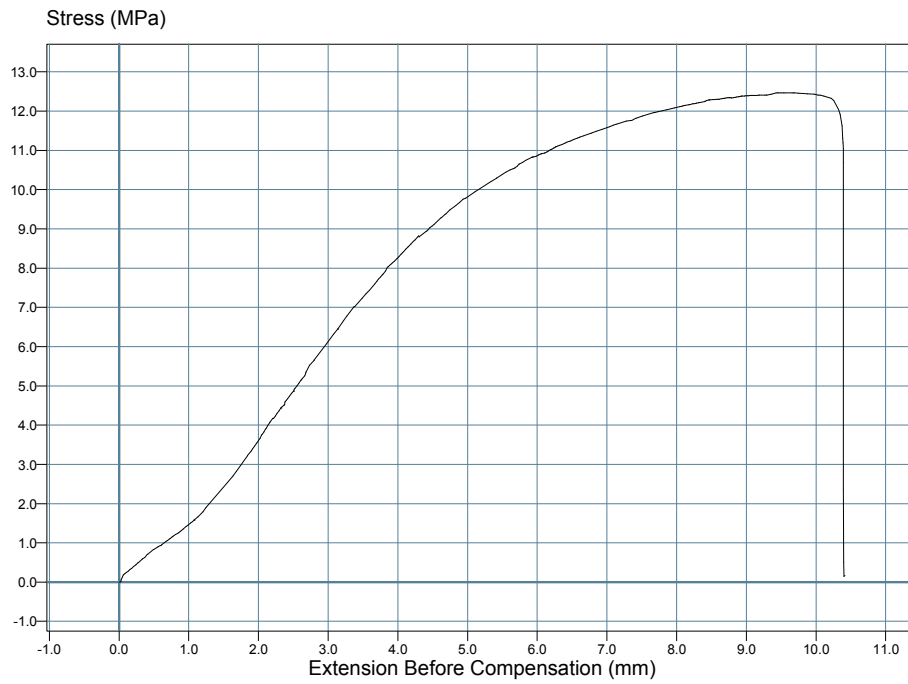


**Figure A. 5** Stress-Strain curve of LDPE-WF-15 MA composition

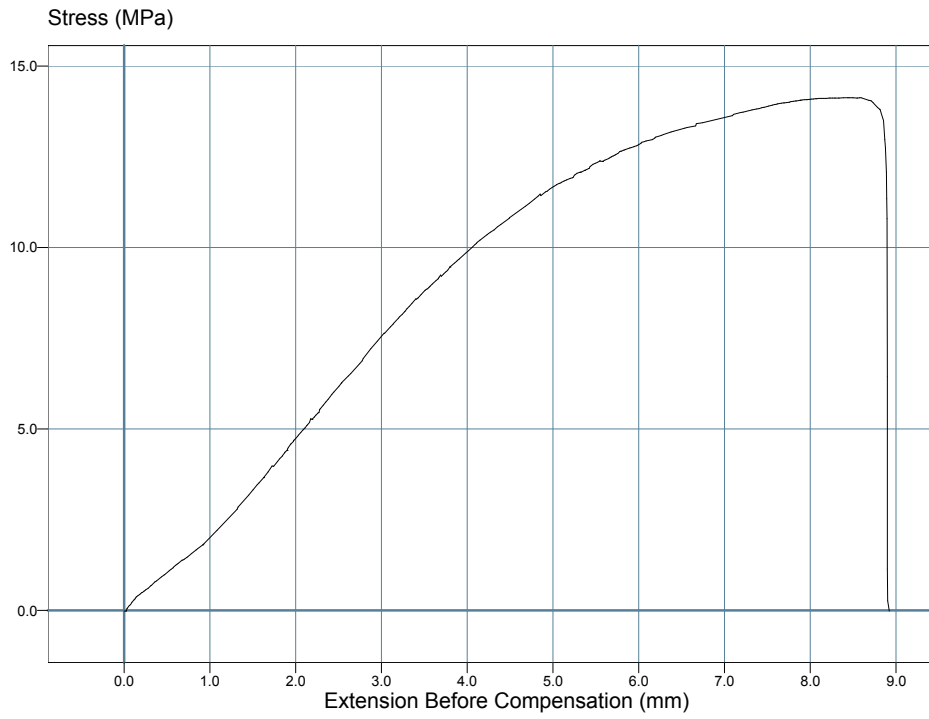


**Figure A. 6** Stress-Strain curve of LDPE-WF-pre 10 MA composition

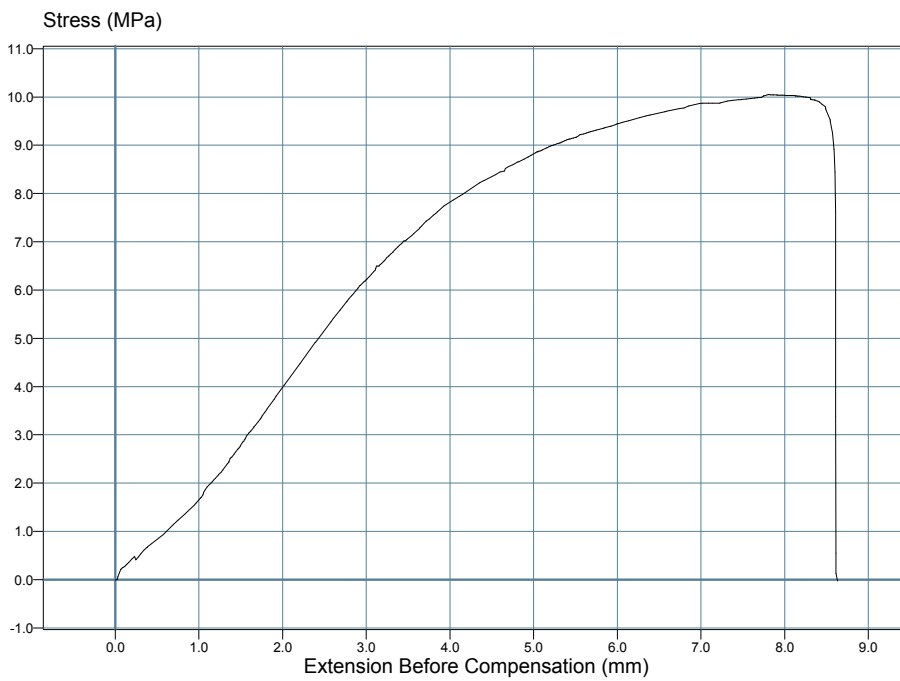


**Figure A. 7** Stress-Strain curve of LDPE-WF-3 GMA composition



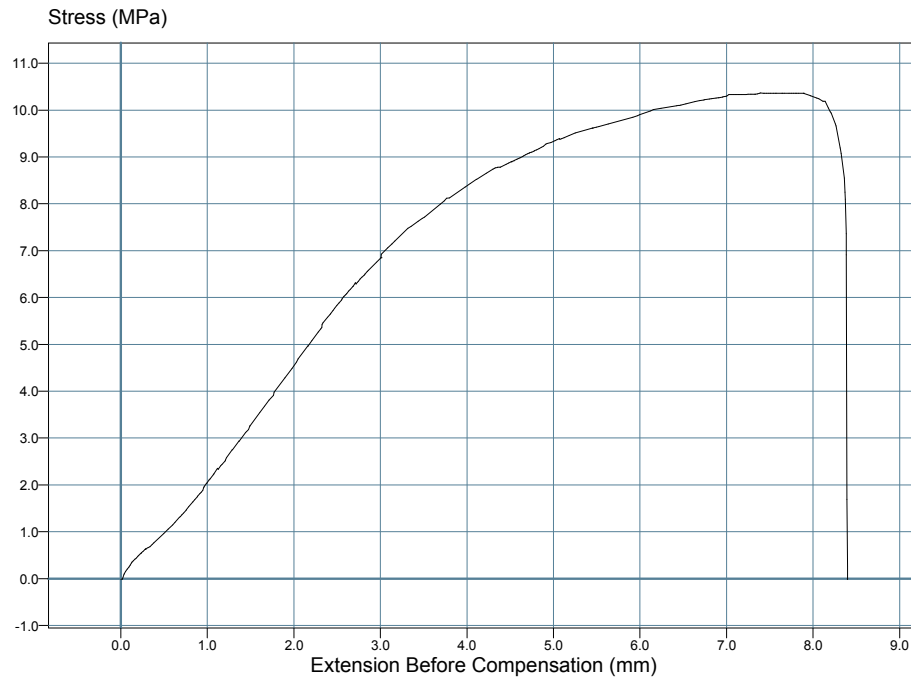


**Figure A. 8** Stress-Strain curve of LDPE-WF-5 GMA composition

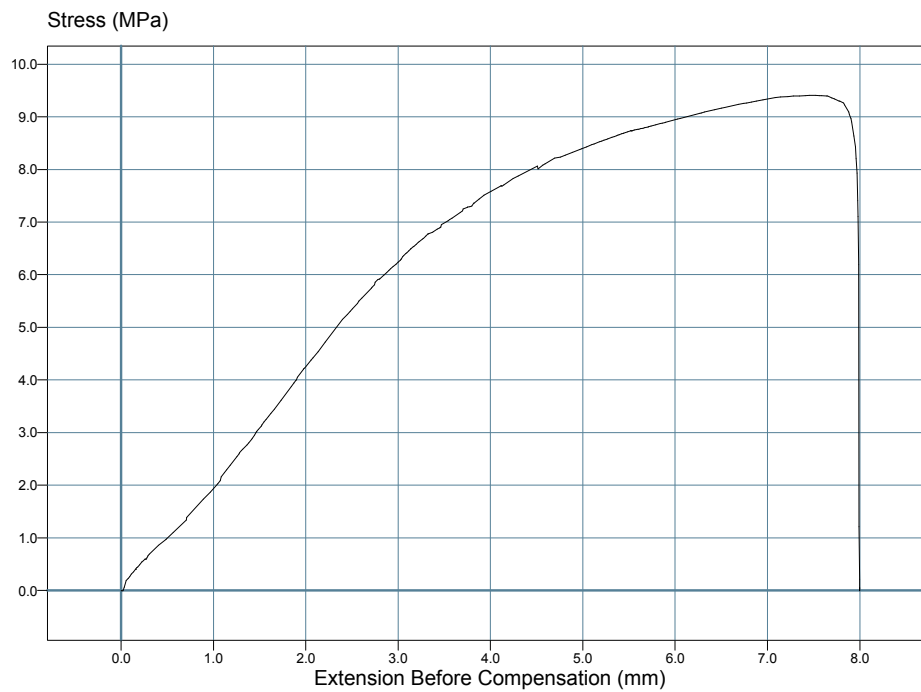


**Figure A. 9** Stress-Strain curve of LDPE-WF-10 GMA composition

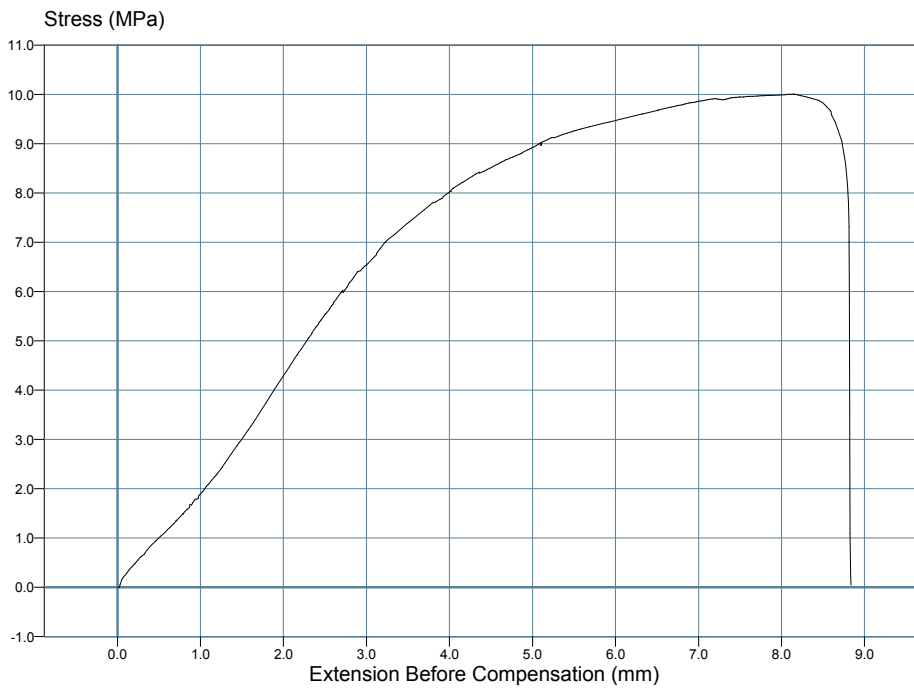


**Figure A. 10** Stress-Strain curve of LDPE-WF-15 GMA composition

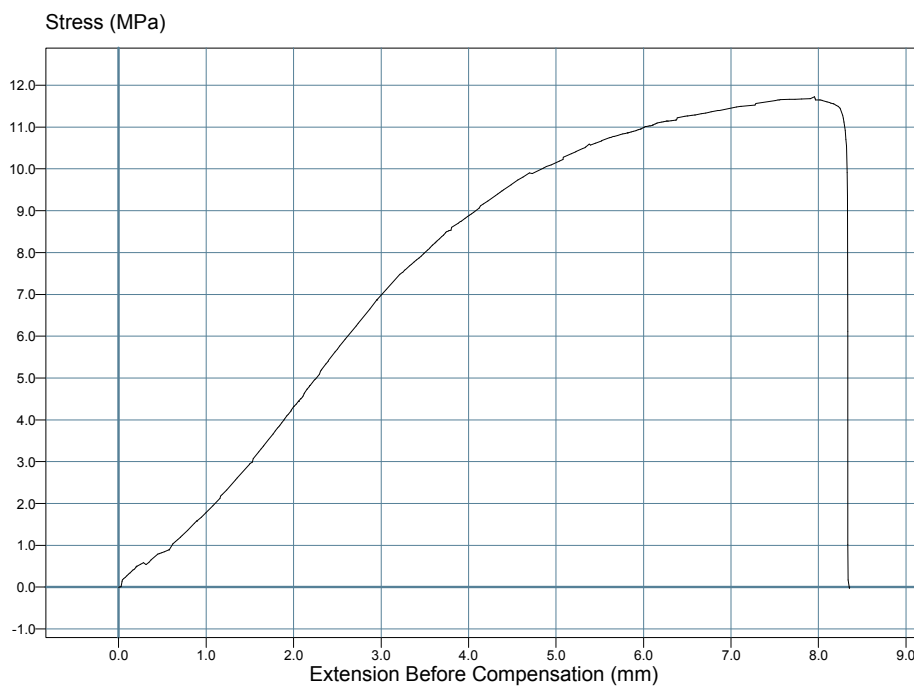


**Figure A. 11** Stress-Strain curve of LDPE-WF-pre 1 GMA composition

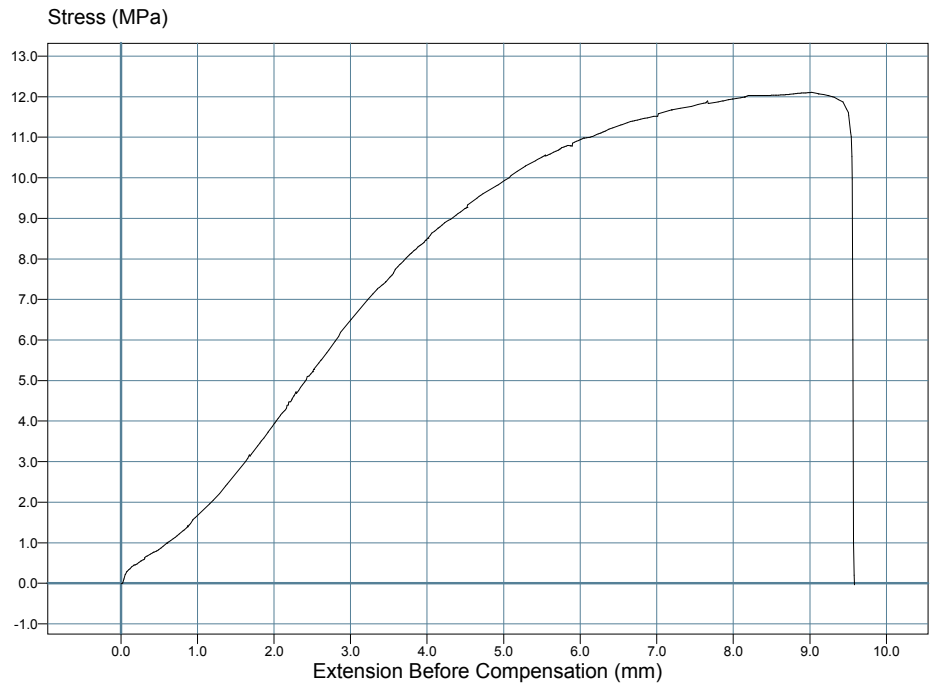


**Figure A. 12** Stress-Strain curve of LDPE-WF-pre 3 GMA composition

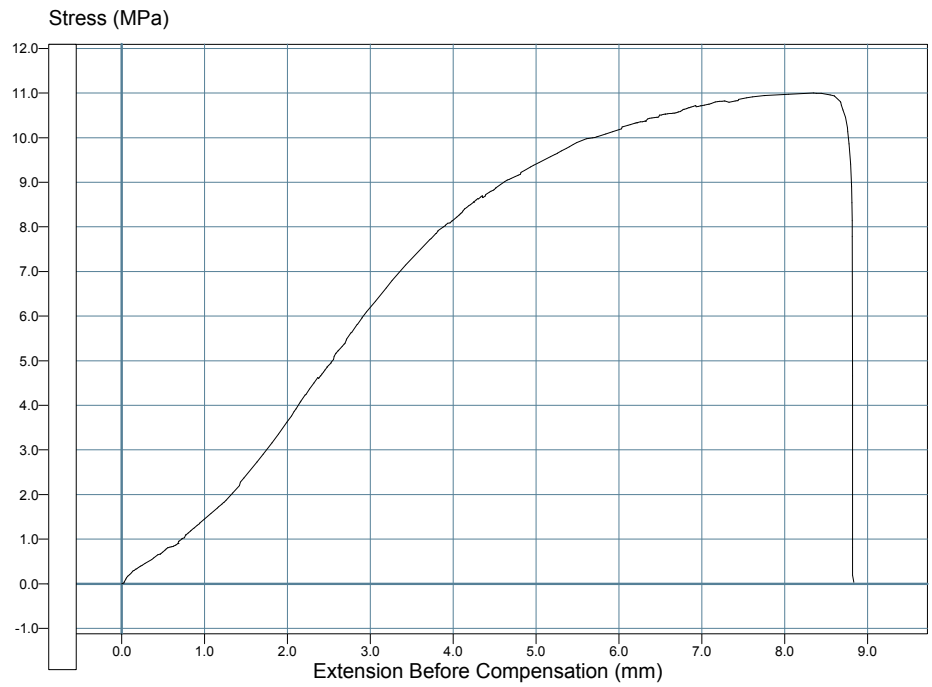


**Figure A. 13** Stress-Strain curve of LDPE-WF-pre 5 GMA composition



## CIRRICULUM VITAE

### PERSONAL INFORMATION:

**Name and Surname:** Yasemin ALTUN

**Date and Place of Birth:** 26/08/1983, Balıkesir (TURKEY)

**Sex:** Female

**Marital Status:** Single

**Nationality:** Republic of Turkey

**Correspondence Address**

Work Address: Roketsan A.Ş. Kemalpaşa Mah. Şehit Yüzbaşı Adem Kutlu Sok. No:21 06780 Elmadağ  
Ankara / TURKEY

Home Address: Yaşamkent Mah. Esenpark Sitesi 3232. sok.  
A-Blok No:14 , Yenimahalle Ankara/TURKEY

**Phone:** +90 505 818 7233 (Mobile)  
+90 312 860 55 00-4324 (Work)  
+90 312 217 37 48 (Home)

**E-mail :** yasemin.altun@roketan.com.tr

### EDUCATIONAL BACKGROUND:

**Ph.D.:** METU Polymer Science and Technology Department, Ankara (3.21/4.00)  
Date of Graduation: February, 2015

**M.S.:** METU Department of Chemistry, Ankara (3.36/4.00)  
Date of Graduation: October, 2008

**B.S.:** METU Department of Chemistry, Ankara (2.87/4.00)  
Date of Graduation: June, 2006

**High School:** Sırrı Yırcalı Anatolian High School, Balıkesir (4.78/5.00)  
Date of Graduation: June, 2001

## **RELEVANT SKILLS**

- Three years of experience of working at polymer chemistry laboratory
- Three years of experience of development in the mechanical and flame retardancy properties of wood flour-polymer composites.
- Four years of experience of research and development of natural products (cyclitol derivatives) and derivatives of carba-sugars that can be the key compounds for the treatment of cancer.
- Five years of experience of working at organic chemistry laboratory.
- Very good knowledge of NMR Spectroscopy.
- Two years of experience of working in a TÜBİTAK project.
- Working knowledge of
  - Fourier Transform Infrared Radiation(FTIR)
  - Gas Chromatography-Mass Spectrometry (GCMS)
  - Ultraviolet-Visible Spectrophotometry (UV-Vis)
  - Viscometer
  - Differential Scanning Calorimetry (DSC)
  - Dissolution Instrument
  - Extruder (microcompounder)
  - Injection Molding Machine
  - Tensile Test Machine
  - Impact Test Machine
  - Compression Molding Press
  - Melt Flow Index Instrument
  - Limiting Oxygen Index Instrument (LOI)
  - UL-94 Vertical Burning Test
  - Horizontal Burning Test

## **WORK EXPERIENCE:**

**July 2013-present:** Engineer at Ballistic Protection and Material Technology Department, Roketsan A. Ş. (Elmadağ-ANKARA)

**September 2006-July 2013:** Research Assistant of the Graduate School of Natural & Applied Sciences at METU, Department of Chemistry (ANKARA)

**June-July 2005:** Internship at Bilim İlaç San. A.Ş. (ÇERKEZKÖY-TEKİRDAĞ)

### **PROFESSIONAL DUTIES:**

**September 2007-2010:** Student Selection and Placement Center (ÖSYM), Assistant of the City Ankara Representative

- Finding and assigning proctors for the physically handicapped candidates' examinations.
- Organization of the proctors who are on duty at the physically handicapped candidates' buildings for all examinations.

### **FOREIGN LANGUAGES:**

- English-fluent
- German-beginner

### **COMPUTER SKILLS:**

**Operating Systems:** Windows 95/98/2000/XP/Vista

**Office and Computer Aided Design Tools:** Microsoft Office, ChemOffice

### **PUBLICATIONS:**

- **Altun, Y.**, Dogan, M., Bayramli, E.; Comparative study of maleated and glycidyl methacrylate functionalized terpolymers as compatibilizers for low-density polyethylene-wood flour composites, *J Appl Polym Sci*, 127 (2), 1010-1016, **2013**
- **Altun, Y.**, Dogan, M., Bayramli, E.; Effect of alkaline treatment and pre-impregnation on mechanical and water absorption properties of pine wood flour containing poly (lactic acid) based green-composites, *J Polym Environ*, 21(3), 850-856, **2013**.
- **Altun, Y.**, Dogan, D., Balci, M., Synthesis of branched carbasugars via photooxygenation and manganese (III) acetate free radical cyclization, *Tetrahedron*, 70 (33), 4884-4890, **2014**.

### **PROFESSIONAL MEETINGS AND ACTIVITIES:**

- International Manufacturing Technologies Exhibition, 25-28 September 2003, İstanbul-Turkey.
- Synthesis of Polyhydroxy Compounds by Using Manganese (III) Acetate, **Yasemin Altun**, Dilem Yardımcı, Metin Balcı, *International Conference on Organic Chemistry*, 5-9 June 2007, Erzurum-Turkey

- Mangan (III) Asetat Oksidasyonu ile Polihidroksi Bileşiklerin Sentezlenmesi, **Yasemin Altun**, Dilem Yardımcı, Metin Balcı, 22. *Ulusal Kimya Kongresi*, 6-10 Ekim 2008, Mağusa-KKTC
- Yeni Bir Yöntemle İnositol Türevi Sentezi, Merve Bekarlar, **Yasemin Altun**, Arif Baran, Metin Balcı, 23. *Ulusal Kimya Kongresi*, 16-20 Haziran 2009, Sivas-Türkiye
- Polihidroksisiklopentan Türevlerinin Sentezi İçin Yeni Bir Yöntem, Dilem Yardımcı Doğan, **Yasemin Altun**, Serdal Kaya, Metin Balcı, 24. *Ulusal Kimya Kongresi*, 29 Haziran- 2 Temmuz 2010, Zonguldak-Türkiye
- The Improvement of Mechanical and Water Absorption Properties Of Poly(Lactic Acid) Based Green-Composites, **Yasemin Altun**, Mehmet Doğan, Erdal Bayramlı, *Kimyevi Maddeler ve Mamülleri Sektöründe 2. AR-GE Proje Pazarı*, 18-19 September 2012, İstanbul-Turkey
- Comparative Study of Maleated and Glycidyl Methacrylate Functionalized Terpolymers as Compatibilizers for LDPE-Wood Flour Composites, **Yasemin Altun**, Mehmet Doğan, Erdal Bayramlı, 26. *Ulusal Kimya Kongresi*, 1-6 October 2012, Fethiye, Muğla-Turkey

#### **PROJECTS INVOLVED:**

- Mangan (III) Asetat ile Hidrokarbonların Oksidasyon Mekanizmasının Araştırılması ve Yeni Doğal Ürün Sentezlerinin Geliştirilmesi. TUBİTAK/106M335 (**Investigation of Oxidation Mechanism of Hydrocarbons with Manganese (III) Acetate and Advancement of New Natural Product Syntheses.**)

#### **LEADERSHIP ACTIVITIES:**

- METU Chemistry Society

**November 2002-September 2005** : Active member of Administrative Committee and

participated in the organization of Traditional Chemistry Week

**September 2005-June 2006** : President of Administrative Committee



**PERSONAL INTERESTS:**

Playing squash, taking photograph, yoga, reading books